BaBar Analysis Document #1586, Version 1
September 15, 2006

Global Fit for Branching Fractions of $B \to D^{(*)}\ell\nu$ Decays and Form Factor Slope of $B \to D\ell\nu$ Decays

Kenji Hamano (University of Victoria)
Robert V. Kowalewski (University of Victoria)

Abstract

We present details of our Global fit analysis in $B \to D^{(*,**)}X\ell\nu$ decays. We use 86×10^6 $B\bar{B}$ events collected by the Babar detector. The primary target of this analysis is to determine the branching fractions of $B \to D\ell\nu$ and $B \to D^*\ell\nu$ decays and the form factor slope of $B \to D\ell\nu$ decay.

Main changes from previous version

1. Introduction. Especially, inclusive-exclusive comparison.

2. Fitting method

3. Constraints on variables in the fit

To Do list

1. Separate electron and muon.

2. List-up selected number of cnadidates after each step of event selection cuts.

3. Justification of sideband subtraction. Sideband was subtracted with an assumption of sideband is linearly disributed. To justify this, pick up a few bins and fit D mass distribution by a combination of a Gaussian peak and ploynomial background. The signal and background yeild from this fit is supposed to be same as sideband subtraction.

4. Plots to compare FF values and weight factor of FF re-weighting.
4-1. $B \to D\ell\nu$
4-1. $B \to D^*\ell\nu$

5. MC validation plots. (make sure 0th, 1st, 2nd components add up to Dlnu.)

6. χ^2 vs ρ_D^2 plots.

7. Systematic uncertainty study.
7-1. Effect of track eff and PID correction.
7-2. Effect of change in $R-1$, R_2. (and ρ^2 ?)
7-3. Effect of uncertainties on the measured values used in the fit.
7-3. Bin by bin error? (Effciciency may change not grobally but bin by bin)

8. LMisID background. Replace by a calculated histogram from data?

9. DiffB background. Check the most recent Babar $B \to X_c \ell \nu$ BAD.

10. The fit result of BF may not be relative?

11. Reduce χ^2
11-1. $B \to D^* \ell \nu$ slope ρ^2. Float this with Gaussian constraint ?
11-2. $B \to D^{**} \ell \nu$ FF re-weighting.
11-3. $B \to D^{(*)} \pi \ell \nu$ FF re-weighting.

Contents

1 Introduction **8**

2 Signal and Background Events **14**
2.1 Signal . . . 14
2.1.1 D^0 modes . . . 14
2.1.2 D^+ modes . . . 15
2.2 Background . . . 15
2.2.1 DiffB . . . 15
2.2.2 DBCascL . . . 16
2.2.3 CascL . . . 16
2.2.4 LMisID . . . 16
2.2.5 Comb . . . 16
2.2.6 RealD . . . 17
2.2.7 Cont . . . 17
2.3 Notation of branching fractions . . . 17

3 Event Selection **20**
3.1 BToDlnu skim . . . 21
3.1.1 Reconstruction of D^0 and D^+ . . . 21
3.1.2 Reconstruction of Dl candidates . . . 22
3.2 Radiative Bhabha veto . . . 22
3.3 Kaon Selection . . . 27
3.4 Vertexing . . . 27
3.5 Thrust cut . . . 27
3.6 Summary of event selection cuts . . . 33

4 Fitting Method **38**
4.1 Binning (i) . . . 38
4.2 MC modes (j) . . . 39
4.3 χ^2 . . . 39
4.4 Number of Events or Candidates N_{ij} . . . 40
4.4.1 Tracking efficiency and PID correction . . . 40
4.4.2 Luminosity normalization . . . 41
4.4.3 Background MC N_{ij}^{Bkgd} . . . 41
4.4.4 Signal MC N_{ij}^{Sig} . . . 41
4.5 Branching fraction weight W_{jk}^{Bkgd} . . . 42

4.6 Form factor weight W_{ijk}^{Sig} . . . 43
4.7 Statistical uncertainty σ_i^{data}, σ_{ij}^{Bkgd} and σ_{ij}^{Sig} . . . 43
4.8 Coefficients C_j^{Bkgd} and C_j^{Sig} . . . 43
4.9 Normalization . . . 43

5 Coefficients in the fitting **45**
5.1 Number of produced B . . . 45
5.2 D^0 MC modes . . . 45
5.2.1 Coefficients for signals C_j^{Sig} . . . 45
5.2.2 Coefficients for backgrounds C_j^{Bkgd} . . . 49
5.3 D^+ MC modes . . . 51
5.3.1 Coefficients for signals C_j^{Sig} . . . 51
5.3.2 Coefficients for backgrounds C_j^{Bkgd} . . . 54

6 Form Factor (FF) Re-weighting **56**
6.1 Normalization . . . 56
6.2 $B \to D\ell\nu$ . . . 56
6.3 $B \to D^*\ell\nu$ . . . 58
6.4 $B \to D_0^*\ell\nu$ . . . 61
6.5 $B \to D_1\ell\nu$ . . . 61
6.6 $B \to D_1'\ell\nu$ . . . 61
6.7 $B \to D_2^*\ell\nu$ . . . 61
6.8 $B \to D\pi\ell\nu$ . . . 61
6.9 $B \to D^*\pi\ell\nu$ . . . 62
6.10 $B \to D\ell\nu$ slope fitting technique . . . 62
6.10.1 Number of events . . . 62
6.10.2 Statistical uncertainty . . . 63
6.10.3 Normalization factor R_N . . . 64

7 Effect of corrections and weights **65**
7.1 Tracking efficiency and PID correction . . . 65
7.2 $B \to D\ell\nu$ FF re-weighting . . . 65
7.3 $B \to D^*\ell\nu$ FF re-weighting . . . 65

8 Constraints on variables in the fit **78**
8.1 f_{+0} . . . 78
8.2 C_{+0} . . . 78
8.3 D^* decay branching fractions . . . 78

8.4 D^{**} decay branching fractions . . . 79
8.5 $B \to D^{(*)}\ell\nu$ decay branching fractions . . . 80
8.6 $B \to D^{**}\ell\nu$ and $B \to D^{(*)}\pi\ell\nu$ decay branching fractions . . . 80
8.6.1 $B \to D_1\ell\nu$ and $B \to D_2^*\ell\nu$ . . . 81
8.6.2 $B \to D_0^*\ell\nu$ and non-resonant $B \to D\pi\ell\nu$ . . . 82
8.6.3 $B \to D_1'\ell\nu$ and non-resonant $B \to D^*\pi\ell\nu$. . . . 84
8.6.4 $B \to D^{**}\ell\nu$ and non-resonant $B \to D^{(*)}\pi\ell\nu$ . . . 85

9 Validation of fit **88**
9.1 Case 1 : FF slope fixed . . . 88
9.2 Case 2 : FF slope with standard parametrization . . . 88
9.3 Case 3 : FF slope with new parametrization . . . 88
9.4 Case 4 : float all ratios . . . 88

10 Fit results **89**
10.1 Constraints on $f_{BpDPiDD0}$ and $f_{BpDSPiDDP1}$ . . . 89
10.2 Fit result . . . 89

11 Systematic Uncertainties **90**

12 Conclusion **91**

13 Acknowledgements **92**

A Decay modes to consider **93**
A.1 Semileptonic $B \to D^{(*,**)}\ell\nu$ decays . . . 93
A.1.1 Semileptonic B^+ decays . . . 93
A.1.2 Semileptonic B^0 decays . . . 93
A.2 D^* and D^{**} decays . . . 93
A.2.1 $D^{*,**+}$ decays . . . 93
A.2.2 $D^{*,**0}$ decays . . . 97
A.3 D^0 and D^+ decays . . . 97
A.3.1 D^0 decays . . . 97
A.3.2 D^+ decays . . . 97
A.3.3 π^0 and K_s^0 . . . 97
A.4 Decay chain . . . 101
A.4.1 B^+ decay chain . . . 101
A.4.2 B^0 decay chain . . . 102
A.5 Background . . . 104

A.5.1 $B \to D^{(*)}\bar{D}^{(*)}(K)$ 104
A.5.2 Doubly Cabbibo suppressed D decay 104

B Numerical values used in MC and fitting **106**
B.1 Measured $B \to D^{(*)}\pi^+\ell^+\nu$ branching fractions 106

C BToDlnu skim rates and luminosities **114**

D Isospin Symmetry **117**
D.1 Semileptonic B decays 117
D.2 D^{**} decays 118

E Classification of D^{**} **120**
E.1 Angular momentum of mesons 120
E.2 Standard classification of mesons 120
E.3 Heavy Quark Effective Theory (HQET) and D, D^* and D^{**} mesons 121
E.4 Decay modes of D^{**} 122

F $\cos\theta_{BY}$ **126**
F.1 $B \to D\ell\nu$ decays 126
F.2 With an additional pion 126
F.3 If D and l come from different B 127

G Velocity transfer w **129**
G.1 w and q^2 129
G.2 $1 \leq w \lesssim 1.5$ 129
G.3 Practical calculation of w 130

H Form Factors (FF) of $B \to D^{(*,**)}X\ell\nu$ decays **131**
H.1 Matrix elements, form factors and decay rates 131
H.1.1 $B \to D\ell\nu$ 131
H.1.2 $B \to D^*\ell\nu$ 132
H.1.3 $B \to D_0^*\ell\nu$ 133
H.1.4 $B \to D_1'\ell\nu$ 134
H.1.5 $B \to D_1\ell\nu$ 134
H.1.6 $B \to D_2^*\ell\nu$ 134
H.2 ISGW2 model 134
H.2.1 $B \to D\ell\nu$ (1^2S_0) 139

H.2.2 $B \to D^*\ell\nu$ (1^3S_0) 139
H.2.3 $B \to D_0^*\ell\nu$ (1^3P_0) 140
H.2.4 $B \to D_1'\ell\nu$ (1^3P_1) 141
H.2.5 $B \to D_1\ell\nu$ (1^1P_1) 141
H.2.6 $B \to D_2^*\ell\nu$ (1^3P_2) 142
H.2.7 $B \to D_1^*\ell\nu$ $(\frac{1}{2}^+)$ 143
H.2.8 $B \to D_1\ell\nu$ $(\frac{3}{2}^+)$ 143
H.2.9 Differential decay rate 144
H.3 LLSW model 144
H.3.1 $B \to D_1\ell\nu$ 144
H.3.2 $B \to D_2^*\ell\nu$ 146
H.3.3 $B \to D_0^*\ell\nu$ 147
H.3.4 $B \to D_1^*\ell\nu$ 148
H.3.5 Differential decay rate using x, y 149
H.4 HQET model 150
H.4.1 Velocity transfer w 150
H.4.2 $B \to D\ell\nu$ 150
H.4.3 $B \to D^*\ell\nu$ 151
H.5 GoityRoberts model 152
H.5.1 $B \to D\pi\ell\nu$ 152
H.5.2 $B \to D^*\pi\ell\nu$ 156

1 Introduction

The Cabbibo-Kobayashi-Maskawa (CKM) Matrix [1][2] plays an important role in quark mixing and CP violation. The matrix elements of it are free parameters of the Standard Model of particle physics and need to be determined by experiments. As a B-factory, Babar can measure some of the CKM matrix elements such as $|V_{ub}|$, $|V_{cb}|$ and $|V_{tb}|$ in a good precision. To extract $|V_{cb}|$, semileptonic $B \to X_c \ell \nu$ decays have been used. Here, X_c denotes a charmed meson. Especially two exclusive decay modes, $B \to D^* \ell \nu$ and $B \to D \ell \nu$ are very useful. However, there are still unsolved problems in these decay modes such as

- $B^0 \to D^{*-} \ell^+ \nu$ decay [1] branching fraction discrepancy
  There are discrepancies between $B^0 \to D^{*-} \ell^+ \nu$ decay branching fraction measurements. Those are summarized in Table 1. The results vary from 0.0459 (BELLE) to 0.0609 (CLEO). And those measurements are not consistent with each other.

- $B^0 \to D^{*-} \ell^+ \nu$, $B^+ \to \bar{D}^{*0} \ell^+ \nu$ branching fraction difference
  There is a significant difference between the branching fractions of $B^0 \to D^{*-} \ell^+ \nu$ and $B^+ \to \bar{D}^{*0} \ell^+ \nu$ decays. To compare these decays, we need to consider decay rates. In the case of $B^0 \to D^{*-} \ell^+ \nu$,

$$\mathcal{B}(B^0 \to D^{*-} \ell^+ \nu) = \frac{\Gamma(B^0 \to D^{*-} \ell^+ \nu)}{\Gamma_{B^0}} = \Gamma(B^0 \to D^{*-} \ell^+ \nu) \tau_{B^0} \quad (1)$$

  where Γ_{B^0} is the total width and τ_{B^0} is the lifetime of B^0. Thus, the ratio of two decay rates is

$$\frac{\Gamma(B^0 \to D^{*-} \ell^+ \nu)}{\Gamma(B^+ \to \bar{D}^{*0} \ell^+ \nu)} = \frac{\mathcal{B}(B^0 \to D^{*-} \ell^+ \nu)}{\tau_{B^0}} \frac{\tau_{B^+}}{\mathcal{B}(B^+ \to \bar{D}^{*0} \ell^+ \nu)} \quad (2)$$

  Using PDG value of $\frac{\tau_{B^+}}{\tau_{B^0}} = 1.071 \pm 0.009$ [10], we define the lifetime adjusted branching fraction of $B^0 \to D^{*-} \ell^+ \nu$ as

$$\begin{aligned} &\hat{\mathcal{B}}(B^0 \to D^{*-} \ell^+ \nu) \equiv \mathcal{B}(B^0 \to D^{*-} \ell^+ \nu) \tfrac{\tau_{B^+}}{\tau_{B^0}} \\ &= (1.071 \pm 0.009) \times \mathcal{B}(B^0 \to D^{*-} \ell^+ \nu) \end{aligned} \quad (3)$$

[1] Charge conjugate modes are implied throughout this text

Hence, the ratio of two decay rates is given by

$$\frac{\Gamma(B^0 \to D^{*-}\ell^+\nu)}{\Gamma(B^+ \to \bar{D}^{*0}\ell^+\nu)} = \frac{\hat{\mathcal{B}}(B^0 \to D^{*-}\ell^+\nu)}{\mathcal{B}(B^+ \to \bar{D}^{*0}\ell^+\nu)} \tag{4}$$

These values are summarized in Table 2. The $B^+ \to \bar{D}^{*0}\ell^+\nu$ branching fraction value from Babar is calculated as follows. Babar measure [13]

$$\frac{\Gamma(B^+ \to \bar{D}^{*0}\ell^+\nu)}{\Gamma(B^+ \to X_c\ell^+\nu)} = 0.611 \pm 0.022 \pm 0.027 \tag{5}$$

Combining this with $\mathcal{B}(B^+ \to X_c\ell^+\nu) = 0.1097 \pm 0.0065$ (see section 4.9), we get

$$\begin{aligned} \mathcal{B}(B^+ \to \bar{D}^{*0}\ell^+\nu) &= (0.611 \pm 0.0348) \times (0.1097 \pm 0.0065) \\ &= 0.0670 \pm 0.0055 \end{aligned} \tag{6}$$

Based on isospin symmetry,

$$\hat{\mathcal{B}}(B^0 \to D^{*-}\ell^+\nu) = \mathcal{B}(B^+ \to \bar{D}^{*0}\ell^+\nu) \tag{7}$$

But, the numbers in the table do not satisfy this condition.

- Inclusive-exclusive disagreement
  There are mainly 10 exclusive decay modes of the type $B \to X_c\ell\nu$ (see Appendix A)
  - $B \to D\ell\nu$
  - $B \to D^*\ell\nu$
  - $B \to D_0^*\ell\nu$
  - $B \to D_1\ell\nu$
  - $B \to D_1'\ell\nu$
  - $B \to D_2^*\ell\nu$
  - $B \to D\pi^+\ell\nu$ (non-resonant)
  - $B \to D\pi^0\ell\nu$ (non-resonant)
  - $B \to D^*\pi^+\ell\nu$ (non-resonant)
  - $B \to D^*\pi^0\ell\nu$ (non-resonant)

The D_0^*, D_1, D_1' and D_2^* are called D^{**} as a whole (see Appendix E). The sum of the branching fractions of these exclusive decays is supposed to be identical to the inclusive $B \to X_c \ell\nu$ branching fractions (this X_c denotes a particle system including a charm quark such as D^* or $D\pi$ etc.). Those branching fractions are summarized in Table 3. In this table, non-resonant $B \to D^{(*)}\pi\ell\nu$ decays and $B \to D^{**}\ell\nu$ decays are combined (see Appendix B). The sum of exclusive modes is consistent with the inclusive branching fraction in case of B^+ decays. However, there is a disagreement in B^0 decays. If $\mathcal{B}(B^0 \to D^{*-}\ell^+\nu)$ is as large as $\mathcal{B}(B^+ \to \bar{D}^{*0}\ell^+\nu)$, which is close to the CLEO value in Table 1, exclusive and inclusive branching fraction agrees. Interesting point is that only CLEO measured both $\mathcal{B}(B^0 \to D^{*-}\ell^+\nu)$ and $\mathcal{B}(B^+ \to \bar{D}^{*0}\ell^+\nu)$. Our analysis can provides another measurement using a different method, and we can also access both $\mathcal{B}(B^0 \to D^{*-}\ell^+\nu)$ and $\mathcal{B}(B^+ \to \bar{D}^{*0}\ell^+\nu)$. Note that D_s modes are not included in the table; however, those contributions are small enough to be negligible.

- $B \to D\ell\nu$ decay form factor slope
  $B \to D\ell\nu$ decay form factor slope, ρ_D^2 (see Appendix H), has never been well measured. Existing measurements are listed in Table 4. The best measurement from BELLE has a 23 % uncertainty. More precise measurement is necessary to address the above issues.

In this analysis, we address these problems. We use a global fit technique to determine exclusive $B \to D\ell\nu$ and $B \to D^*\ell\nu$ branching fractions and $B \to D\ell\nu$ form factor slope. We do not explicitly reconstruct D^* or D^{**}. Thus, we do not have to rely on slow pion reconstruction. We also do not depend on Monte Carlo simulation (MC) to determine efficiency to reconstruct and detect a specific decay mode. This is a different approach from the existing measurements listed above. We, however, depend on MC to construct the probability density functions (PDF) to be used in the fit. Details of our fit technique is explained in section 4. Since we use a different approach, our results are useful to solve the above problems.

In the following section 2, we explain the signal and background events and define our notation of branching fractions. The data set and event selections used in this analysis is described in section 3. In section 4, fitting method is explained in detail. In our fit, branching fractions are include in the coefficients, which is explained in section 5. We also need to re-weight

Branching Fraction	Experiment (year)	Decay mode
$0.0459 \pm 0.0023 \pm 0.0040$	BELLE (2002) [3]	$B^0 \to D^{*-}\ell^+\nu$
$0.0470 \pm 0.0013^{+0.0036}_{-0.0031}$	DELPHI (2001) [4]	$B^0 \to D^{*-}\ell^+\nu$
$0.0490 \pm 0.0007^{+0.0036}_{-0.0035}$	BABAR (2005) [5]	$B^0 \to D^{*-}\ell^+\nu$
$0.0526 \pm 0.0020 \pm 0.0046$	OPAL (2000) [6]	$B^0 \to D^{*-}\ell^+\nu$
$0.0553 \pm 0.0026 \pm 0.0052$	ALEPH (1997) [7]	$B^0 \to D^{*-}\ell^+\nu$
$0.0590 \pm 0.0022 \pm 0.0050$	DELPHI (2004) [8]	$B^0 \to D^{*-}\ell^+\nu$
$0.0609 \pm 0.0019 \pm 0.0040$	CLEO (2003) [9]	$B^0(B^+) \to D^{*-}(\bar{D}^{*0})\ell^+\nu$

Table 1: $B^0 \to D^{*-}\ell^+\nu$ branching fractions from different experiments. The first uncertainty is statistical and the second one is systematic. In the most right column, the decay modes measured in each analysis are listed. Only CLEO (2003) measured both $B^0 \to D^{*-}\ell^+\nu$ and $B^+ \to \bar{D}^{*0}\ell^+\nu$ modes.

Experiment [Reference]	BELLE (2005) [12]	BABAR (2006) [5][13]
$\mathcal{B}(B^0 \to D^{*-}\ell^+\nu)$	0.0470 ± 0.0024	0.0490 ± 0.0037
$\hat{\mathcal{B}}(B^0 \to D^{*-}\ell^+\nu)$	0.0503 ± 0.0026	0.0525 ± 0.0040
$\mathcal{B}(B^+ \to \bar{D}^{*0}\ell^+\nu)$	0.0606 ± 0.0025	0.0670 ± 0.0055

Table 2: $B^0 \to D^{*-}\ell^+\nu$ and $B^+ \to \bar{D}^{*0}\ell^+\nu$ branching fractions from two experiments. The first uncertainty is statistical and the second one is systematic. The lifetime adjusted branching fraction, $\hat{\mathcal{B}}$ is defined in the text.

Decay mode (B^+)	Branching Fraction (%)	Reference
$B^+ \to \bar{D}^0 \ell^+ \nu$	2.15 ± 0.22	[10]
$B^+ \to \bar{D}^{*0} \ell^+ \nu$	6.5 ± 0.5	[10]
$B^+ \to D^- \pi^+ \ell^+ \nu$	0.53 ± 0.10	[10]
$B^+ \to \bar{D}^0 \pi^0 \ell^+ \nu$	0.265 ± 0.05	Isospin symmetry
$B^+ \to D^{*-} \pi^+ \ell^+ \nu$	0.64 ± 0.15	[10]
$B^+ \to \bar{D}^{*0} \pi^0 \ell^+ \nu$	0.32 ± 0.075	Isospin symmetry
Sum of exclusive modes	10.41 ± 0.61	
Inclusive $B^+ \to X_c \ell^+ \nu$	10.97 ± 0.65	section 4.9
Decay mode (B^0)	Branching Fraction (%)	Reference
$B^0 \to D^- \ell^+ \nu$	2.13 ± 0.18	[10]
$B^0 \to D^{*-} \ell^+ \nu$	5.20 ± 0.24	[10]
$B^0 \to \bar{D}^0 \pi^- \ell^+ \nu$	0.32 ± 0.095	[10]
$B^0 \to D^- \pi^0 \ell^+ \nu$	0.16 ± 0.0475	Isospin symmetry
$B^0 \to \bar{D}^{*0} \pi^- \ell^+ \nu$	0.65 ± 0.16	[10]
$B^0 \to D^{*-} \pi^0 \ell^+ \nu$	0.325 ± 0.08	Isospin symmetry
Sum of exclusive modes	8.79 ± 0.41	
Inclusive $B^0 \to X_c \ell^+ \nu$	10.25 ± 0.60	section 4.9

Table 3: Branching fractions of $B \to X_c \ell \nu$ type of decays. $B \to D^{(*)} \pi \ell \nu$ decays include not only non-resonant $B \to D^{(*)} \pi \ell \nu$ decays but also $B \to D^{**} \ell \nu$ decays.

ρ_D^2	Experiment (year)	Decay mode
$0.97 \pm 0.98 \pm 0.38$	ALEPH (1997) [14]	$B^0 \to D^- \ell^+ \nu$
$1.12 \pm 0.22 \pm 0.14$	BELLE (2002) [15]	$B^0 \to D^- \ell^+ \nu$
$1.27 \pm 0.25 \pm 0.14$	CLEO (1999) [16]	$B^0 \to D^- \ell^+ \nu$ and $B^+ \to \bar{D}^0 \ell^+ \nu$

Table 4: Form factor slope ρ_D^2 from different experiments. The first uncertainty is statistic and the second one is systematic.

MC in the fit, and the re-weighting is described in section 6. The effect of tracking efficiency and PID correction and of form factor re-weighting is shown in section 7. Constraints on our fit is discussed in section 8. Validation of the fit method using MC is described in section 9. In section 10, the results of the fitting are presented. The systematic uncertainties are considered in section 11. We summarize our final results in section 12. In Appendix, useful information on physics related to this analysis is described in detail.

2 Signal and Background Events

2.1 Signal

We are interested in $B \to D^{(*,**)}X\ell\nu$ decays. We reconstruct either D^0 or D^+ and a lepton (electron or muon) to form a Dl candidate as a candidate of a B meson. We do not explicitly reconstruct D^* or D^{**}. However, we can access those because, as described in Appendix A, all D^* and D^{**} eventually decay into either D^0 or D^+. We separate decay modes into two categories: the decay modes to produce D^0 and to produce D^+.

2.1.1 D^0 modes

The decay processes to produce D^0 are

- $B^+ \to \bar{D}^0\ell^+\nu$
- $B^+ \to \bar{D}^{*0}\ell^+\nu$ with $\bar{D}^{*0} \to \bar{D}^0\pi^0$ or $\bar{D}^{*0} \to \bar{D}^0\gamma$
- $B^0 \to D^{*-}\ell^+\nu$ with $D^{*-} \to \bar{D}^0\pi^-$
- $B^+ \to \bar{D}^{**0}\ell^+\nu$ with $\bar{D}^{**0} \to D^0\pi^0$
  $B^+ \to \bar{D}^{**0}\ell^+\nu$ with $\bar{D}^{**0} \to D^{*0}\pi^0$ and $D^{*0} \to \bar{D}^0\pi^0$ or $D^{*0} \to \bar{D}^0\gamma$
  $B^+ \to \bar{D}^{**0}\ell^+\nu$ with $\bar{D}^{**0} \to D^{*-}\pi^+$ and $D^{*-} \to \bar{D}^0\pi^-$
- $B^0 \to D^{**-}\ell^+\nu$ with $D^{**-} \to \bar{D}^0\pi^-$
  $B^0 \to D^{**-}\ell^+\nu$ with $D^{**-} \to \bar{D}^{*0}\pi^-$ and $\bar{D}^{*0} \to \bar{D}^0\pi^0$ or $\bar{D}^{*0} \to \bar{D}^0\gamma$
  $B^0 \to D^{**-}\ell^+\nu$ with $D^{**-} \to D^{*+}\pi^0$ and $D^{*+} \to \bar{D}^0\pi^+$
- $B^+ \to \bar{D}^0\pi^0\ell^+\nu$
- $B^0 \to \bar{D}^0\pi^-\ell^+\nu$
- $B^+ \to \bar{D}^{*0}\pi^0\ell^+\nu$ with $\bar{D}^{*0} \to \bar{D}^0\pi^0$ or $\bar{D}^{*0} \to \bar{D}^0\gamma$
  $B^+ \to D^{*-}\pi^+\ell^+\nu$ with $D^{*-} \to \bar{D}^0\pi^-$
- $B^0 \to \bar{D}^{*0}\pi^-\ell^+\nu$ with $\bar{D}^{*0} \to \bar{D}^0\pi^0$ or $\bar{D}^{*0} \to \bar{D}^0\gamma$
  $B^0 \to D^{*-}\pi^0\ell^+\nu$ with $D^{*-} \to \bar{D}^0\pi^-$

2.1.2 D^+ modes

The decay processes to produce D^+ are

- $B^0 \to D^- \ell^+ \nu$
- $B^0 \to D^{*-} \ell^+ \nu$ with $D^{*-} \to D^- \pi^0$ or $D^{*-} \to D^- \gamma$
- $B^0 \to D^{**-} \ell^+ \nu$ with $D^{**-} \to D^- \pi^0$
  $B^0 \to D^{**-} \ell^+ \nu$ with $D^{**-} \to D^{*-} \pi^0$ and $D^{*-} \to D^- \pi^0$ or $D^{*-} \to D^- \gamma$
- $B^+ \to \bar{D}^{**0} \ell^+ \nu$ with $\bar{D}^{**0} \to D^- \pi^+$
  $B^+ \to \bar{D}^{**0} \ell^+ \nu$ with $\bar{D}^{**0} \to D^{*-} \pi^+$ and $D^{*-} \to D^- \pi^0$ or $D^{*-} \to D^- \gamma$
- $B^0 \to D^- \pi^0 \ell^+ \nu$
- $B^+ \to D^- \pi^+ \ell^+ \nu$
- $B^0 \to D^{*-} \pi^0 \ell^+ \nu$ with $D^{*-} \to D^- \pi^0$ or $D^{*-} \to D^- \gamma$
- $B^+ \to D^{*-} \pi^+ \ell^+ \nu$ with $D^{*-} \to D^- \pi^0$ or $D^{*-} \to D^- \gamma$

2.2 Background

Backgrounds are categorized into seven : "DiffB", "DBCascL", "CascL", "LMisID", "Comb", "RealD", "Cont", as described in the following subsections. The DiffB, DBCascL, CascL, LMisID and RealD are peaking backgrounds, and the Comb and Cont are non-peaking backgrounds. Thus, Comb and Cont almost disappear after D mass sideband subtraction. See also Figure 8-11.

2.2.1 DiffB

D and ℓ come from different B, and ℓ come directly from B.
One example of this type of background is

- $B^+ \to \bar{D}^0 \ell^+ \nu$
- $B^- \to D^{(*)0} D^{*-} K^0$ with $D^{*-} \to D^- \pi^0$ or $D^{*-} \to D^- \gamma$

These ℓ^+ from B^+ and D^- from B^- form a Dl candidate as if $B^0 \to D^{(*)-} \ell^+ \nu$.
Another example is

- $B^+ \to \bar{D}^0 \ell^+ \nu$
- $B^- \to D^0 X$
  with doubly Cabbibo suppressed decay $D^0 \to K^+ \pi^-$

This $K^+\pi^-$ from B^- is reconstructed as $\bar{D}^0$ and combined with ℓ^+ to form a Dl candidate.

2.2.2 DBCascL

D and ℓ come from different B, and ℓ does not directly come from B.
An example is

- $B^+ \to \bar{D}^0 X_1$
- $B^- \to D^0 X_2$ with $D^0 \to K^- \ell^+ \nu$

These $\bar{D}^0$ from B^+ and ℓ^+ from $B^-(D^0)$ form a Dl candidate as if $B^+ \to \bar{D}^0 \ell^+ \nu$.

2.2.3 CascL

ℓ does not directly come from B, and D and ℓ come from same B
One example of this type of background is

- $B^+ \to \bar{D}^0 D^{*0} K^+$
  with $\bar{D}^0 \to K^+ \ell^- \bar{\nu}$ and $D^{*0} \to D^0 \pi^0$

These ℓ^- and D^0 form a Dl candidate as if $B^- \to D^0 \ell^- \bar{\nu}$

2.2.4 LMisID

The lepton in a Dl candidate is a mis identified K, π or p. A typical mis identification is between μ and π.

2.2.5 Comb

Combinatorial background from $B\bar{B}$ events. This is the case that reconstructed D is not real. Most of the cases, the kaon and pion do not come from same D or not directly come from D. In our analysis, D^0 has much less Comb background than D^+ because D^0 is reconstructed from two particles (one K and one π) whereas D^+ is reconstructed from three particles (one K and two π) (see section 3.1.1).

2.2.6 RealD

$c\bar{c}$ background including real D. One or both of the $c\bar{c}$ is hadronized to D (or $\bar{D}$) and those D are reconstructed.

2.2.7 Cont

Continuum background from $c\bar{c}$, $s\bar{s}$, $u\bar{u}$, $d\bar{d}$ and $\tau^+\tau^-$ events. All $s\bar{s}$, $u\bar{u}$, $d\bar{d}$ and $\tau^+\tau^-$ events and D mis-reconstructed $c\bar{c}$ events are in this category.

2.3 Notation of branching fractions

We define branching fractions as follows. The value used in the MC simulation SP5/SP6 and PDG values are given in Appendix B. See also Appendix E.4.

- B decays
  - $B_{BpD} \equiv \mathcal{B}(B^+ \to \bar{D}^0\ell^+\nu)$
  - $B_{B0D} \equiv \mathcal{B}(B^0 \to D^-\ell^+\nu)$
  - $B_{BpDS} \equiv \mathcal{B}(B^+ \to \bar{D}^{*0}\ell^+\nu)$
  - $B_{B0DS} \equiv \mathcal{B}(B^0 \to D^{*-}\ell^+\nu)$
  - $B_{BpDD0} \equiv \mathcal{B}(B^+ \to \bar{D}_0^{*0}\ell^+\nu)$
  - $B_{B0DD0} \equiv \mathcal{B}(B^0 \to D_0^{*-}\ell^+\nu)$
  - $B_{BpDD1} \equiv \mathcal{B}(B^+ \to \bar{D}_1^0\ell^+\nu)$
  - $B_{B0DD1} \equiv \mathcal{B}(B^0 \to D_1^-\ell^+\nu)$
  - $B_{BpDDP1} \equiv \mathcal{B}(B^+ \to \bar{D}_1^{\prime 0}\ell^+\nu)$
  - $B_{B0DDP1} \equiv \mathcal{B}(B^0 \to D_1^{\prime -}\ell^+\nu)$
  - $B_{BpDD2} \equiv \mathcal{B}(B^+ \to \bar{D}_2^{*0}\ell^+\nu)$
  - $B_{B0DD2} \equiv \mathcal{B}(B^0 \to D_2^{*-}\ell^+\nu)$
  - $B_{BpDPp} \equiv \mathcal{B}(B^+ \to D^-\pi^+\ell^+\nu)$
  - $B_{BpDP0} \equiv \mathcal{B}(B^+ \to \bar{D}^0\pi^0\ell^+\nu)$
  - $B_{B0DPp} \equiv \mathcal{B}(B^0 \to \bar{D}^0\pi^-\ell^+\nu)$
  - $B_{B0DP0} \equiv \mathcal{B}(B^0 \to D^-\pi^0\ell^+\nu)$

- $B_{BpDSPp} \equiv \mathcal{B}(B^+ \to D^{*-}\pi^+\ell^+\nu)$
- $B_{BpDSP0} \equiv \mathcal{B}(B^+ \to \bar{D}^{*0}\pi^0\ell^+\nu)$
- $B_{B0DSPp} \equiv \mathcal{B}(B^0 \to \bar{D}^{*0}\pi^-\ell^+\nu)$
- $B_{B0DSP0} \equiv \mathcal{B}(B^0 \to D^{*-}\pi^0\ell^+\nu)$

- D^{**} decays
  - $B_{DD0pDPp} \equiv \mathcal{B}(D_0^{*+} \to D^0\pi^+)$
  - $B_{DD0pDP0} \equiv \mathcal{B}(D_0^{*+} \to D^+\pi^0)$
  - $B_{DD00DPp} \equiv \mathcal{B}(D_0^{*0} \to D^+\pi^-)$
  - $B_{DD00DP0} \equiv \mathcal{B}(D_0^{*0} \to D^0\pi^0)$
  - $B_{DD1pDSPp} \equiv \mathcal{B}(D_1^+ \to D^{*0}\pi^+)$
  - $B_{DD1pDSP0} \equiv \mathcal{B}(D_1^+ \to D^{*+}\pi^0)$
  - $B_{DD10DSPp} \equiv \mathcal{B}(D_1^0 \to D^{*+}\pi^-)$
  - $B_{DD10DSP0} \equiv \mathcal{B}(D_1^0 \to D^{*0}\pi^0)$
  - $B_{DDP1pDSPp} \equiv \mathcal{B}(D_1'^+ \to D^{*0}\pi^+)$
  - $B_{DDP1pDSP0} \equiv \mathcal{B}(D_1'^+ \to D^{*+}\pi^0)$
  - $B_{DDP10DSPp} \equiv \mathcal{B}(D_1'^0 \to D^{*+}\pi^-)$
  - $B_{DDP10DSP0} \equiv \mathcal{B}(D_1'^0 \to D^{*0}\pi^0)$
  - $B_{DD2pDPp} \equiv \mathcal{B}(D_2^{*+} \to D^0\pi^+)$
  - $B_{DD2pDP0} \equiv \mathcal{B}(D_2^{*+} \to D^+\pi^0)$
  - $B_{DD2pDSPp} \equiv \mathcal{B}(D_2^{*+} \to D^{*0}\pi^+)$
  - $B_{DD2pDSP0} \equiv \mathcal{B}(D_2^{*+} \to D^{*+}\pi^0)$
  - $B_{DD20DPp} \equiv \mathcal{B}(D_2^{*0} \to D^+\pi^-)$
  - $B_{DD20DP0} \equiv \mathcal{B}(D_2^{*0} \to D^0\pi^0)$
  - $B_{DD20DSPp} \equiv \mathcal{B}(D_2^{*0} \to D^{*+}\pi^-)$
  - $B_{DD20DSP0} \equiv \mathcal{B}(D_2^{*0} \to D^{*0}\pi^0)$

- D^* decays
  - $B_{DSpDPp} \equiv \mathcal{B}(D^{*+} \to D^0\pi^+)$

- $B_{DSpDP0} \equiv \mathcal{B}(D^{*+} \to D^+\pi^0)$
- $B_{DSpDG} \equiv \mathcal{B}(D^{*+} \to D^+\gamma)$
- $B_{DS0DP0} \equiv \mathcal{B}(D^{*0} \to D^0\pi^0)$
- $B_{DS0DG} \equiv \mathcal{B}(D^{*0} \to D^0\gamma)$

- D decays
  - $B_{Dp} \equiv \mathcal{B}(D^+ \to K^-\pi^+\pi^+)$
  - $B_{D0} \equiv \mathcal{B}(D^0 \to K^-\pi^+)$

3 Event Selection

We use the data sample of approximately 86×10^6 $B\bar{B}$-pairs, collected by the BaBar detector. This corresponds to the integrated luminosity of 210.5 fb^{-1}. A description of the BaBar detector can be found elsewhere [17]. The $B\bar{B}$-pairs are produced from $\Upsilon(4S)$ resonance created by the asymmetric e^+e^- collider, PEP-II, at the Stanford Linear Accelerator Centre (SLAC). We use analysis-26 (release 16.1.5) to analyze Run1-4 data and SP5/SP6 MC.
In the following event selection, we used the uncertainty on signal to optimize our cuts. Since we apply D mass sideband subtraction to reduce combinatorial and continuum backgrounds, we need to consider signal yields and background yields at the D mass peak and in the D mass sideband. We denote those as S_p, B_p, S_s and B_s. The total yield at the peak, N_p, and in the sideband, N_s, are given by the sum of signal and background yields

$$\begin{aligned} N_p &= S_p + B_p \\ N_s &= S_s + B_s \end{aligned} \tag{8}$$

B_p can be the sum of a peaking background $(B_p)_{\rm peak}$ and a non-peaking background $(B_p)_{\rm non-peak}$

$$B_p = (B_p)_{\rm peak} + (B_p)_{\rm non-peak} \tag{9}$$

B_s is, in good approximation,

$$B_s = (B_p)_{\rm non-peak} \tag{10}$$

Thus,

$$B_p = (B_p)_{\rm peak} + B_s \qquad \Rightarrow \qquad (B_p)_{\rm peak} = B_p - B_s \tag{11}$$

The signal yield, S, after sideband subtraction is

$$S = N_p - N_s - (B_p)_{\rm peak} = (S_p + B_p) - (S_s + B_s) - (B_p - B_s) = S_p - S_s \tag{12}$$

and its variance is

$$\sigma_S^2 = N_p + N_s + \sigma^2_{\rm peaking} = S_p + B_p + S_s + B_s + \sigma^2_{\rm peaking} \tag{13}$$

where $\sigma_{\rm peaking}$ is the uncertainty of peaking background. Therefore, the uncertainty on signal is given by

$$\frac{\sigma_S}{S} = \frac{\sqrt{S_p + B_p + S_s + B_s + \sigma^2_{\rm peaking}}}{S_p - S_s} \tag{14}$$

Supposing σ_{peaking} is proportional to the yield of peaking background $(B_p)_{\text{peak}}$,

$$\sigma_{\text{peaking}} = \rho \cdot (B_p)_{\text{peak}} \tag{15}$$

where ρ is the coefficient. Then,

$$\frac{\sigma_S}{S} = \frac{\sqrt{S_p + B_p + S_s + B_s + [\rho \cdot (B_p)_{\text{peak}}]^2}}{S_p - S_s} \tag{16}$$

In the following optimization, we set $\rho = 0$. Thus,

$$\frac{\sigma_S}{S} = \frac{\sqrt{S_p + B_p + S_s + B_s}}{S_p - S_s} \tag{17}$$

We use 30fb^{-1} of Run3 MC to study the effect of the following cuts.

3.1 BToDlnu skim

First, the collected data is precessed to select only $B \to D^{(*)}\ell\nu$ events. This process is done by BaBar collaboration and the produced data set is called BToDlnu skim. In this subsection, we summarize the selection criteria of BToDlnu skim. See also Appendix C.

3.1.1 Reconstruction of D^0 and D^+

D^0 is reconstructed by the following 4 modes:

- $D^0 \to K^-\pi^+$
- $D^0 \to K^-\pi^+\pi^+\pi^-$
- $D^0 \to K^-\pi^+\pi^+\pi^0$
- $D^0 \to \bar{K}^0\pi^+\pi^-$

D^+ is reconstructed by the following 2 modes:

- $D^+ \to K^-\pi^+\pi^+$
- $D^+ \to \bar{K}^0\pi^+$

For K^-, GoodTracksLoose (GTL) is used to reconstruct D^0, but KLHNotPion is used to reconstruct D^+. We apply the same KLHNotPion to D^0 as described in subsection 3.3.
We use only $D^0 \to K^-\pi^+$ mode and $D^+ \to K^-\pi^+\pi^-$ mode as described in subsection 3.2.
D^* is also reconstructed in the BToDlnu skim, but we do not use the reconstructed D^* in our analysis because we do not want to rely on the reconstruction of D^*, which has problems in reconstruction of soft pions from D^* decay.

3.1.2 Reconstruction of Dl candidates

Electrons and muons are are selected by PID selectors.

- PidLHElectron selector for electrons
- muMicroTight selector for muons

are used in the BToDlnu skims. These leptons are combined with D^0 or D^+ to form Dl candidates. Since neutrinos cannot be detected, we cannot reconstruct B mesons. These Dl candidates are the candidates of B mesons. Only one true Dl-pair can be produced from one B meson. However, tens of Dl candidates are usually reconstructed in a event.
The following cuts are also applied

- Lepton momentum cut
  $0.8 < p^* < 3.0$ GeV, where p^* is the lepton momentum in the $\Upsilon(4S)$ rest frame.
- Lepton and kaon charge correlation cut
  The kaon and lepton from the same B meson must have the same sign of charge. See Appendix A.

3.2 Radiative Bhabha veto

We apply radiative Bhabha veto as follows:

- Define the following variables
  $nTrk$ = number of GoodTracksLoose
  $nGam$ = number of CalorNeutral with $E_\gamma > 80$ MeV

$nConv$ = number of identified $\gamma \to e^+e^-$ pairs
= number of gammaConversionDefault
$nTrk2 = nTrk - 2 \cdot nConv$
$nGam2 = nGam + nConv$
$mult2 = nTrk2 + \frac{nGam2}{2}$

- The Radiative Bhabha veto then requires
  $nTrk \geq 4$ and $mult2 \geq 5$

Figure 1 and 2 are the D^0 mass plots before and after Bhabha veto, corresponding to four D^0 reconstruction modes. From top to bottom, $D^0 \to K^-\pi^+$, $D^0 \to K^-\pi^+\pi^+\pi^-$, $D^0 \to K^-\pi^+\pi^0$, $D^0 \to \bar{K}^0\pi^+$. Figure 3 and 4 are the D^+ mass plots before and after Bhabha veto, corresponding to two D^+ reconstruction modes. From top to bottom, $D^+ \to K^-\pi^+\pi^+$ and $D^+ \to \bar{K}^0\pi^+$. In these plots, star is the On Peak data, green is the B^+B^- MC, yellow is the $B^0\bar{B}^0$ MC, blue is the Off Peak data, magenta is the $c\bar{c}$ MC, cyan is the uds MC, and grey is the $\tau^+\tau^-$ MC. From these plots, we can observe

- Use $D^0 \to K^-\pi^+$ and $D^+ \to K^-\pi^+\pi^+$ modes.
  Only $D^0 \to K^-\pi^+$ and $D^+ \to K^-\pi^+\pi^+$ modes show a clear D mass peak. Thus, we decide to use these modes in our analysis.

- Better data MC agreement.
  After Bhabha veto, data MC agreement is much better in $D^0 \to K^-\pi^+$ mode, and slightly better in $D^+ \to K^-\pi^+\pi^+$ mode.

- Good agreement between Off Peak data and continuum MC.
  In the $D^0 \to K^-\pi^+$ and $D^+ \to K^-\pi^+\pi^+$ modes, Off Peak data and continuum MC (sum of $c\bar{c}$, uds and $\tau^+\tau^-$ MC) agree well. Hence, we use continuum MC in our analysis to enjoy the benefit of larger statistics.

As a matter of fact, if we first apply the remaining event selections described in the following subsections, then almost all radiative Bhabha events are cut out by those selections. And, the effect of radiative Bhabha veto becomes almost negligible. However, as radiative Bhabha veto significantly reduce the size of data, we first apply this cut.
In Figure 4, Data and MC does not agree well even in $D^+ \to K^-\pi^+\pi^+$ mode, but the agreement improves after the remaining selections.

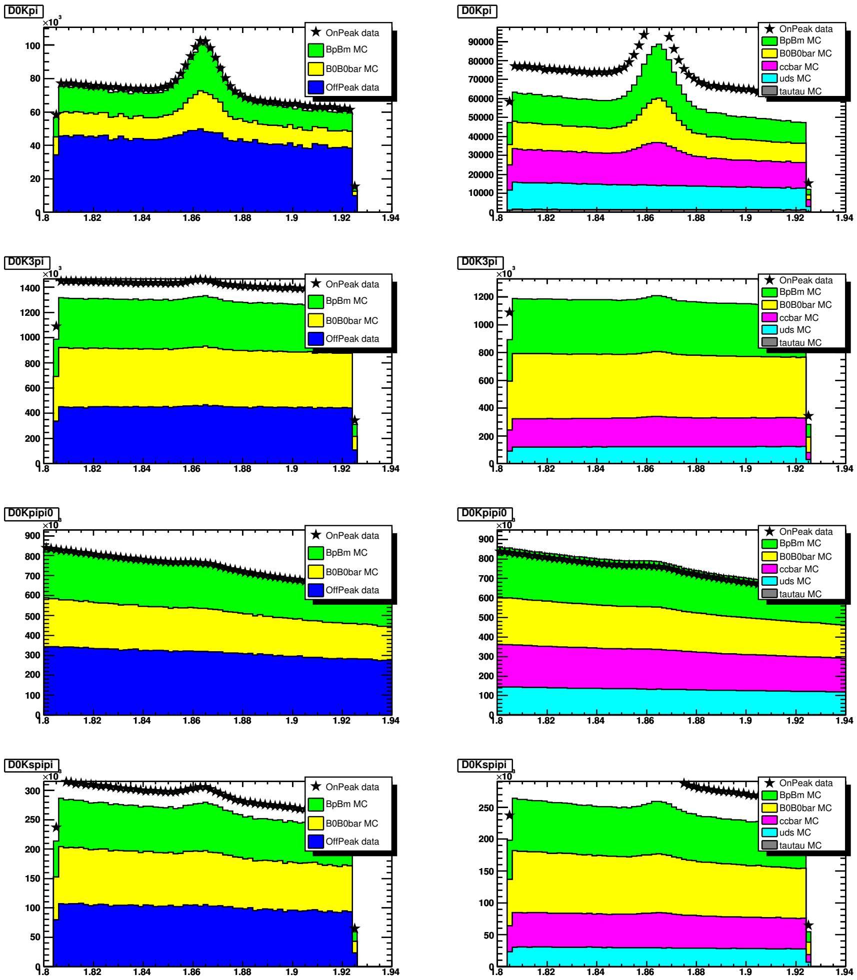

Figure 1: D^0 mass plot before applying Bhabha veto. From top to bottom, $D^0 \to K^-\pi^+$, $D^0 \to K^-\pi^+\pi^+\pi^-$, $D^0 \to K^-\pi^+\pi^0$, $D^0 \to \bar{K}^0\pi^+$. Star is the On Peak data, green is the B^+B^- MC, yellow is the $B^0\bar{B}^0$ MC, blue is the Off Peak data, magenta is the $c\bar{c}$ MC, cyan is the uds MC, and grey is the $\tau^+\tau^-$ MC.

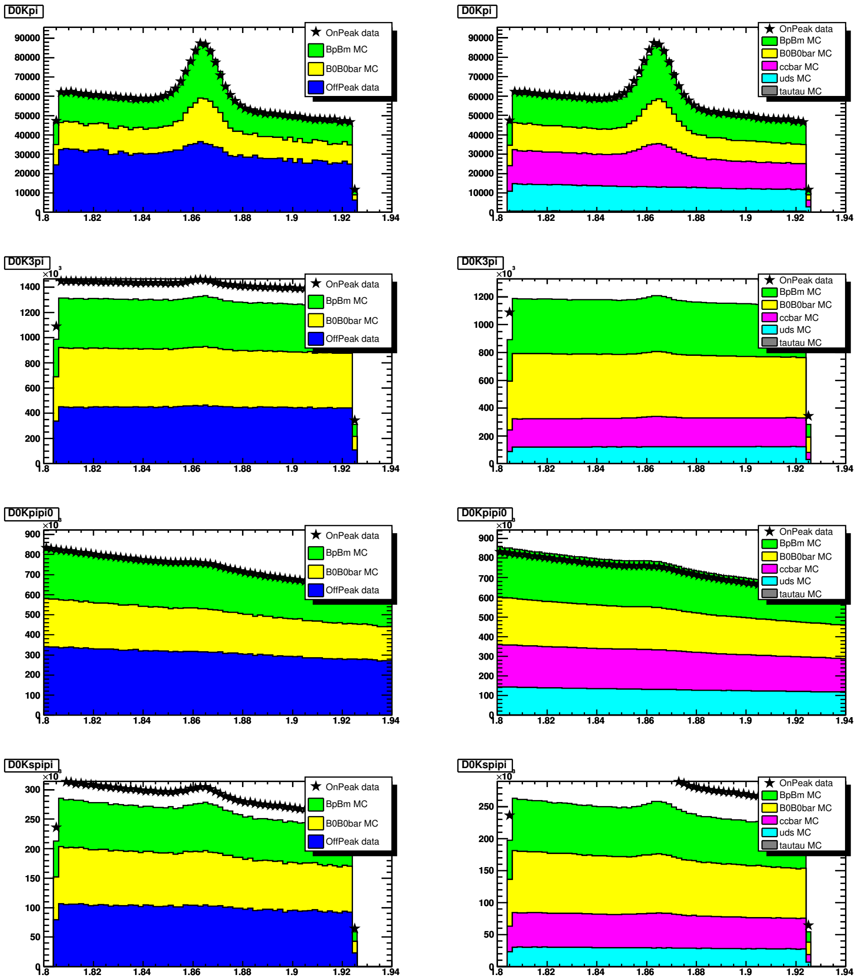

Figure 2: D^0 mass plot after applying Bhabha veto. From top to bottom, $D^0 \to K^-\pi^+$, $D^0 \to K^-\pi^+\pi^+\pi^-$, $D^0 \to K^-\pi^+\pi^0$, $D^0 \to \bar{K}^0\pi^+$. Star is the On Peak data, green is the B^+B^- MC, yellow is the $B^0\bar{B}^0$ MC, blue is the Off Peak data, magenta is the $c\bar{c}$ MC, cyan is the uds MC, and grey is the $\tau^+\tau^-$ MC.

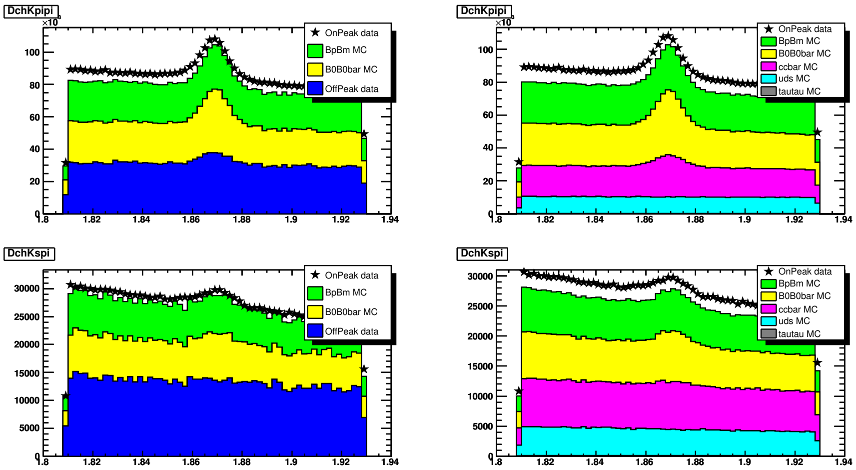

Figure 3: D^+ mass plot before applying Bhabha veto. From top to bottom, $D^+ \to K^-\pi^+\pi^+$ and $D^+ \to \bar{K}^0\pi^+$. Star is the On Peak data, green is the B^+B^- MC, yellow is the $B^0\bar{B}^0$ MC, blue is the Off Peak data, magenta is the $c\bar{c}$ MC, cyan is the uds MC, and grey is the $\tau^+\tau^-$ MC.

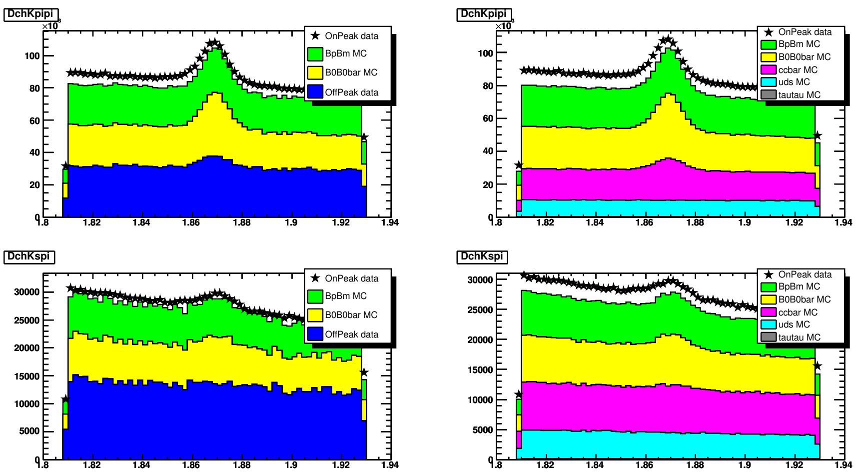

Figure 4: D^+ mass plot after applying Bhabha veto. From top to bottom, $D^+ \to K^-\pi^+\pi^+$ and $D^+ \to \bar{K}^0\pi^+$. Star is the On Peak data, green is the B^+B^- MC, yellow is the $B^0\bar{B}^0$ MC, blue is the Off Peak data, magenta is the $c\bar{c}$ MC, cyan is the uds MC, and grey is the $\tau^+\tau^-$ MC.

D^0	Before KLHNotPion	After KLHNotPion
S_p	141247	132576
S_s	7103	4767
B_p	1179211	695544
B_s	1097176	615404
$\frac{\sigma_S}{S}$	0.0116	0.0094

Table 5: Signal and background yield and the uncertainty on signal in both before and after KLHNotPion

3.3 Kaon Selection

In BToDlnu skim, for K^-, GoodTracksLoose (GTL) is used to reconstruct D^0, but KLHNotPion is used to reconstruct D^+. We apply KLHNotPion to D^0 reconstruction as well to reduce kaon misidentification. Signal and background yield and the uncertainty on signal in both before and after KLHNotPion are given in Table 5. We can reduce the uncertainty on signal by 19 %, keeping 94 % of signal events (candidates).

3.4 Vertexing

No vertexing is done in BToDlnu skim, hence, we apply TreeFitter to D vertex and B vertex. By B vertex, we mean the vertex of Dl combination. We cut on the probability value, $P(\chi^2, dof)$, calculated by the χ^2 and the number of degrees of freedom (dof) of the vertex fitting. Table 6 shows the uncertainty on signal with variety of $P(\chi^2, dof)$ of D and B vertexing. The optimum cut is

$$P^D(\chi^2, dof) > 0.01, \quad P^B(\chi^2, dof) > 0.01, \tag{18}$$

3.5 Thrust cut

$B\bar{B}$ events are isotropic and other $q\bar{q}$ events tend to go back to back in the $\Upsilon(4S)$ rest frame. This is because the mass difference between $\Upsilon(4S)$ and, for example, $D\bar{D}$-pair is big and produced D mesons carry rather large

D^0	$P^D(\chi^2, dof) > 0.1$	0.01	0.001	0.0001
$P^B(\chi^2, dof) > 0.1$			0.006220	
0.01	0.006357	0.006169	0.006165	0.006165
0.001		0.006232	0.006236	0.006240
0.0001			0.006283	

D^+	$P^D(\chi^2, dof) > 0.1$	0.01	0.001	0.0001
$P^B(\chi^2, dof) > 0.1$			0.012825	
0.01		0.012979	0.012997	0.012997
0.001		0.013133	0.013238	0.013260
0.0001			0.013349	

Table 6: The change in the uncertainty on signal with variety of $P(\chi^2, dof)$ of D and B vertexing.

momentum. Thus, we can separate $q\bar{q}$ events from $B\bar{B}$ events using thrust axis. We calculate thrust axis of Dl candidate and "non-Dl" particles in each event. Here, "non-Dl" particles mean all charged tracks and calorimeter energy deposits other than the ones used to reconstruct the Dl candidate. Dl is supposed to be one B in the event; thus, non-Dl should be the other B in the event. We then calculate $|\cos\theta_{Dl-nonDl}|$, which is the cosine of the angle between thrust axis of Dl candidate and non-Dl particles. Those are shown in Figure 5, 6 and 7. Figure 5 is for D^0 case and Figure 6 is for D^+ case. Figure 7 is $B \to D^{(*,**)0}(\pi)\ell\nu$ signal only. It is almost flat for signal events but peaked at $|\cos\theta_{Dl-nonDl}| = 1$ for $q\bar{q}$ events as expected.
To optimize the cut, we calculate the uncertainty on signal by changing cuts. Table 7 show the result. Optimum point may be around $|\cos\theta_{Dl-nonDl}| < 0.86$. However, since no big difference between 0.84 and 0.88, looser cut is the best choice. We chose the cut

$$\cos\theta_{Dl-nonDl} < 0.88 \tag{19}$$

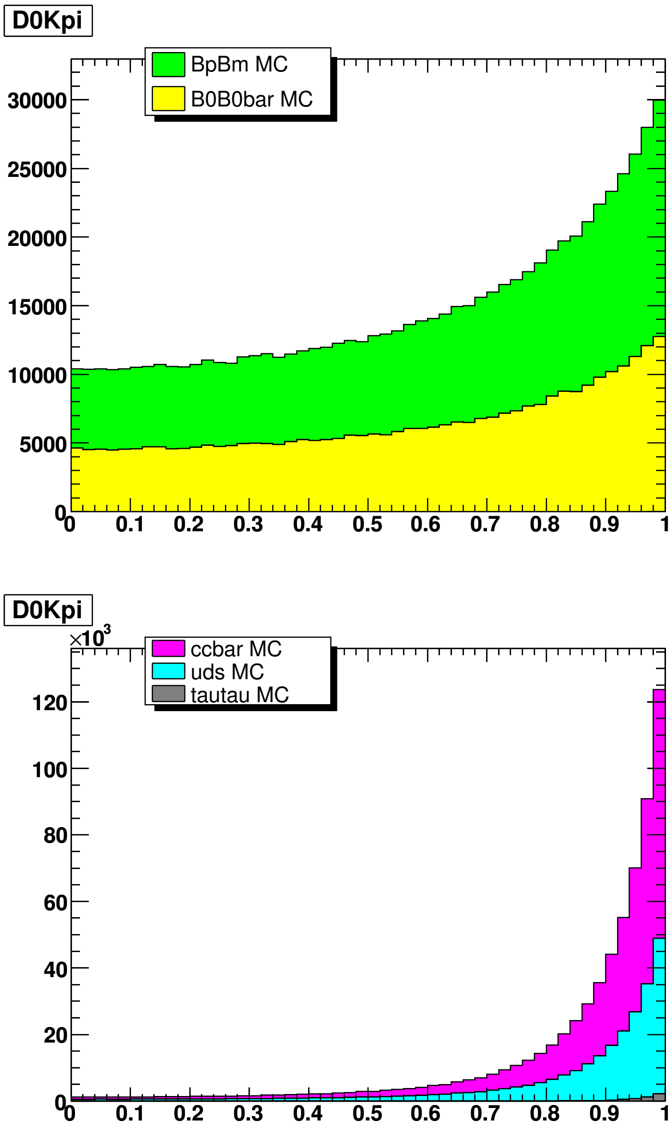

Figure 5: $|\cos\theta_{Dl-non\,Dl}|$ plot for D^0 case. Green is B^+B^-, yellow is $B^0\bar{B}^0$, magenta is $c\bar{c}$, light blue is uds and grey is $\tau^+\tau^-$.

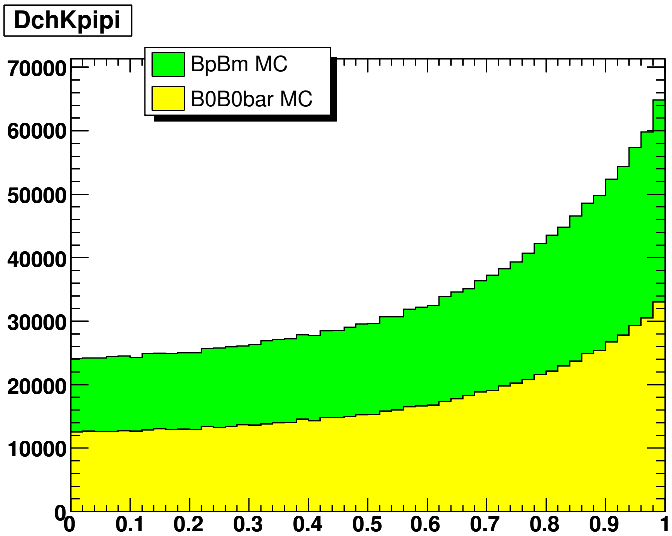

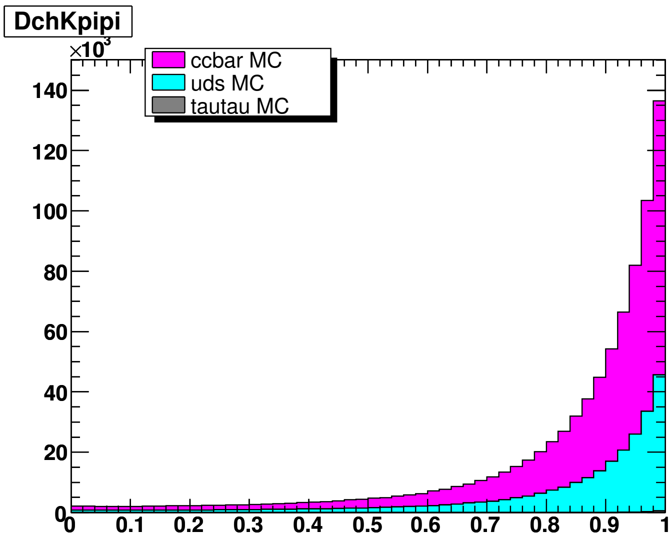

Figure 6: $|\cos\theta_{Dl-non\,Dl}|$ plot for D^+ case. Green is B^+B^-, yellow is $B^0\bar{B}^0$, magenta is $c\bar{c}$, light blue is uds and grey is $\tau^+\tau^-$.

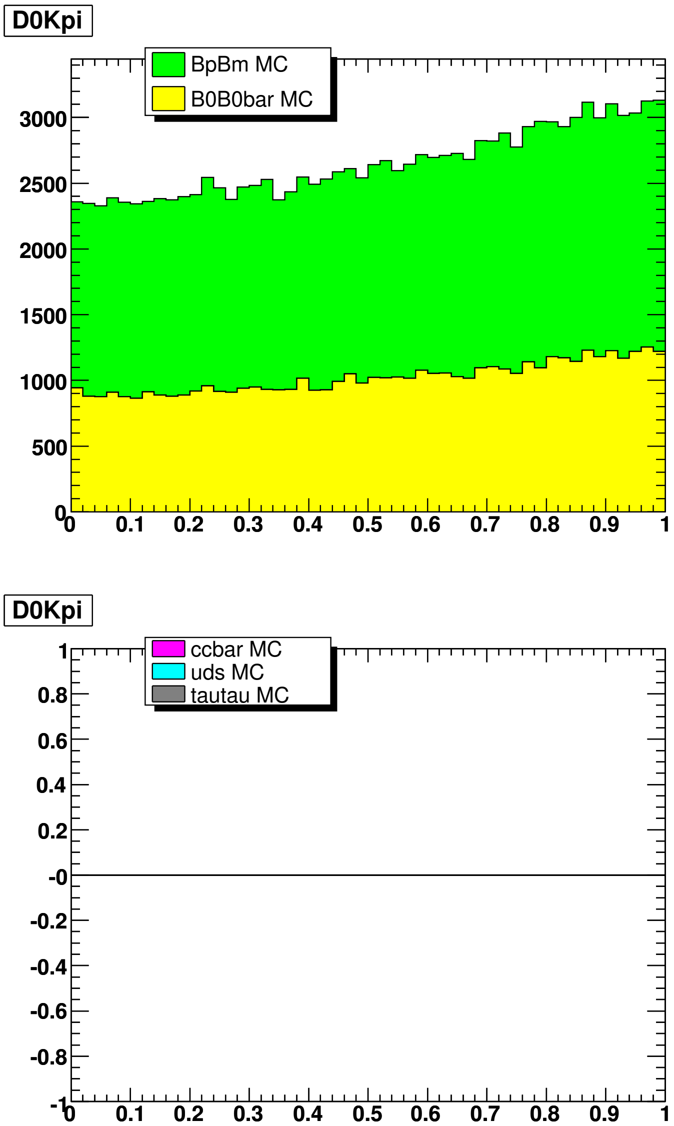

Figure 7: $|\cos\theta_{Dl-non\,Dl}|$ plot for $D \to D^{(*,**)0}(\pi)\ell\nu$ signal events. Green is B^+B^-, yellow is $B^0\bar{B}^0$. Magenta is $c\bar{c}$, light blue is uds and grey is $\tau^+\tau^-$, but no entries for these colours.

D^0	S_p	B_p	S_s	B_s	$\frac{\sigma_S}{S}$
no cut	125263	471940	3089	404153	0.0082032
$\lvert\cos\theta_{Dl-nonDl}\rvert < 0.96$	119398	381608	2932	323204	0.0078089
0.92	113723	321612	2806	269657	0.0075850
0.88	107990	278126	2671	231447	0.0074777
0.84	102236	245488	2524	202894	0.0074588
0.80	96666	219108	2391	180300	0.0074889
D^+	S_p	B_p	S_s	B_s	$\frac{\sigma_S}{S}$
no cut	75639	892051	2242	834640	0.0183024
$\lvert\cos\theta_{Dl-nonDl}\rvert < 0.96$	71978	770507	2123	721253	0.0179134
0.92	68588	680920	2007	637638	0.0177021
0.88	65277	610372	1893	571458	0.017632
0.84	61832	551900	1788	517354	0.017726
0.80	58513	502329	1673	471165	0.0178871

Table 7: The change in the uncertainty on signal with variety of $|\cos\theta_{Dl-nonDl}|$ cuts.

cuts	S_p	S_s	B_p	B_s
BToDlnu skim				
Bhabha veto				
KLHNotPion				
$P^D(\chi^2, dof) > 0.01$ $P^B(\chi^2, dof) > 0.01$				
$\lvert\cos\theta_{Dl-nonDl}\rvert < 0.88$				

Table 8: The summary of event selection cuts.

3.6 Summary of event selection cuts

The cuts we applied and the number of selected candidates after the cuts are shown in Table 8.
Figure 8 - 11 shows the D mass, lepton momentum, D momentum and $\cos\theta_{B-Dl}$ after all cuts. The excess of MC events is corrected by PID and tracking correction (see section 7). The structure at 1 GeV in the D^+ momentum plot is a statistical fluctuation or binning effect.

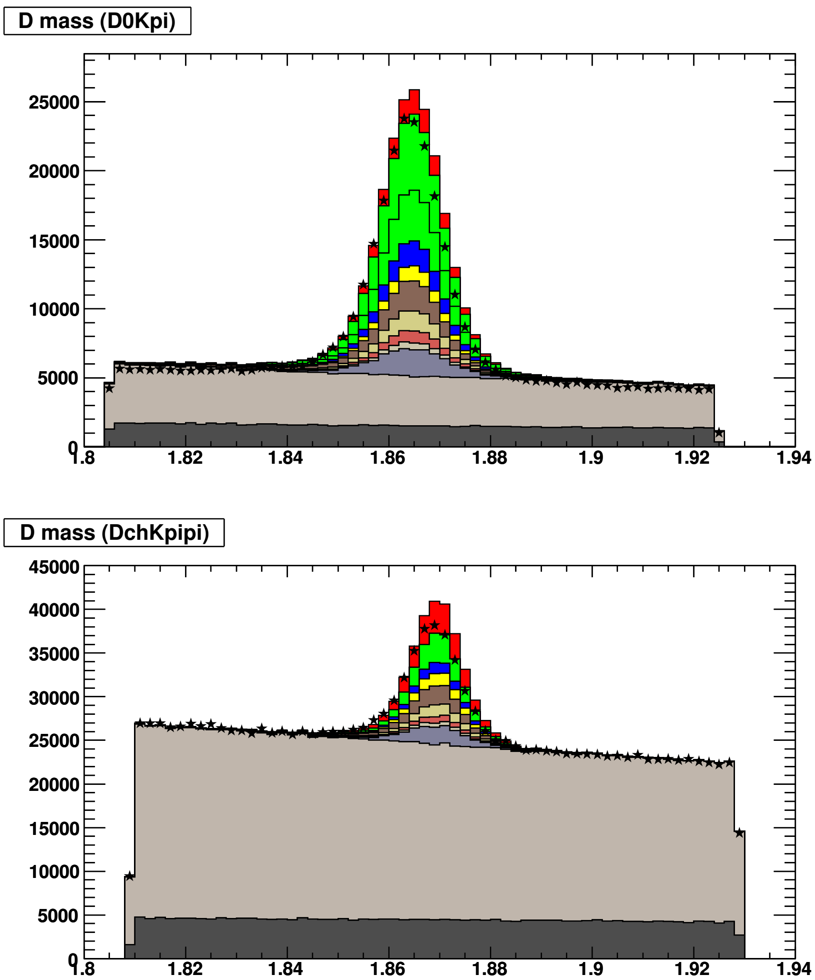

Figure 8: D mass plot after all cuts. The top is D^0 and the bottom is D^+. Red is $B \to D\ell\nu$, green is $B \to D^*\ell\nu$, blue is $B \to D^{**}\ell\nu$, yellow is non-resonant $B \to D^{(*)}\pi\ell\nu$, and the rest is background. Dark brown is DiffB, light brown is DBCascL, dark red is CascL, light grey is LMisID, blue-gray is RealD, grey is Comb, and dark grey is Cont.

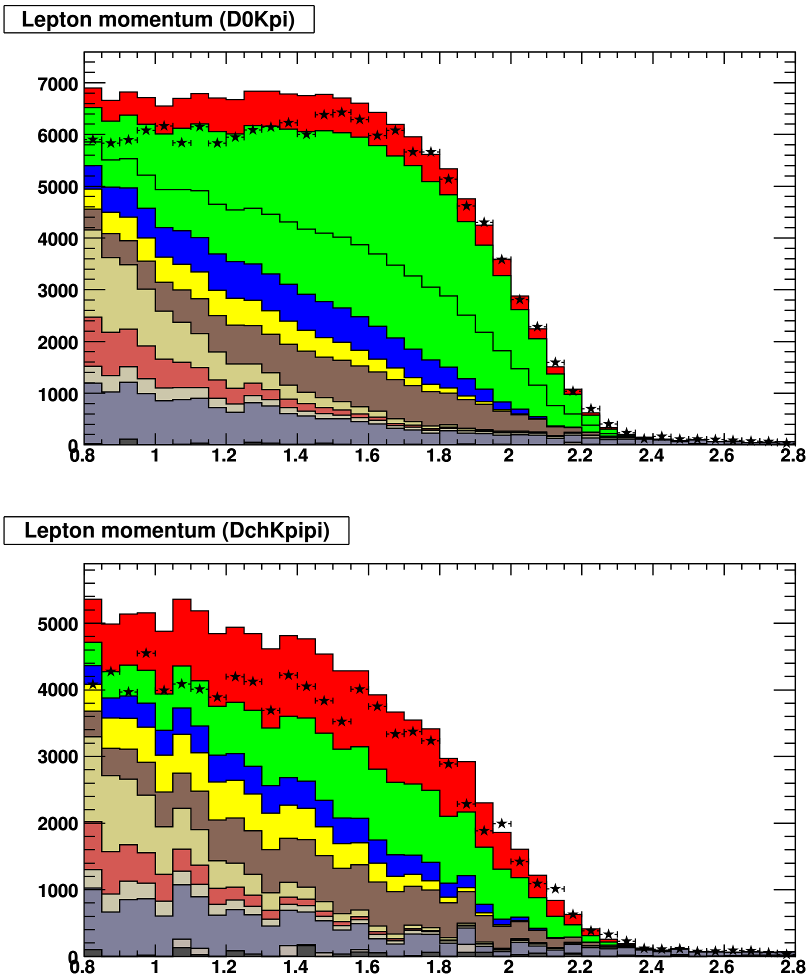

Figure 9: Lepton momentum plot after all cuts and D mass sideband subtraction. The top is D^0 and the bottom is D^+. Red is $B \to D\ell\nu$, green is $B \to D^*\ell\nu$, blue is $B \to D^{**}\ell\nu$, yellow is non-resonant $B \to D^{(*)}\pi\ell\nu$, and the rest is background. Dark brown is DiffB, light brown is DBCascL, dark red is CascL, light grey is LMisID, blue-gray is RealD, grey is Comb, and dark grey is Cont. Comb and Cont are almost disappeared after D mass sideband subtraction. Negative values are not appeared in the plot.

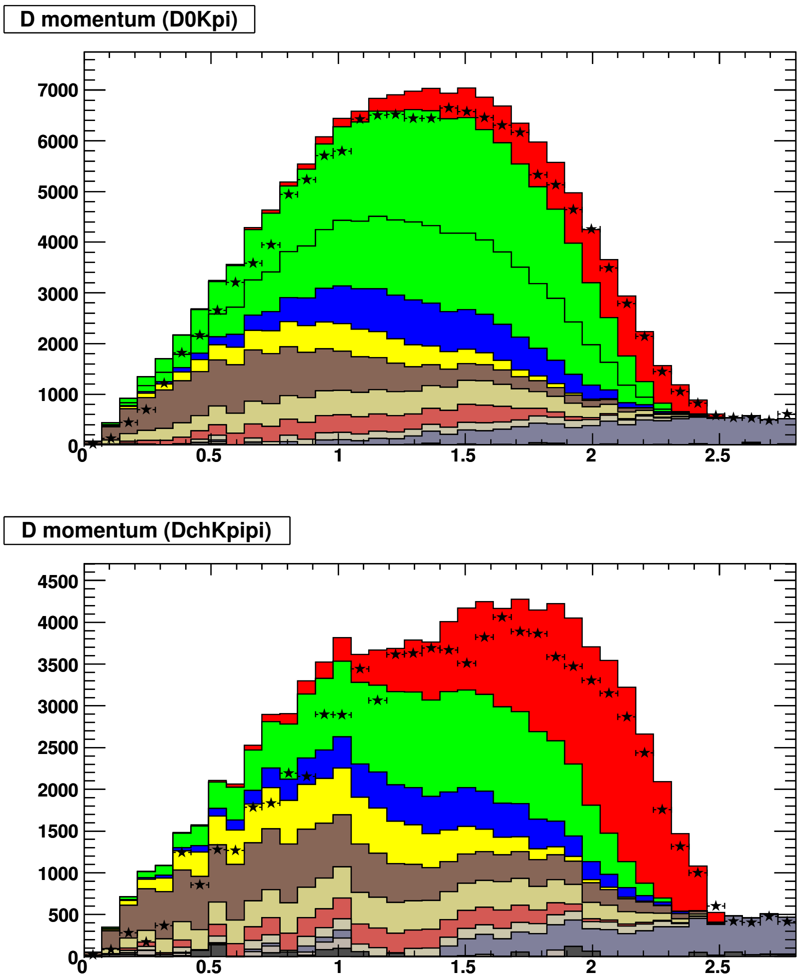

Figure 10: D momentum plot after all cuts and D mass sideband subtraction. The top is D^0 and the bottom is D^+. Red is $B \to D\ell\nu$, green is $B \to D^*\ell\nu$, blue is $B \to D^{**}\ell\nu$, yellow is non-resonant $B \to D^{(*)}\pi\ell\nu$, and the rest is background. Dark brown is DiffB, light brown is DBCascL, dark red is CascL, light grey is LMisID, blue-gray is RealD, grey is Comb, and dark grey is Cont. Comb and Cont are almost disappeared after D mass sideband subtraction. Negative values are not appeared in the plot.

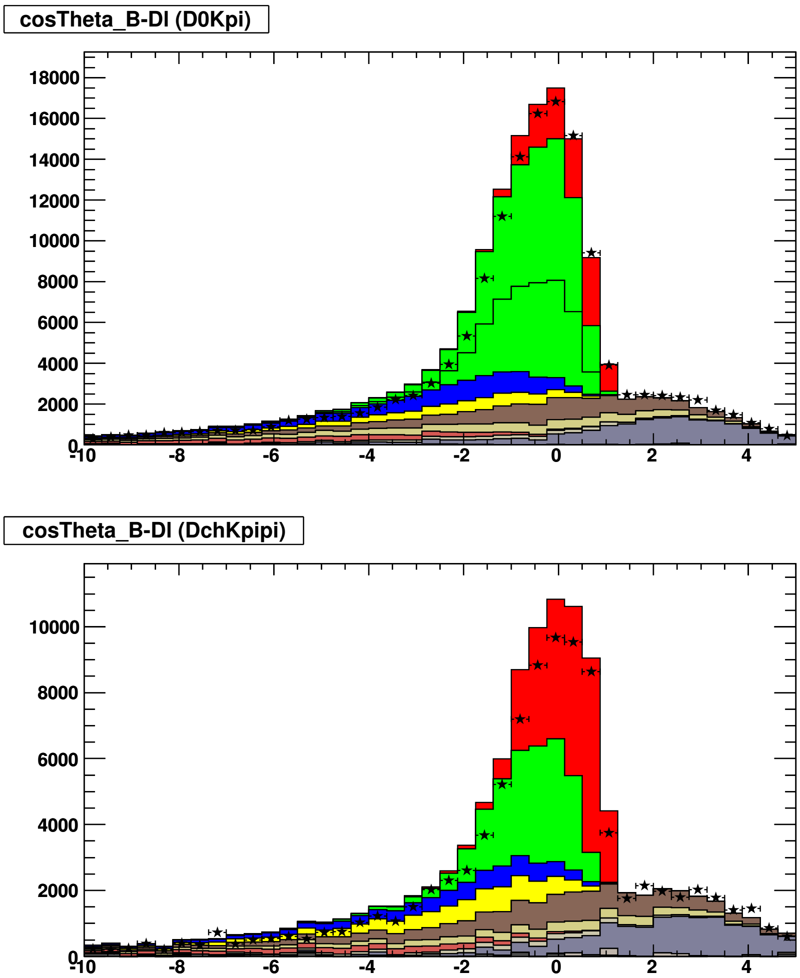

Figure 11: $\cos\theta_{B-Dl}$ plot after all cuts and D mass sideband subtraction. The top is D^0 and the bottom is D^+. Red is $B \to D\ell\nu$, green is $B \to D^*\ell\nu$, blue is $B \to D^{**}\ell\nu$, yellow is non-resonant $B \to D^{(*)}\pi\ell\nu$, and the rest is background. Dark brown is DiffB, light brown is DBCascL, dark red is CascL, light grey is LMisID, blue-gray is RealD, grey is Comb, and dark grey is Cont. Comb and Cont are almost disappeared after D mass sideband subtraction. Negative values are not appeared in the plot.

4 Fitting Method

We use binned χ^2 fitting.

4.1 Binning (i)

We use 3D binning by three variables :

- lepton momentum in the CM frame p^*_ℓ
- D momentum in the CM frame p^*_D
- $\cos\theta_{B-Dl}$ (see Appendix F)

In the $B \to D\ell\nu$ decays, there are only three independent kinematic variables. For example, in Figure 12, supposing D^* is D and does not decay, independent variables can be

- The magnitude of lepton momentum
- The magnitude of D momentum
- The angle θ_ℓ

because χ and θ_V are irrelevant. We chose three variables, p^*_ℓ, p^*_D and $\cos\theta_{B-Dl}$, because this combination is most efficient and simple to separate each signal decay modes and backgrounds. As we can see from Figures 9-11, the shape of each MC mode is quite different. Especially, $\cos\theta_{B-Dl}$ and p^*_D have a significant separation power.
The actual binning we used is

- p^*_ℓ (4 bins (GeV)) : 0.8, 1.2, 1.6, 2.0, 2.4
- p^*_D (6 bins (GeV)) : 0.2, 0.6, 1.0, 1.4, 1.8, 2.2, 2.6
- $\cos\theta_{B-Dl}$ (5 bins) : -10, -2.5, -1.1, 0, 1.1, 5

The binning of $\cos\theta_{B-Dl}$ and p^*_D is finer than p^*_ℓ because the former two parameters have more discrimination power than the latter. We tried many different binning to optimize binning. We also tried $\cos\theta_{D-\ell}$ (the cosine of the angle between D and ℓ in the CM frame) instead of $\cos\theta_{B-Dl}$ to assure that $\cos\theta_{B-Dl}$ is a better parameter.

4.2 MC modes (j)

There are 29 D^0 MC modes and 28 D^+ MC modes as listed in section 5. See also Appendix A and section 2.

4.3 χ^2

The χ^2 is

$$\chi^2 = \sum_{i=\mathrm{bin}}^{D^0} \frac{(N_i^{data} - \sum_j C_j^{Bkgd} N_{ij}^{Bkgd} - \sum_j C_j^{Sig} N_{ij}^{Sig})^2}{(\sigma_i^{data})^2 + \sum_j (C_j^{Bkgd}\sigma_{ij}^{Bkgd})^2 + \sum_j (C_j^{Sig}\sigma_{ij}^{Sig})^2}$$
$$+ \sum_{i=\mathrm{bin}}^{D^+} \frac{(N_i^{data} - C_{+0}\sum_j C_j^{Bkgd} N_{ij}^{Bkgd} - C_{+0}\sum_j C_j^{Sig} N_{ij}^{Sig})^2}{(\sigma_i^{data})^2 + C_{+0}\sum_j (C_j^{Bkgd}\sigma_{ij}^{Bkgd})^2 + C_{+0}\sum_j (C_j^{Sig}\sigma_{ij}^{Sig})^2} \quad (20)$$

where, i represents each bin and j represents each MC mode. Quantities in the χ^2 are:

- N_i^{data}
  The number of data events or candidates in the i-th bin
- N_{ij}^{Bkgd}
  The number of j-th MC background events or candidates in the i-th bin, normalized to data luminosity. The effect of data MC differences from tracking and PID are included. Details are in section 4.4 and 4.4.3.
- C_j^{Bkgd}
  The coefficient of each MC background (j). These allow us to float each component of background in the fit. Details are in section 5.
- N_{ij}^{Sig}
  The number of j-th MC signal events or candidates in the i-th bin. The effect of data MC differences from tracking and PID are included. The effect of form factors is also included. Details are in section 4.4 and 4.4.4.
- C_j^{Sig}
  The coefficient of each MC signal mode (j). This consists of branching fractions. Details are in section 5.

- σ_i^{data}
  The statistical uncertainty of N_i^{data}. Details are in section 4.7.

- σ_{ij}^{Bkgd}
  The statistical uncertainty of N_{ij}^{Bkgd}. Details are in section 4.7.

- σ_{ij}^{Sig}
  The statistical uncertainty of N_{ij}^{Sig}. Details are in section 4.7.

- C_{+0}
  This coefficient is to account for possible MC modelling difference between D^+ and D^0 modes. We expect this to be consistent with 1.

Note that the resulting branching fractions from this fitting are relative values. We need to normalize them so that the sum of exclusive branching fractions agrees with the inclusive branching fraction. See section 4.9 for details.

4.4 Number of Events or Candidates N_{ij}

We calculate the number of events or candidates from MC using MC truth information. We use five generic MC samples: ($l =$) BpBm, B0B0bar, ccbar, uds and tautau. Tracking efficiency and PID corrections are applied to adjust MC. MCs are also luminosity normalized to data.

4.4.1 Tracking efficiency and PID correction

MC is modelling actual data quite well. However, tracking efficiency and PID efficiency are not completely equal in both data and MC, no matter how sophisticated the codes to reconstruct charged tracks and to identify particles are. Tracking efficiency and PID corrections are the corrections to account for the residual difference between data and MC. Both corrections are done in similar way.

- Tracking efficiency correction
  Tracking efficiency correction factors are given for each charged track. There are 3 charged tracks to reconstruct a $D^0 l$ candidate, and 4 charged tracks to reconstruct a $D^+ l$ candidate. We multiply those correction factors of charged tracks to get r_k^{Trk} for each candidate (k).

- PID correction
  PID correction factors (called weights) are given one for each PID selector. Thus, we have one for lepton (PidLHElectron for electrons and muMicroTight for muons) and another for kaon (KLHNotPion). We multiply these two weights to get r_k^{PID} for each candidate (k).

The effect of these corrections is shown in the section 7.1

4.4.2 Luminosity normalization

All MC are normalized to data by luminosity. Supposing data luminosity is $\mathcal{L}^{data}$ and MC (sample l) luminosity is $\mathcal{L}_l^{MC}$, the normalization factor r_l^{Lumi} is given by

$$r_l^{Lumi} = \frac{\mathcal{L}^{data}}{\mathcal{L}_l^{MC}} \tag{21}$$

where the luminosity of MC is calculated by the generated number of events and its cross section. Details are in Appendix C.

4.4.3 Background MC N_{ij}^{Bkgd}

The number of background events or candidates N_{ij}^{Bkgd} is given by

$$N_{ij}^{Bkgd} = \sum_l \left(r_l^{Lumi} \sum_k r_k^{Trk} r_k^{PID} W_{jk}^{Bkgd} \right) \tag{22}$$

The sum over k is taken in each MC sample (l), in each MC mode (j) and in each bin (i). W_{jk}^{Bkgd} is the branching fraction weight described in section 4.5. These weights are calculated candidate by candidate (k) in each decay mode (j).

4.4.4 Signal MC N_{ij}^{Sig}

The number of signal events or candidates N_{ij}^{Sig} is given by

$$N_{ij}^{MC} = \sum_l \left(r_l^{Lumi} \sum_k r_k^{Trk} r_k^{PID} W_{ijk}^{Sig} \right) \tag{23}$$

The sum over k is taken in each MC sample (l), in each MC mode (j), and in each bin (i). W^{Sig}_{ijk} is the form factor weight described in section 6. These weights are calculated candidate by candidate (k) in each decay mode (j) and depend on i.

4.5 Branching fraction weight W^{Bkgd}_{jk}

Recent measurements of $D \to K^{(*)} e\nu$ decay branching fractions are quite different from the ones used in our MC. In SP5/SP6 MC the following branching fractions are used

$$\begin{aligned} \mathcal{B}(D^+ \to \bar{K}^0 e\nu) &= 0.0670 \\ \mathcal{B}(D^+ \to \bar{K}^{*0} e\nu) &= 0.0480 \end{aligned} \tag{24}$$

and the sum of all semileptonic modes is

$$\mathcal{B}(D^+ \to X e\nu) = 0.1372 \tag{25}$$

The most recent results from CLEO-c [18][19] are

$$\begin{aligned} \mathcal{B}(D^+ \to \bar{K}^0 e\nu) &= 0.0871 \pm 0.0038 \pm 0.0037 = 0.0871 \pm 0.0053 \\ \mathcal{B}(D^+ \to \bar{K}^{*0} e\nu) &= 0.0556 \pm 0.0027 \pm 0.0023 = 0.0556 \pm 0.00354 \\ \mathcal{B}(D^+ \to X e\nu) &= 0.1613 \pm 0.0020 \pm 0.0033 \end{aligned} \tag{26}$$

Thus, we need to correct or re-weight our MC. This weight affect only on DBCascL, CascL and RealD backgrounds. For example, in the case of

- $B^+ \to D^{*-} D^+ K^+$
  with $D^{*-} \to \bar{D}^0 \pi^-$ and $D^+ \to \bar{K}^0 e^+ \nu$
  and these $\bar{D}^0$ and e^+ form a Dl candidate as if $B^+ \to \bar{D}^0 e^+ \nu$

The number of this background is given by

$$\begin{aligned} &N = (\text{number of produced } B^+B^- \text{ pairs}) \times \\ &\mathcal{B}(B^+ \to D^{*-} D^+ K^+) \mathcal{B}(D^{*-} \to \bar{D}^0 \pi^-) \mathcal{B}(D^+ \to \bar{K}^0 e^+ \nu) \mathcal{B}(D^0 \to K^- \pi^+) \end{aligned} \tag{27}$$

Thus, it is proportional to $\mathcal{B}(D^+ \to \bar{K}^0 e^+ \nu)$. This means that the weight is given by the ratio of new and old branching fractions.
We apply

$$W^{Bkgd}_{jk} = \frac{0.0871}{0.0670} = 1.30 \tag{28}$$

for candidates (k) which electron come from $D^+ \to \bar{K}^0 e\nu$ decay, and

$$W_{jk}^{Bkgd} = \frac{0.0556}{0.0480} = 1.16 \tag{29}$$

for candidates (k) which electron come from $D^+ \to \bar{K}^{*0} e\nu$ decay.
When some of branching fractions are increased, some of other branching fractions of D^+ must be decreased to keep the sum of all branching fraction being 1. As measurement of inclusive $\mathcal{B}(D^+ \to Xe\nu)$ increased accordingly, we need to decrease something other than $D^+ \to Xe\nu$ type of decays. $D^+ \to X\mu\nu$ type of decay branching fractions are well measured and cannot be changed. The change in $\mathcal{B}(B^+ \to K^-\pi^+\pi^+)$ is taken care of in C_j^{Bkgd} and C_j^{Sig}. So something else must be changed. However, those something else do not affect to reconstruct Dl and have only negligible effect on our analysis.

4.6 Form factor weight W_{ijk}^{Sig}

This is described in section 6

4.7 Statistical uncertainty σ_i^{data}, σ_{ij}^{Bkgd} and σ_{ij}^{Sig}

We add statistical uncertainty quadratically. (Need justification?)

4.8 Coefficients C_j^{Bkgd} and C_j^{Sig}

This is described in section 5

4.9 Normalization

The branching fractions from the fit are relative branching fractions. We need to normalize them to agree with the inclusive branching fraction :

$$\begin{aligned} &B_{BpD} + B_{BpDS} + (B_{BpDD0} + B_{BpDD1} + B_{BpDDP1} + B_{BpDD2}) \\ &+(B_{BpDPp} + B_{BpDP0} + B_{BpDSPp} + B_{BpDSP0}) = \mathcal{B}(B^+ \to X_c \ell^+ \nu) \end{aligned} \tag{30}$$

and

$$\begin{aligned} &B_{B0D} + B_{B0DS} + (B_{B0DD0} + B_{B0DD1} + B_{B0DDP1} + B_{B0DD2}) \\ &+(B_{B0DPp} + B_{B0DP0} + B_{B0DSPp} + B_{B0DSP0}) = \mathcal{B}(B^0 \to X_c \ell^+ \nu) \end{aligned} \tag{31}$$

In SP5/SP6 the following value is used :

$$\mathcal{B}(B^+ \to X_c\ell\nu) = \mathcal{B}(B^0 \to X_c\ell\nu) = 0.104 \tag{32}$$

From PDG [10]

$$\begin{aligned} \mathcal{B}(B \to X_u\ell\nu) &= 0.1081 \pm 0.0014 \\ \mathcal{B}(B \to X\ell\nu) &= 0.00233 \pm 0.00022 \end{aligned} \tag{33}$$

Thus,

$$\begin{aligned} \mathcal{B}(B \to X_c\ell\nu) &= (0.1081 \pm 0.0014) - (0.00233 \pm 0.00022) \\ &= 0.10577 \pm 0.001417 \end{aligned} \tag{34}$$

Combining this with lifetime ratio [10]

$$t_{+0} \equiv \frac{\tau_{B^+}}{\tau_{B^0}} = 1.071 \pm 0.009 \tag{35}$$

we can calculate B^+ and B^0 separately. By assuming B^+ and B^0 contributions are equal,

$$\mathcal{B}(B^+ \to \bar{X}_c^0\ell^+\nu) + \mathcal{B}(B^0 \to X_c^-\ell^+\nu) = 2\mathcal{B}(B \to X_c\ell\nu) \tag{36}$$

From isospin symmetry

$$\mathcal{B}(B^+ \to \bar{X}_c^0\ell^+\nu) = t_{+0}\mathcal{B}(B^0 \to X_c^-\ell^+\nu) \tag{37}$$

Thus

$$\mathcal{B}(B^+ \to \bar{X}_c^0\ell^+\nu) = \frac{2t_{+0}}{1+t_{+0}}\mathcal{B}(B \to X_c\ell\nu) = 0.1094 \pm 0.0018 \tag{38}$$

and

$$\mathcal{B}(B^+ \to \bar{X}_c^0\ell^+\nu) = \frac{2}{1+t_{+0}}\mathcal{B}(B \to X_c\ell\nu) = 0.1021 \pm 0.0014 \tag{39}$$

We use these values in our fit.

5 Coefficients in the fitting

5.1 Number of produced B

Branching fractions of B^+B^- and $B^0\bar{B}^0$ of $\Upsilon(4S)$ resonance are denoted by

$$
\begin{aligned}
f_{+-} &= \mathcal{B}(\Upsilon(4S) \to B^+B^-) \\
f_{00} &= \mathcal{B}(\Upsilon(4S) \to B^0\bar{B}^0)
\end{aligned}
\tag{40}
$$

In the first approximation, $f_{+-} = f_{00} = 0.5$. We define the ratio of these two branching fractions

$$f_{+0} \equiv \frac{f_{+-}}{f_{00}} \tag{41}$$

Supposing N of $B\bar{B}$-pairs are produced, the number of produced B for neutral B modes is

$$N_{neut}^{prod} = 2f_{00}N \tag{42}$$

and for charged B modes

$$N_{chrg}^{prod} = 2f_{+-}N = f_{+0}N_{neut}^{prod} \tag{43}$$

In SP5/SP6 MC

$$f_{+0}^{SP6} = 1 \tag{44}$$

is used.

5.2 D^0 MC modes

5.2.1 Coefficients for signals C_j^{Sig}

There are 15 signal MC modes (j). The coefficient of each mode is given by taking ratio between new and old branching fraction factors, F_j and F_j^{SP6} as explained below.

$$C_j^{Sig} = \frac{F_j}{F_j^{SP6}} \tag{45}$$

The branching fraction factors are

- $j = 15 : B^+ \to \bar{D}^0\ell^+\nu$
  Number of produced events are

$$N_{15} = N_{chrg}^{prod} B_{BpD} B_{D^0} = N_{neut}^{prod} f_{+0} B_{BpD} B_{D^0} \tag{46}$$

As N_{neut}^{prod} is common, it will be cancelled by taking a ratio. Thus, the branching fraction factor is

$$F_{15} = f_{+0} B_{BpD} B_{D^0} \tag{47}$$

The coefficient is given by taking ratio with SP5/SP6 values

$$C_{15} = \frac{f_{+0} B_{BpD} B_{D^0}}{f_{+0}^{SP6} B_{BpD}^{SP6} B_{D^0}^{SP6}} \tag{48}$$

- $j = 16 : \; B^+ \to \bar{D}^{*0} \ell^+ \nu$
  The decays contribute to this mode are
  $B^+ \to \bar{D}^{*0} \ell^+ \nu$ with $\bar{D}^{*0} \to \bar{D}^0 + \gamma/\pi^0$
  The branching fraction factor is

$$\begin{aligned} F_{16} &= f_{+0} B_{BpDS} (B_{DS0DP0} + B_{DS0DG}) B_{D^0} \\ &= f_{+0} B_{BpDS} B_{D^0} \end{aligned} \tag{49}$$

- $j = 17 : \; B^0 \to D^{*-} \ell^+ \nu$
  The decays contribute to this mode are
  $B^0 \to D^{*-} \ell^+ \nu$ with $D^{*-} \to \bar{D}^0 \pi^-$
  The branching fraction factor is

$$F_{17} = B_{B0DS} B_{DSpDPp} B_{D^0} \tag{50}$$

- $j = 18 : \; B^+ \to \bar{D}_0^{*0} \ell^+ \nu$
  The decays contribute to this mode are
  $B^+ \to \bar{D}_0^{*0} \ell^+ \nu$ with $\bar{D}_0^{*0} \to \bar{D}^0 \pi^0$
  The branching fraction factor is

$$F_{18} = f_{+0} B_{BpDD0} B_{DD00DP0} B_{D^0} \tag{51}$$

- $j = 19 : \; B^0 \to D_0^{*-} \ell^+ \nu$
  The decays contribute to this mode are
  $B^0 \to D_0^{*-} \ell^+ \nu$ with $D_0^{**-} \to \bar{D}^0 \pi^-$
  The branching fraction factor is

$$F_{19} = B_{B0DD0} B_{DD0pDPp} B_{D^0} \tag{52}$$

- $j = 20:\ B^+ \to \bar{D}_1^0 \ell^+ \nu$
  The decays contribute to this mode are
  $B^+ \to \bar{D}_1^0 \ell^+ \nu$ with $\bar{D}_1^0 \to D^{*-}\pi^+$ and $D^{*-} \to \bar{D}^0\pi^-$
  $B^+ \to \bar{D}_1^0 \ell^+ \nu$ with $\bar{D}_1^0 \to \bar{D}^{*0}\pi^0$ and $\bar{D}^{*0} \to \bar{D}^0 + \gamma/\pi^0$
  The branching fraction factor is

$$\begin{aligned}
&F_{20} = f_{+0} B_{BpDD1} B_{DD10DSPp} B_{DSpDPp} B_{D^0} \\
&+ f_{+0} B_{BpDD1} B_{DD10DSP0} (B_{DS0DP0} + B_{DS0DG}) B_{D^0} \\
&= f_{+0} B_{BpDD1} (B_{DD10DSPp} B_{DSpDPp} + B_{DD10DSP0}) B_{D^0}
\end{aligned} \tag{53}$$

- $j = 21:\ B^0 \to D_1^- \ell^+ \nu$
  The decays contribute to this mode are
  $B^0 \to D_1^- \ell^+ \nu$ with $D_1^- \to D^{*-}\pi^0$ and $D^{*-} \to \bar{D}^0\pi^-$
  $B^0 \to D_1^- \ell^+ \nu$ with $D_1^- \to \bar{D}^{*0}\pi^-$ and $\bar{D}^{*0} \to \bar{D}^0 + \gamma/\pi^0$
  The branching fraction factor is

$$\begin{aligned}
&F_{21} = B_{B0DD1} B_{DD1pDSP0} B_{DSpDPp} B_{D^0} \\
&+ B_{B0DD1} B_{DD1pDSPp} (B_{DS0DP0} + B_{DS0DG}) B_{D^0} \\
&= B_{B0DD1} (B_{DD1pDSP0} B_{DSpDPp} + B_{DD1pDSPp}) B_{D^0}
\end{aligned} \tag{54}$$

- $j = 22:\ B^+ \to \bar{D}_1'^0 \ell^+ \nu$
  The decays contribute to this mode are
  $B^+ \to \bar{D}_1'^0 \ell^+ \nu$ with $\bar{D}_1'^0 \to D^{*-}\pi^+$ and $D^{*-} \to \bar{D}^0\pi^-$
  $B^+ \to \bar{D}_1'^0 \ell^+ \nu$ with $\bar{D}_1'^0 \to \bar{D}^{*0}\pi^0$ and $\bar{D}^{*0} \to \bar{D}^0 + \gamma/\pi^0$
  The branching fraction factor is

$$\begin{aligned}
&F_{22} = f_{+0} B_{BpDDP1} B_{DDP10DSPp} B_{DSpDPp} B_{D^0} \\
&+ f_{+0} B_{BpDDP1} B_{DDP10DSP0} (B_{DS0DP0} + B_{DS0DG}) B_{D^0} \\
&= f_{+0} B_{BpDDP1} (B_{DDP10DSPp} B_{DSpDPp} + B_{DDP10DSP0}) B_{D^0}
\end{aligned} \tag{55}$$

- $j = 23:\ B^0 \to D_1'^- \ell^+ \nu$
  The decays contribute to this mode are
  $B^0 \to D_1'^- \ell^+ \nu$ with $D_1'^- \to D^{*-}\pi^0$ and $D^{*-} \to \bar{D}^0\pi^-$
  $B^0 \to D_1'^- \ell^+ \nu$ with $D_1'^- \to \bar{D}^{*0}\pi^-$ and $\bar{D}^{*0} \to \bar{D}^0 + \gamma/\pi^0$

The branching fraction factor is

$$\begin{aligned}
F_{23} &= B_{B0DDP1}B_{DDP1pDSP0}B_{DSpDPp}B_{D^0} \\
&+B_{B0DDP1}B_{DDP1pDSPp}(B_{DS0DP0}+B_{DS0DG})B_{D^0} \\
&= B_{B0DDP1}(B_{DDP1pDSP0}B_{DSpDPp}+B_{DDP1pDSPp})B_{D^0}
\end{aligned} \tag{56}$$

- $j=24:\ B^+ \to \bar{D}_2^{*0}\ell^+\nu$
  The decays contribute to this mode are
  $B^+ \to \bar{D}_2^{*0}\ell^+\nu$ with $\bar{D}_2^{*0} \to D^{*-}\pi^+$ and $D^{*-} \to \bar{D}^0\pi^-$
  $B^+ \to \bar{D}_2^{*0}\ell^+\nu$ with $\bar{D}_2^{*0} \to \bar{D}^{*0}\pi^0$ and $\bar{D}^{*0} \to \bar{D}^0+\gamma/\pi^0$
  $B^+ \to \bar{D}_2^{*0}\ell^+\nu$ with $\bar{D}_2^{*0} \to \bar{D}^0\pi^0$
  The branching fraction factor is

$$\begin{aligned}
F_{24} &= f_{+0}B_{BpDD2}B_{DD20DSPp}B_{DSpDPp}B_{D^0} \\
&+f_{+0}B_{BpDD2}B_{DD20DSP0}(B_{DS0DP0}+B_{DS0DG})B_{D^0}+f_{+0}B_{BpDD2}B_{DD20DP0}B_{D^0} \\
&= f_{+0}B_{BpDD2}(B_{DD20DSPp}B_{DSpDPp}+B_{DD20DSP0}+B_{DD20DP0})B_{D^0}
\end{aligned} \tag{57}$$

- $j=25:\ B^0 \to D_2^{*-}\ell^+\nu$
  The decays contribute to this mode are
  $B^0 \to D_2^{*-}\ell^+\nu$ with $D_2^{*-} \to D^{*-}\pi^0$ and $D^{*-} \to \bar{D}^0\pi^-$
  $B^0 \to D_2^{*-}\ell^+\nu$ with $D_2^{*-} \to \bar{D}^{*0}\pi^-$ and $\bar{D}^{*0} \to \bar{D}^0+\gamma/\pi^0$
  $B^0 \to D_2^{*-}\ell^+\nu$ with $D_2^{*-} \to \bar{D}^0\pi^-$
  The branching fraction factor is

$$\begin{aligned}
F_{25} &= B_{B0DD2}B_{DD2pDSP0}B_{DSpDPp}B_{D^0} \\
&+B_{B0DD2}B_{DD2pDSPp}(B_{DS0DP0}+B_{DS0DG})B_{D^0}+B_{B0DD2}B_{DD2pDPp}B_{D^0} \\
&= B_{B0DD2}(B_{DD2pDSP0}B_{DSpDPp}+B_{DD2pDSPp}+B_{DD2pDPp})B_{D^0}
\end{aligned} \tag{58}$$

- $j=26:\ B^+ \to \bar{D}^0\pi^0\ell^+\nu$
  The branching fraction factor is

$$F_{26} = f_{+0}B_{BpDP0}B_{D^0} \tag{59}$$

- $j=27:\ B^0 \to \bar{D}^0\pi^-\ell^+\nu$
  The branching fraction factor is

$$F_{27} = B_{B0DPp}B_{D^0} \tag{60}$$

- $j = 28: \ B^+ \to D^* \pi \ell^+ \nu$
  The decays contribute to this mode are
  $B^+ \to D^{*-} \pi^+ \ell^+ \nu$ with $D^{*-} \to \bar{D}^0 + \pi^-$
  $B^+ \to \bar{D}^{*0} \pi^0 \ell^+ \nu$ with $\bar{D}^{*0} \to \bar{D}^0 + \gamma/\pi^0$
  The branching fraction factor is

$$\begin{aligned} & F_{28} = f_{+0} B_{BpDSPp} B_{DSpDPp} B_{D^0} \\ & + f_{+0} B_{BpDSP0} (B_{DS0DP0} + B_{DS0DG}) B_{D^0} \\ & = f_{+0} (B_{BpDSPp} B_{DSpDPp} + B_{BpDSP0}) B_{D^0} \end{aligned} \tag{61}$$

- $j = 29: \ B^0 \to D^* \pi \ell^+ \nu$
  The decays contribute to this mode are
  $B^0 \to D^{*-} \pi^0 \ell^+ \nu$ with $D^{*-} \to \bar{D}^0 + \pi^-$
  $B^0 \to \bar{D}^{*0} \pi^- \ell^+ \nu$ with $\bar{D}^{*0} \to \bar{D}^0 + \gamma/\pi^0$
  The branching fraction factor is

$$\begin{aligned} & F_{29} = B_{B0DSP0} B_{DSpDPp} B_{D^0} \\ & + B_{B0DSPp} (B_{DS0DP0} + B_{DS0DG}) B_{D^0} \\ & = (B_{B0DSP0} B_{DSpDPp} + B_{B0DSPp}) B_{D^0} \end{aligned} \tag{62}$$

5.2.2 Coefficients for backgrounds C_j^{Bkgd}

There are 14 background MC modes (j). The coefficient of each mode is

- $j = 1$, DiffB from $B^+ B^-$

$$C_1^{Bkgd} = C_{DiffB}^{D^0} \frac{f_{+0} B_{D0}}{f_{+0}^{SP6} B_{D0}^{SP6}} \tag{63}$$

- $j = 2$, DiffB from $B^0 \bar{B}^0$

$$C_2^{Bkgd} = C_{DiffB}^{D^0} \frac{B_{D0}}{B_{D0}^{SP6}} \tag{64}$$

- $j = 3$, DBCascL from $B^+ B^-$

$$C_3^{Bkgd} = C_{DBCascL}^{D^0} \frac{f_{+0} B_{D0}}{f_{+0}^{SP6} B_{D0}^{SP6}} \tag{65}$$

- $j = 4$, DBCascL from $B^0\bar{B}^0$

$$C_4^{Bkgd} = C_{DBCascL}^{D^0} \frac{B_{D0}}{B_{D0}^{SP6}} \tag{66}$$

- $j = 5$, CascL from B^+B^-

$$C_5^{Bkgd} = C_{CascL}^{D^0} \frac{f_{+0} B_{D0}}{f_{+0}^{SP6} B_{D0}^{SP6}} \tag{67}$$

- $j = 6$, CascL from $B^0\bar{B}^0$

$$C_6^{Bkgd} = C_{CascL}^{D^0} \frac{B_{D0}}{B_{D0}^{SP6}} \tag{68}$$

- $j = 7$, LMisID from B^+B^-

$$C_7^{Bkgd} = C_{LMisID}^{D^0} \frac{f_{+0} B_{D0}}{f_{+0}^{SP6} B_{D0}^{SP6}} \tag{69}$$

- $j = 8$, LMisID from $B^0\bar{B}^0$

$$C_8^{Bkgd} = C_{LMisID}^{D^0} \frac{B_{D0}}{B_{D0}^{SP6}} \tag{70}$$

- $j = 9$, Comb from B^+B^-

$$C_9^{Bkgd} = \frac{f_{+0} B_{D0}}{f_{+0}^{SP6} B_{D0}^{SP6}} \tag{71}$$

- $j = 10$, Comb from $B^0\bar{B}^0$

$$C_{10}^{Bkgd} = \frac{B_{D0}}{B_{D0}^{SP6}} \tag{72}$$

- $j = 11$, RealD from $c\bar{c}$

$$C_{11}^{Bkgd} = C_{RealD}^{D^0} \frac{B_{D0}}{B_{D0}^{SP6}} \tag{73}$$

- $j = 12$, Cont from $c\bar{c}$

$$C_{12}^{Bkgd} = \frac{B_{D0}}{B_{D0}^{SP6}} \tag{74}$$

- $j = 13$, Cont from uds

$$C_{13}^{Bkgd} = \frac{B_{D0}}{B_{D0}^{SP6}} \tag{75}$$

- $j = 14$, Cont from $\tau^+\tau^-$

$$C_{14}^{Bkgd} = \frac{B_{D0}}{B_{D0}^{SP6}} \tag{76}$$

These five coefficients, $C_{DiffB}^{D^0}$, $C_{DBCascL}^{D^0}$, $C_{CascL}^{D^0}$, $C_{LMisID}^{D^0}$ and $C_{RealD}^{D^0}$ correspond to five peaking background components. These coefficients can be floated in the fit to account for our lack of knowledge in the MC simulation. Since Comb and Cont backgrounds are almost zero after D mass sideband subtraction, we do not float the coefficients of them.

5.3 D^+ MC modes

5.3.1 Coefficients for signals C_j^{Sig}

There are 14 signal MC modes (j). The branching fraction factor of each mode is

- $j = 15$: $B^0 \to D^-\ell^+\nu$
  The branching fraction factor is

$$F_{15} = B_{B0D} B_{Dp} \tag{77}$$

- $j = 16$: $B^0 \to D^{*-}\ell^+\nu$
  The decays contribute to this mode are
  $B^0 \to D^{*-}\ell^+\nu$ with $D^{*-} \to D^- + \gamma/\pi^0$
  The branching fraction factor is

$$F_{16} = B_{B0DS}(B_{DSpDP0} + B_{DSpDG}) B_{Dp} \tag{78}$$

- $j = 17: \; B^+ \to \bar{D}_0^{*0} \ell^+ \nu$
  The decays contribute to this mode are
  $B^+ \to \bar{D}_0^{*0} \ell^+ \nu$ with $\bar{D}_0^{*0} \to D^- + \pi^+$
  The branching fraction factor is

$$F_{17} = f_{+0} B_{BpDD0} B_{DD00DPp} B_{Dp} \tag{79}$$

- $j = 18: \; B^0 \to D_0^{*-} \ell^+ \nu$
  The decays contribute to this mode are
  $B^0 \to D_0^{*-} \ell^+ \nu$ with $D_0^{*-} \to D^- \pi^0$
  The branching fraction factor is

$$F_{18} = B_{B0DD0} B_{DD0pDP0} B_{Dp} \tag{80}$$

- $j = 19: \; B^+ \to \bar{D}_1^0 \ell^+ \nu$
  The decays contribute to this mode are
  $B^+ \to \bar{D}_1^0 \ell^+ \nu$ with $\bar{D}_1^0 \to D^{*-} + \pi^+$ and $D^{*-} \to D^- + \pi^0/\gamma$
  The branching fraction factor is

$$F_{19} = f_{+0} B_{BpDD1} B_{DD10DSPp} (B_{DSpDP0} + B_{DSpDG}) B_{Dp} \tag{81}$$

- $j = 20: \; B^0 \to D_1^- \ell^+ \nu$
  The decays contribute to this mode are
  $B^0 \to D_1^- \ell^+ \nu$ with $D_1^- \to D^{*-} \pi^0$ and $D^{*-} \to D^- + \pi^0/\gamma$
  The branching fraction factor is

$$F_{20} = B_{B0DD1} B_{DD1pDSP0} (B_{DSpDP0} + B_{DSpDG}) B_{Dp} \tag{82}$$

- $j = 21: \; B^+ \to \bar{D}_1'^0 \ell^+ \nu$
  The decays contribute to this mode are
  $B^+ \to \bar{D}_1'^0 \ell^+ \nu$ with $\bar{D}_1'^0 \to D^{*-} + \pi^+$ and $D^{*-} \to D^- + \pi^0/\gamma$
  The branching fraction factor is

$$F_{21} = f_{+0} B_{BpDDP1} B_{DDP10DSPp} (B_{DSpDP0} + B_{DSpDG}) B_{Dp} \tag{83}$$

- $j = 22: \; B^0 \to D_1'^- \ell^+ \nu$
  The decays contribute to this mode are
  $B^0 \to D_1'^- \ell^+ \nu$ with $D_1'^- \to D^{*-} \pi^0$ and $D^{*-} \to D^- + \pi^0/\gamma$
  The branching fraction factor is

$$F_{22} = B_{B0DDP1} B_{DDP1pDSP0} (B_{DSpDP0} + B_{DSpDG}) B_{Dp} \tag{84}$$

- $j = 23:\ B^+ \to \bar{D}_2^{*0}\ell^+\nu$
  The decays contribute to this mode are
  $B^+ \to \bar{D}_2^{*0}\ell^+\nu$ with $\bar{D}_2^{*0} \to D^{*-} + \pi^+$ and $D^{*-} \to D^- + \pi^0/\gamma$
  $B^+ \to \bar{D}_2^{*0}\ell^+\nu$ with $\bar{D}_2^{*0} \to D^- + \pi^+$
  The branching fraction factor is

$$F_{23} = f_{+0} B_{BpDD2}[B_{DD20DSPp}(B_{DSpDP0} + B_{DSpDG}) + B_{DD20DPp}]B_{Dp} \tag{85}$$

- $j = 24:\ B^0 \to D_2^{*-}\ell^+\nu$
  The decays contribute to this mode are
  $B^0 \to D_2^{*-}\ell^+\nu$ with $D_2^{*-} \to D^{*-}\pi^0$ and $D^{*-} \to D^- + \pi^0/\gamma$
  $B^0 \to D_2^{*-}\ell^+\nu$ with $D_2^{*-} \to D^-\pi^0$
  The branching fraction factor is

$$F_{24} = B_{B0DD2}[B_{DD2pDSP0}(B_{DSpDP0} + B_{DSpDG}) + B_{DD2pDP0}]B_{Dp} \tag{86}$$

- $j = 25:\ B^+ \to D^-\pi^+\ell^+\nu$
  The branching fraction factor is

$$F_{25} = f_{+0} B_{BpDPp} B_{Dp} \tag{87}$$

- $j = 26:\ B^0 \to D^-\pi^0\ell^+\nu$
  The branching fraction factor is

$$F_{26} = B_{B0DP0} B_{Dp} \tag{88}$$

- $j = 27:\ B^+ \to D^{*-}\pi^+\ell^+\nu$
  The decays contribute to this mode are
  $B^+ \to D^{*-}\pi^+\ell^+\nu$ with $D^{*-} \to D^- + \gamma/\pi^0$
  The branching fraction factor is

$$F_{27} = f_{+0} B_{BpDSPp}(B_{DSpDP0} + B_{DSpDG})B_{Dp} \tag{89}$$

- $j = 28:\ B^0 \to D^{*-}\pi^0\ell^+\nu$
  The decays contribute to this mode are
  $B^0 \to D^{*-}\pi^0\ell^+\nu$ with $D^{*-} \to D^- + \gamma/\pi^0$
  The branching fraction factor is

$$F_{28} = B_{B0DSP0}(B_{DSpDP0} + B_{DSpDG})B_{Dp} \tag{90}$$

5.3.2 Coefficients for backgrounds C_j^{Bkgd}

There are 14 background MC modes (j). The coefficient of each mode is

- $j = 1$, DiffB from B^+B^-

$$C_1^{Bkgd} = C_{DiffB}^{D^+} \frac{f_{+0} B_{Dp}}{f_{+0}^{SP6} B_{Dp}^{SP6}} \tag{91}$$

- $j = 2$, DiffB from $B^0\bar{B}^0$

$$C_2^{Bkgd} = C_{DiffB}^{D^+} \frac{B_{Dp}}{B_{Dp}^{SP6}} \tag{92}$$

- $j = 3$, DBCascL from B^+B^-

$$C_3^{Bkgd} = C_{DBCascL}^{D^+} \frac{f_{+0} B_{Dp}}{f_{+0}^{SP6} B_{Dp}^{SP6}} \tag{93}$$

- $j = 4$, DBCascL from $B^0\bar{B}^0$

$$C_4^{Bkgd} = C_{DBCascL}^{D^+} \frac{B_{Dp}}{B_{Dp}^{SP6}} \tag{94}$$

- $j = 5$, CascL from B^+B^-

$$C_5^{Bkgd} = C_{CascL}^{D^+} \frac{f_{+0} B_{Dp}}{f_{+0}^{SP6} B_{Dp}^{SP6}} \tag{95}$$

- $j = 6$, CascL from $B^0\bar{B}^0$

$$C_6^{Bkgd} = C_{CascL}^{D^+} \frac{B_{Dp}}{B_{Dp}^{SP6}} \tag{96}$$

- $j = 7$, LMisID from B^+B^-

$$C_7^{Bkgd} = C_{LMisID}^{D^+} \frac{f_{+0} B_{Dp}}{f_{+0}^{SP6} B_{Dp}^{SP6}} \tag{97}$$

- $j = 8$, LMisID from $B^0\bar{B}^0$

$$C_8^{Bkgd} = C_{LMisID}^{D^+}\frac{B_{Dp}}{B_{Dp}^{SP6}} \tag{98}$$

- $j = 9$, Comb from B^+B^-

$$C_9^{Bkgd} = \frac{f_{+0}B_{Dp}}{f_{+0}^{SP6}B_{Dp}^{SP6}} \tag{99}$$

- $j = 10$, Comb from $B^0\bar{B}^0$

$$C_{10}^{Bkgd} = \frac{B_{Dp}}{B_{Dp}^{SP6}} \tag{100}$$

- $j = 11$, RealD from $c\bar{c}$

$$C_{11}^{Bkgd} = C_{RealD}^{D^+}\frac{B_{Dp}}{B_{Dp}^{SP6}} \tag{101}$$

- $j = 12$, Cont from $c\bar{c}$

$$C_{12}^{Bkgd} = \frac{B_{Dp}}{B_{Dp}^{SP6}} \tag{102}$$

- $j = 13$, Cont from uds

$$C_{13}^{Bkgd} = \frac{B_{Dp}}{B_{Dp}^{SP6}} \tag{103}$$

- $j = 14$, Cont from $\tau^+\tau^-$

$$C_{14}^{Bkgd} = \frac{B_{Dp}}{B_{Dp}^{SP6}} \tag{104}$$

These five coefficients, $C_{DiffB}^{D^+}$, $C_{DBCascL}^{D^+}$, $C_{CascL}^{D^+}$, $C_{LMisID}^{D^+}$ and $C_{RealD}^{D^+}$ correspond to five peaking background components. These coefficients can be floated in the fit to account for our lack of knowledge in the MC simulation.

6 Form Factor (FF) Re-weighting

We use SP5/SP6 MC for our analysis. However, there have been some improvements of form factors (FF) since SP5/SP6 MC were generated. To take those improvements into account, form factor re-weighting is necessary.

6.1 Normalization

When we change parameters of form factors, we need to make sure that total rates stay same. Thus, we need a normalization factor, R_N, such that

$$\Gamma = \int \frac{d\Gamma(\text{old FF})}{dx} dx = R_N \int \frac{d\Gamma(\text{new FF})}{dy} dy \tag{105}$$

We can do the integration numerically by using the Monte Carlo method.

In the following subsections, the FF weight factor W_{jk}^{Sig} is explained for each decay mode. See Appendix H for details of form factors.

6.2 $B \to D\ell\nu$

In this mode, ISGW2 model [23][24] is used in MC. The model is a type of quark models. We need to change it to HQET (Heavy Quark Effective Theory) model [25][26].
The differential decay rate in the ISGW2 model is given by

$$\begin{aligned} \frac{d\Gamma(B \to D\ell\nu)}{dq^2} &= \frac{G_F^2 |V_{cb}|^2}{192\pi^3 m_B^3} \left[(q^2 - m_B^2 - m_D^2)^2 - 4m_B^2 m_D^2\right]^{3/2} |f_+(q^2)|^2 \\ &= \frac{G_F^2 |V_{cb}|^2 m_D^3}{24\pi^3} \left[\left(\frac{m_B^2 + m_D^2 - q^2}{2m_B m_D}\right)^2 - 1\right]^{3/2} |f_+(q^2)|^2 \end{aligned} \tag{106}$$

where $f_+(q^2)$ is the form factor. The differential decay rate in HQET model is given by

$$\frac{d\Gamma(B \to D\ell\nu)}{dw} = \frac{G_F^2 |V_{cb}|^2}{48\pi^3} (m_B + m_D)^2 m_D^3 (w^2 - 1)^{3/2} |h_+(w)|^2 \tag{107}$$

where w is the velocity transfer (see Appendix G), and $h_+(w)$ is the form factor. These two form factors are related by

$$h_+(w) = R f_+(q^2) \tag{108}$$

where

$$R = \frac{2\sqrt{m_B m_D}}{m_B + m_D} \simeq 0.88 \tag{109}$$

q^2 is related to w by

$$w = \frac{m_B^2 + m_D^2 - q^2}{2m_B m_D} \quad \text{or} \quad q^2 = m_B^2 + m_D^2 - 2m_B m_D w \tag{110}$$

In HQET model, we can set

$$h_+(w) = h_+(1)[1 - \rho_D^2(w-1)] \tag{111}$$

where $h_+(1)$ is given by a Lattice QCD calculation [27]

$$h_+(1) = 1.074 \pm 0.018 \pm 0.016 = 1.074 \pm 0.024 \tag{112}$$

and ρ_D^2 is the slope of $B \to D\ell\nu$ FF. The weight is given by the ratio of these two models

$$W_{jk}^{Sig}(w_k) = \frac{[h_+(1)]^2[1-\rho_D^2(w-1)]^2}{[Rf_+(q^2)]^2} R_N \tag{113}$$

where, the normalization factor, R_N, is given by

$$\int_0^{11.64} \left[\left(\frac{m_B^2 + m_D^2 - q^2}{2m_B m_D}\right)^2 - 1\right]^{3/2} [Rf_+(q^2)]^2 \frac{dq^2}{2m_B m_D}$$
$$= R_N \int_1^{1.590} (w^2-1)^{3/2}[h_+(1)]^2[1-\rho_D^2(w-1)]^2 dw \tag{114}$$

Or, we can use a different parametrization proposed by [28]

$$h_+(w) = h_+(1)[1 - 8\rho_D^2 z + (51\rho_D^2 - 10)z^2 - (252\rho_D^2 - 84)z^3] \tag{115}$$

where

$$z = \frac{\sqrt{w+1} - \sqrt{2}}{\sqrt{w+1} + \sqrt{2}} \tag{116}$$

The weight is given by the ratio of this change and original SP5/SP6

$$W_{jk}^{Sig}(w_k) = \frac{[h_+(1)]^2[1 - 8\rho_D^2 z + (51\rho_D^2 - 10)z^2 - (252\rho_D^2 - 84)z^3]^2}{[Rf_+(q^2)]^2} R_N \tag{117}$$

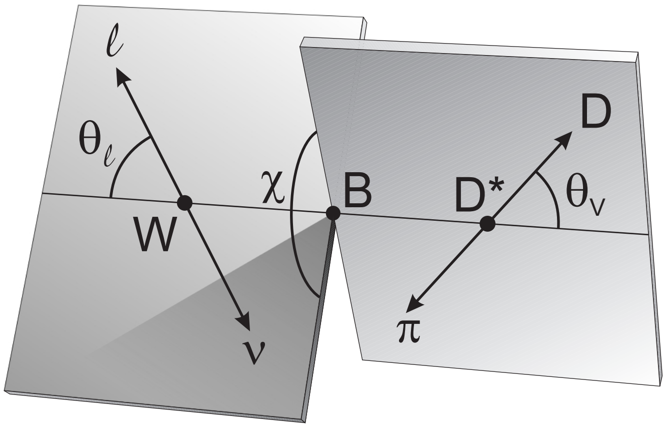

Figure 12: Geometry of $B \to D^* \ell \nu$ decay.

where, the normalization factor, R_N, is given by

$$\int_0^{11.64} \frac{dq^2}{2m_B m_D} \left[\left(\frac{m_B^2 + m_D^2 - q^2}{2m_B m_D} \right)^2 - 1 \right]^{3/2} [Rf_+(q^2)]^2$$
$$= R_N \int_1^{1.590} dw \ \ (w^2-1)^{3/2} [h_+(1)]^2 \times$$
$$\left[1 - 8\rho_D^2 z + (51\rho_D^2 - 10)z^2 - (252\rho_D^2 - 84)z^3\right]^2 \qquad (118)$$

6.3 $B \to D^* \ell \nu$

We need three kinematic variables to describe this decay. We usually chose $\cos\theta_\ell$, $\cos\theta_V$ and χ as shown in the figure 12. The definition of these variables are

- $\cos\theta_\ell$: the cosine of the angle between the directions of "the ℓ in the W rest frame" and "the W in the B rest frame".
- $\cos\theta_V$: the cosine of the angle between the directions of "the D in the D^* rest frame" and "the D^* in the B rest frame".
- χ : the azimuthal angle between the planes formed by "W-ℓ system' ' and "$D^* - D$ system".

HQET model is used and the differential decay rate is given by

$$\begin{aligned}
\frac{d\Gamma(B\to D^*\ell\nu)}{dw d\cos\theta_V d\cos\theta_\ell d\chi} \;=\; & \frac{3G_F^2}{4(4\pi)^4}|V_{cb}|^2 m_B m_{D^*}^2 r\sqrt{w^2-1}(1-2wr+r^2)\times \\
& [(1-\cos\theta_\ell)^2\sin^2\theta_V|H_+(w)|^2 \\
& +(1+\cos\theta_\ell)^2\sin^2\theta_V|H_-(w)|^2 \\
& +4\sin^2\theta_\ell\cos^2\theta_V|H_0(w)|^2 \\
& -4\sin\theta_\ell(1-\cos\theta_\ell)\sin\theta_V\cos\theta_V\cos\chi H_+(w)H_0(w) \\
& +4\sin\theta_\ell(1+\cos\theta_\ell)\sin\theta_V\cos\theta_V\cos\chi H_-(w)H_0(w) \\
& -2\sin^2\theta_\ell\sin^2\theta_V\cos 2\chi H_+(w)H_-(w)]
\end{aligned} \tag{119}$$

where r is the mass ratio

$$r = \frac{m_{D^*}}{m_B} \tag{120}$$

$H_i(w)$ are

$$H_i = -m_B\frac{R^*(1-r^2)(w+1)}{2\sqrt{1-2wr+r^2}}h_{A_1}(w)\widetilde{H}_i(w) \tag{121}$$

where R^* is

$$R^* = \frac{2\sqrt{m_B m_{D^*}}}{m_B+m_{D^*}} \tag{122}$$

and $\widetilde{H}_i(w)$ are

$$\begin{aligned}
\widetilde{H}_\pm(w) &= \tfrac{\sqrt{1-2wr+r^2}}{1-r}\left(1\mp\sqrt{\tfrac{w-1}{w+1}}R_1(w)\right) \\
\widetilde{H}_0(w) &= 1+\tfrac{w-1}{1-r}\left(1-R_2(w)\right)
\end{aligned} \tag{123}$$

were R_1 and R_2 are the form factor ratios. To make the notation simple, we define

$$\begin{aligned}
& c_L \equiv \cos\theta_\ell \\
& c_V \equiv \cos\theta_V \\
& c_\chi \equiv \cos\chi \\
& h_\pm(w) \equiv (1-r)\widetilde{H}_\pm(w) = \sqrt{1-2wr+r^2}\left(1\mp\sqrt{\tfrac{w-1}{w+1}}R_1\right) \\
& h_0(w) \equiv (1-r)\widetilde{H}_0(w) = (1-r)+(w-1)\left(1-R_2\right)
\end{aligned} \tag{124}$$

then

$$\begin{aligned}\frac{d\Gamma(B\to D^*\ell\nu)}{dwd\cos\theta_V d\cos\theta_\ell d\chi} \;=\;& f(w)\times[h_{A_1}(w)]^2 \\ & [(1-c_L)^2(1-c_V^2)h_+^2+(1+c_L)^2(1-c_V^2)h_-^2 \\ & +4(1-c_L^2)c_V^2h_0^2-2(1-c_L^2)(1-c_V^2)(2c_\chi^2-1)h_+h_- \\ & -4\sqrt{1-c_L^2}(1-c_L)\sqrt{1-c_V^2}c_Vc_\chi h_+h_0 \\ & +4\sqrt{1-c_L^2}(1+c_L)\sqrt{1-c_V^2}c_Vc_\chi h_-h_0]\end{aligned} \tag{125}$$

where

$$\begin{aligned} f(w) \equiv & \frac{3G_F^2}{4(4\pi)^4}|V_{cb}|^2 m_B m_{D^*}^2 r\sqrt{w^2-1}(1-2wr+r^2)\times \\ & \left[m_B\frac{2\sqrt{(m_Bm_{D^*})}}{m_B+m_{D^*}}\frac{(1-r^2)(w+1)}{2\sqrt{1-2wr+r^2}}\frac{1}{(1-r)}\right]^2 \\ = & \frac{3G_F^2}{4(4\pi)^4}|V_{cb}|^2\frac{m_B^4m_{D^*}^3}{(m_B+m_{D^*})^2}r(1+r)^2(w+1)^2\sqrt{w^2-1} \end{aligned} \tag{126}$$

In SP5/SP6 MC, the values of parameters are

$$\begin{aligned} R_1^0 &= 1.18 \\ R_2^0 &= 0.72 \\ \rho_0^2 &= 0.92 \end{aligned} \tag{127}$$

where the standard parameterization for the slope ρ^2 is used. Hence, $h_{A_1}(w)$ is given by

$$h_{A_1}(w) = h_{A_1}(1)\left(1-\rho^2(w-1)\right) \tag{128}$$

The values from a recent Babar measurement [31] are

$$\begin{aligned} R_1 &= 1.396\pm0.060\pm0.035\pm0.027 = 1.396\pm0.0745 \\ R_2 &= 0.885\pm0.040\pm0.022\pm0.013 = 0.885\pm0.0474 \\ \rho^2 &= 1.145\pm0.059\pm0.030\pm0.035 = 1.145\pm0.075 \end{aligned} \tag{129}$$

where a different parameterization [28] is used for the slope :

$$h_{A_1}(w) = h_{A_1}(1)\left(1-8\rho^2z+(53\rho^2-15)z^2-(231\rho^2-91)z^3\right) \tag{130}$$

where

$$z = \frac{\sqrt{w+1}-\sqrt{2}}{\sqrt{w+1}+\sqrt{2}} \tag{131}$$

The weight is given by taking the ratio of decay rates which calculated by using old and new form factor parameters. The factors $f(w)$ and $|h_{A_1}(1)|^2$ are cancelled by taking ratio.
The normalization factor R_N is given by

$$\begin{aligned} &\int_1^{1.504} dw \int_{-1}^{1} d\cos\theta_V \int_{-1}^{1} d\cos\theta_\ell \int_0^{2\pi} d\chi \frac{d\Gamma(\text{old parameters})}{dw d\cos\theta_V d\cos\theta_\ell d\chi} \\ &= R_N \int_1^{1.504} dw \int_{-1}^{1} d\cos\theta_V \int_{-1}^{1} d\cos\theta_\ell \int_0^{2\pi} d\chi \frac{d\Gamma(\text{new parameters})}{dw d\cos\theta_V d\cos\theta_\ell d\chi} \end{aligned} \tag{132}$$

Again, factors

$$\frac{3G_F^2}{4(4\pi)^4}|V_{cb}|^2 \frac{m_B^4 m_{D^*}^3}{(m_B+m_{D^*})^2} r(1+r)^2 \tag{133}$$

and $|h_{A_1}(1)|^2$ are cancelled.
The effect of these new FF parameters is shown in the section 7.3.

6.4 $B \to D_0^* \ell\nu$

$$W_{jk}^{Sig}(w_k) = ? \tag{134}$$

6.5 $B \to D_1 \ell\nu$

$$W_{jk}^{Sig}(w_k) = ? \tag{135}$$

6.6 $B \to D_1' \ell\nu$

$$W_{jk}^{Sig}(w_k) = ? \tag{136}$$

6.7 $B \to D_2^* \ell\nu$

$$W_{jk}^{Sig}(w_k) = ? \tag{137}$$

6.8 $B \to D\pi \ell\nu$

$$W_{jk}^{Sig}(w_k) = ? \tag{138}$$

6.9 $B \to D^* \pi \ell \nu$

$$W_{jk}^{Sig}(w_k) = ? \tag{139}$$

6.10 $B \to D\ell\nu$ slope fitting technique

To fit for $B \to D\ell\nu$ slope, it is not efficient to go through the calculation of the weight event by event. The following is a better way to do fitting.

6.10.1 Number of events

We may rewrite the weight (Equation (113))

$$W_{jk}^{Sig}(w_k) = \left[\frac{[h_+(1)]^2}{[Rf_+(q^2)]^2} - \frac{2(w-1)[h_+(1)]^2}{[Rf_+(q^2)]^2}\rho_D^2 + \frac{(w-1)^2[h_+(1)]^2}{[Rf_+(q^2)]^2}\left(\rho_D^2\right)^2 \right] R_N \tag{140}$$

Hence, we define

$$W_{jk}^{Sig}(w_k) \equiv \left[W_{jk}^0(w_k) - W_{jk}^1(w_k)\rho_D^2 + W_{jk}^2(w_k)\left(\rho_D^2\right)^2 \right] R_N \tag{141}$$

Then, the number of events is

$$\begin{aligned} N_{ij}^{Sig} = & \left[\sum_l \left(r_l^{Lumi} \sum_{k \in i,j,l} r_k^{Trk} r_k^{PID} W_{jk}^0 \right) \right. \\ & - \sum_l \left(r_l^{Lumi} \sum_{k \in i,j,l} r_k^{Trk} r_k^{PID} W_{jk}^1 \right) \rho_D^2 \\ & \left. + \sum_l \left(r_l^{Lumi} \sum_{k \in i,j,l} r_k^{Trk} r_k^{PID} W_{jk}^2 \right) \left(\rho_D^2\right)^2 \right] R_N \end{aligned} \tag{142}$$

Hence

$$N_{ij}^{Sig} \equiv \left[N_{ij}^{MC0} - N_{ij}^{MC1}\rho_D^2 + N_{ij}^{MC2}\left(\rho_D^2\right)^2 \right] R_N \tag{143}$$

Instead of going through event by event in fitting, first we create these three histograms (N_{ij}^{MC0}, N_{ij}^{MC1} and N_{ij}^{MC2}), and then use those histograms in fitting.
In another parametrization (Equation (115)).

$$\begin{aligned} & 1 - 8\rho_D^2 z + (51\rho_D^2 - 10)z^2 - (252\rho_D^2 - 84)z^3 \\ & = (1 - 10z^2 + 84z^3) - (8z - 51z^2 + 252z^3)\rho_D^2 \end{aligned} \tag{144}$$

Thus, by replacing

$$\begin{aligned}
&1 \to (1 - 10z^2 + 84z^3) \\
&(w-1) \to (8z - 51z^2 + 252z^3)
\end{aligned} \tag{145}$$

we can use the same method

6.10.2 Statistical uncertainty

Calculation of statistical uncertainty is a little bit tricky. To simplify the notation, we write the number of events at D mass peak

$$N_P^0 = N_{1P} - N_{2P}\rho_D^2 + N_{3P}\left(\rho_D^2\right)^2, \quad N_P = R_N \cdot N_P^0 \tag{146}$$

and at D mass sideband

$$N_S^0 = N_{1S} - N_{2S}\rho_D^2 + N_{3S}\left(\rho_D^2\right)^2, \quad N_S = R_N \cdot N_S^0 \tag{147}$$

The number of events after D mass sideband subtraction is

$$\begin{aligned}
&N = rN_P - rN_S \\
&= \left[r(N_{1P} - N_{1S}) - r(N_{2P} - N_{2S})\rho_D^2 + r(N_{3P} - N_{3S})\left(\rho_D^2\right)^2\right] R_N
\end{aligned} \tag{148}$$

where r is the luminosity normalization factor. The statistical uncertainties for peak and sidebands are

$$\varepsilon_P = rR_N\sqrt{N_P^0}, \quad \varepsilon_S = rR_N\sqrt{N_S^0} \tag{149}$$

Hence

$$\begin{aligned}
\varepsilon &= \sqrt{\varepsilon_P^2 + \varepsilon_S^2} = rR_N\sqrt{N_P^0 + N_S^0} \\
&= rR_N\sqrt{(N_{1P}^0 + N_{1S}^0) - (N_{2P}^0 + N_{2S}^0)\rho_D^2 + (N_{3P}^0 + N_{3S}^0)\left(\rho_D^2\right)^2}
\end{aligned} \tag{150}$$

When we make three component histograms

$$\begin{aligned}
N_1 &= r(N_{1P}^0 - N_{1S}^0), \quad \varepsilon_1 = r\sqrt{N_{1P}^0 + N_{1S}^0} \\
N_2 &= r(N_{2P}^0 - N_{2S}^0), \quad \varepsilon_2 = r\sqrt{N_{2P}^0 + N_{2S}^0} \\
N_3 &= r(N_{3P}^0 - N_{3S}^0), \quad \varepsilon_3 = r\sqrt{N_{3P}^0 + N_{3S}^0}
\end{aligned} \tag{151}$$

Hence, number of events is

$$N = \left[N_1 - N_2 \rho_D^2 + N_3 \left(\rho_D^2 \right)^2 \right] R_N \tag{152}$$

as written in the above. The uncertainty is

$$\varepsilon = R_N \sqrt{\varepsilon_1^2 - \varepsilon_2^2 \rho_D^2 + \varepsilon_3^2 \left(\rho_D^2 \right)^2} \tag{153}$$

6.10.3 Normalization factor R_N

It is also not efficient to calculate normalization factor R_N every time the fit calculate χ^2. We make a table of ρ_D^2 vs R_N, and the fit read in R_N from this table. In this way, we can significantly speed up fitting. In practise, we devide ρ_D^2 by the step

$$\Delta \rho_D^2 = 0.001 \tag{154}$$

and make tables. In the fit, we linearly interpolate the steps to get R_N for a given ρ_D^2.

7 Effect of corrections and weights

7.1 Tracking efficiency and PID correction

7.2 $B \to D\ell\nu$ FF re-weighting

7.3 $B \to D^*\ell\nu$ FF re-weighting

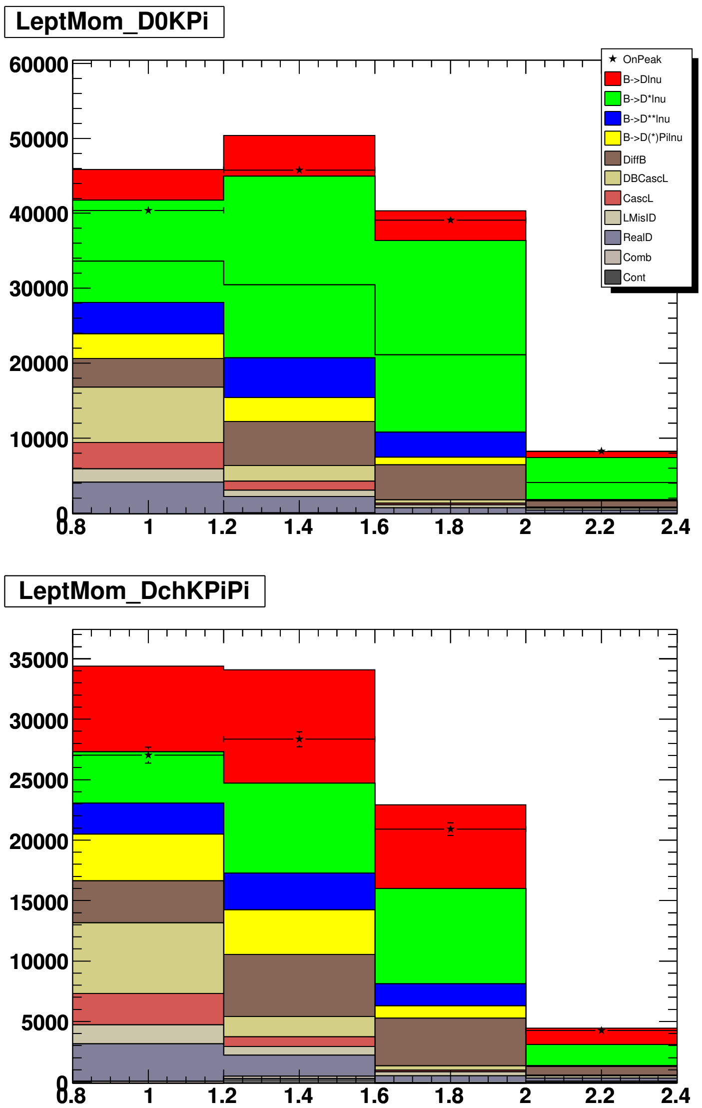

Figure 13: Lepton momentum plot before applying tracking efficiency and PID correction. Summed over D momentum and $cos\theta_{B-Dl}$ bins. Red is $B \to D\ell\nu$, green is $B \to D^{*}\ell\nu$, blue is $B \to D^{**}\ell\nu$, yellow is non-resonant $B \to D^{(*)}\pi\ell\nu$, and the rest is background. Dark brown is DiffB, light brown is DBCascL, dark red is CascL, light grey is LMisID, blue-gray is RealD, grey is Comb, and dark grey is Cont.

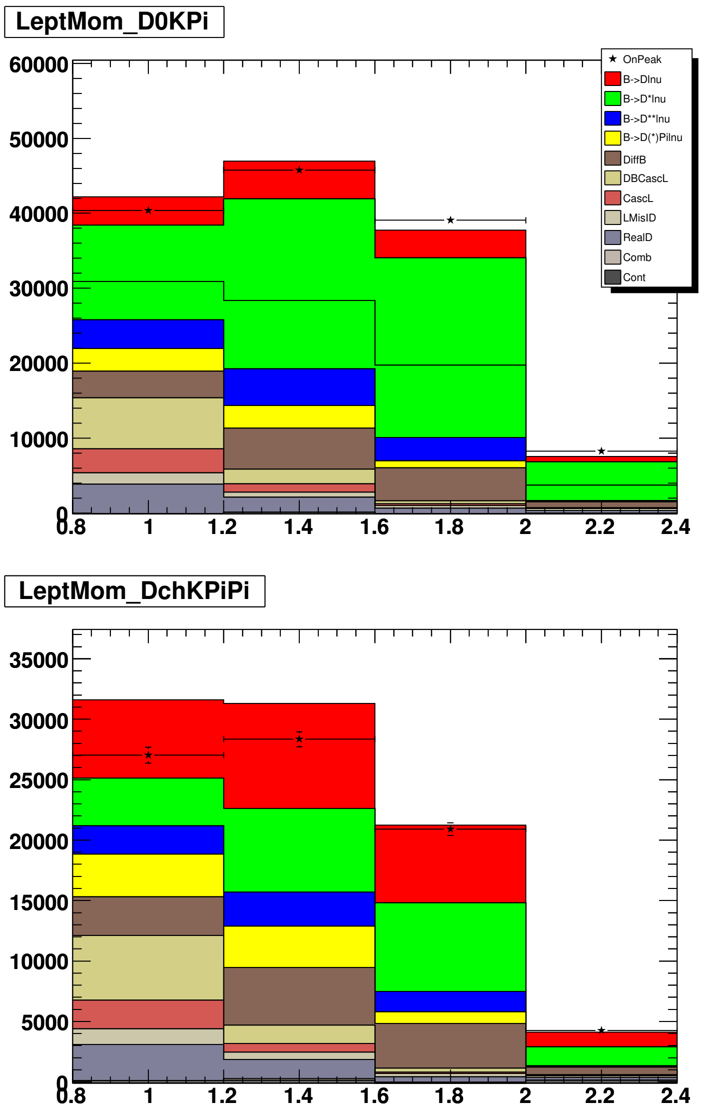

Figure 14: Lepton momentum plot after applying tracking efficiency and PID correction. Summed over D momentum and $cos\theta_{B-Dl}$ bins. Red is $B \rightarrow D\ell\nu$, green is $B \rightarrow D^{*}\ell\nu$, blue is $B \rightarrow D^{**}\ell\nu$, yellow is non-resonant $B \rightarrow D^{(*)}\pi\ell\nu$, and the rest is background. Dark brown is DiffB, light brown is DBCascL, dark red is CascL, light grey is LMisID, blue-gray is RealD, grey is Comb, and dark grey is Cont.

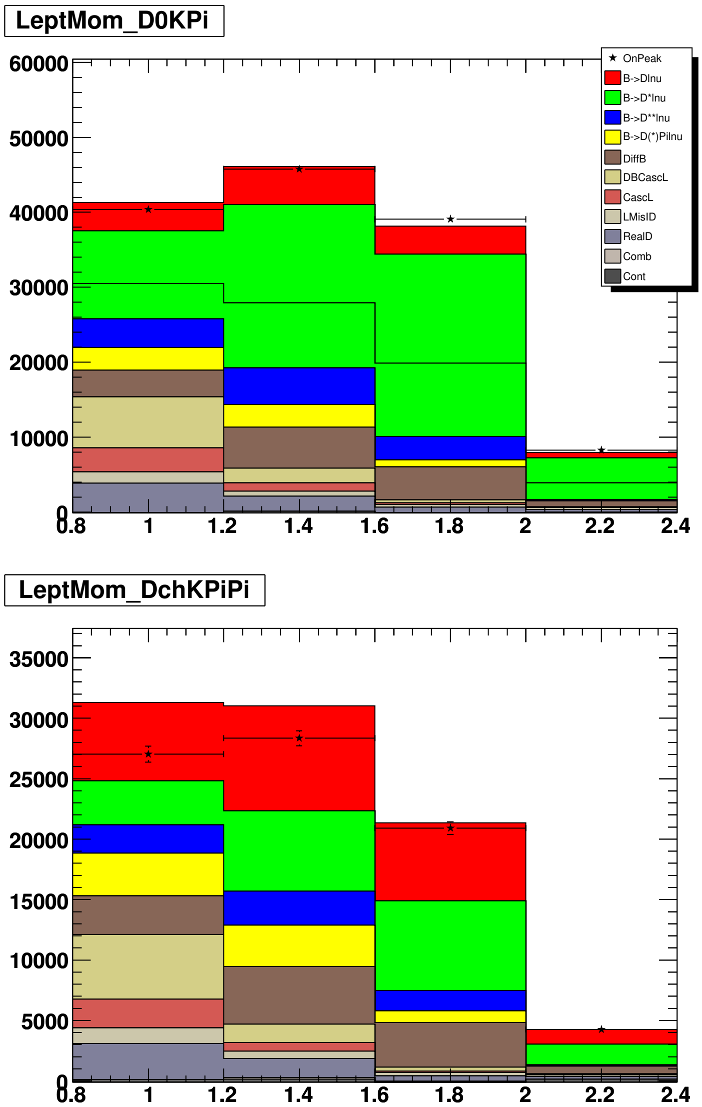

Figure 15: Lepton momentum plot after applying new $B \to D^{*}\ell\nu$ form factor parameters. Summed over D momentum and $cos\theta_{B-Dl}$ bins. Red is $B \to D\ell\nu$, green is $B \to D^{*}\ell\nu$, blue is $B \to D^{**}\ell\nu$, yellow is non-resonant $B \to D^{(*)}\pi\ell\nu$, and the rest is background. Dark brown is DiffB, light brown is DBCascL, dark red is CascL, light grey is LMisID, blue-gray is RealD, grey is Comb, and dark grey is Cont.

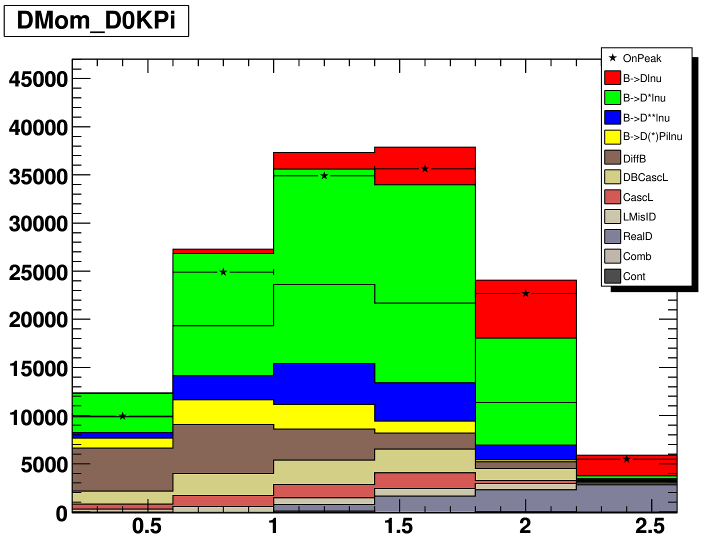

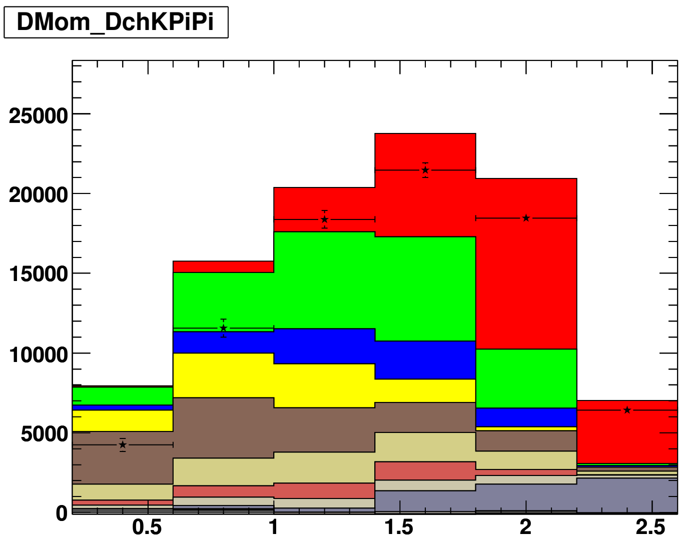

Figure 16: D momentum plot before applying tracking efficiency and PID correction. Summed over the lepton momentum and $cos\theta_{B-Dl}$ bins. Red is $B \to D\ell\nu$, green is $B \to D^{*}\ell\nu$, blue is $B \to D^{**}\ell\nu$, yellow is non-resonant $B \to D^{(*)}\pi\ell\nu$, and the rest is background. Dark brown is DiffB, light brown is DBCascL, dark red is CascL, light grey is LMisID, blue-gray is RealD, grey is Comb, and dark grey is Cont.

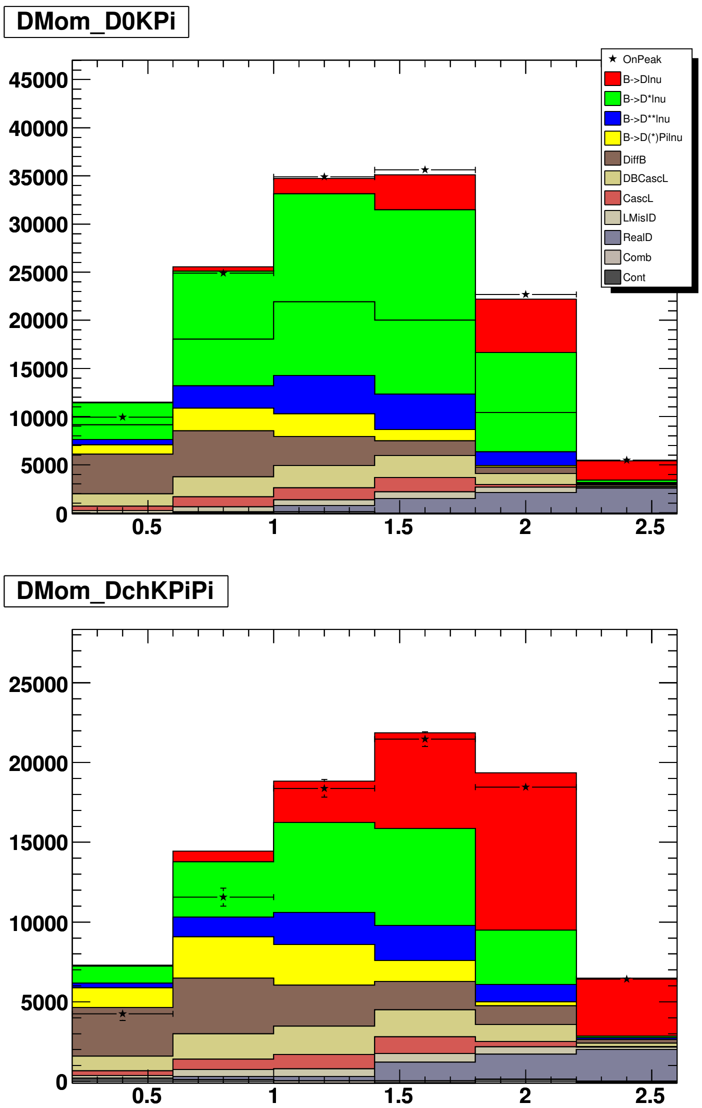

Figure 17: D momentum plot after applying tracking efficiency and PID correction. Summed over the lepton momentum and $cos\theta_{B-Dl}$ bins. Red is $B \to D\ell\nu$, green is $B \to D^{*}\ell\nu$, blue is $B \to D^{**}\ell\nu$, yellow is non-resonant $B \to D^{(*)}\pi\ell\nu$, and the rest is background. Dark brown is DiffB, light brown is DBCascL, dark red is CascL, light grey is LMisID, blue-gray is RealD, grey is Comb, and dark grey is Cont.

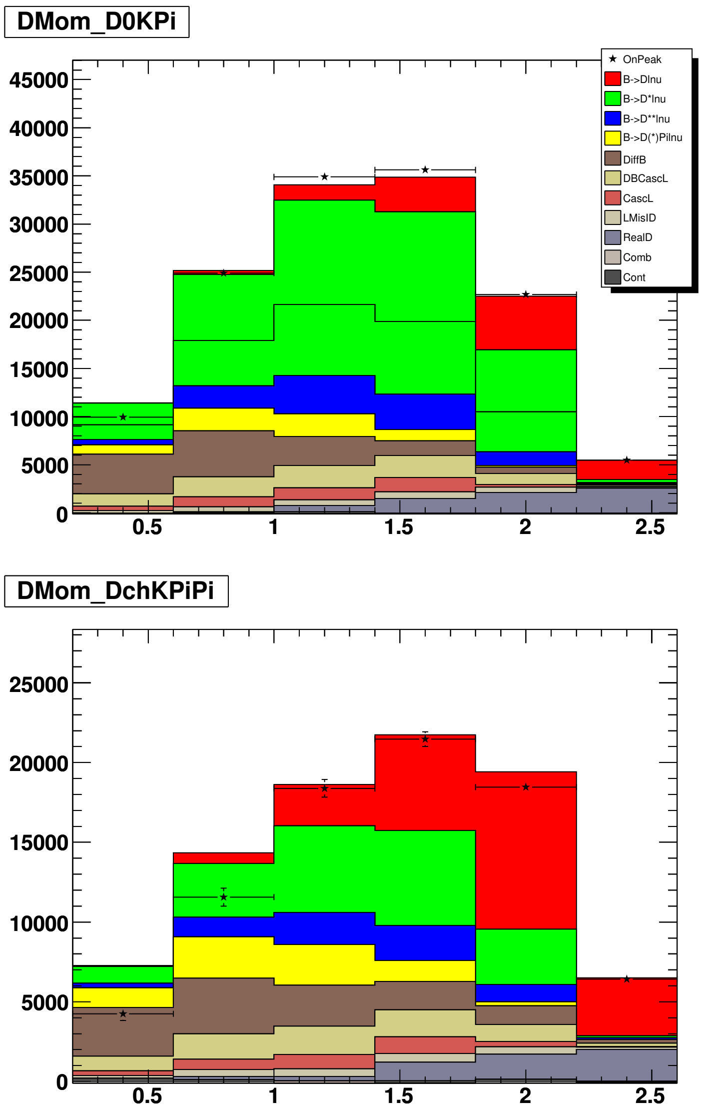

Figure 18: D momentum plot after applying new $B \to D^*\ell\nu$ form factor parameters. Summed over the lepton momentum and $cos\theta_{B-Dl}$ bins. Red is $B \to D\ell\nu$, green is $B \to D^*\ell\nu$, blue is $B \to D^{**}\ell\nu$, yellow is non-resonant $B \to D^{(*)}\pi\ell\nu$, and the rest is background. Dark brown is DiffB, light brown is DBCascL, dark red is CascL, light grey is LMisID, blue-gray is RealD, grey is Comb, and dark grey is Cont.

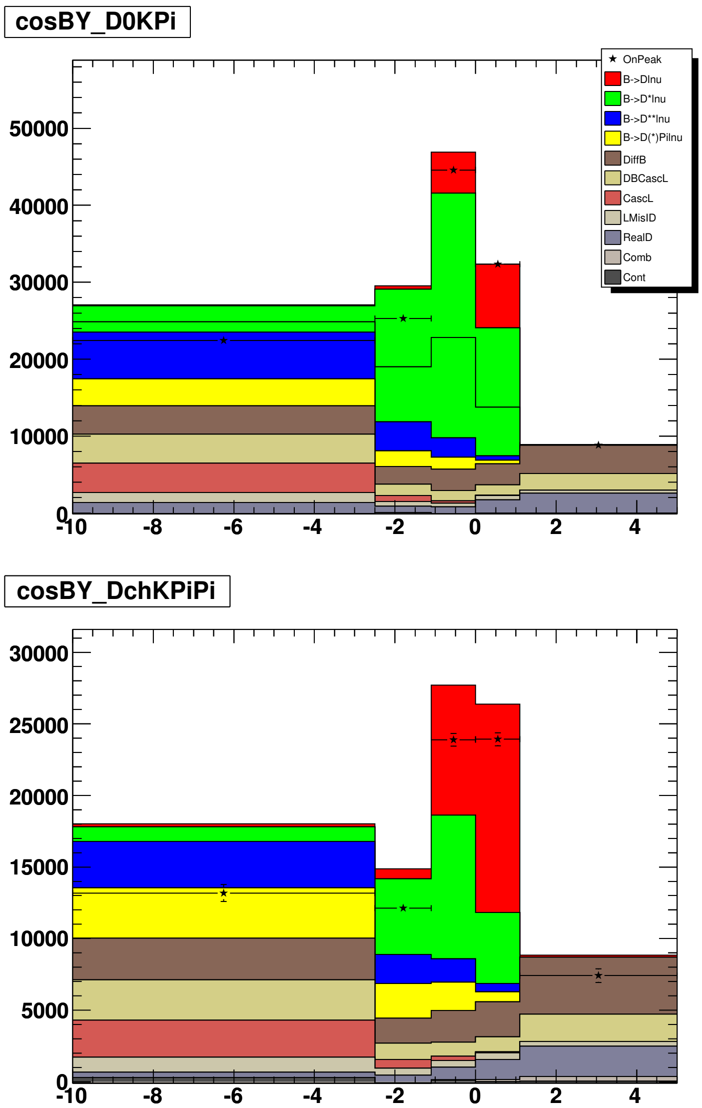

Figure 19: $cos\theta_{B-Dl}$ plot before applying tracking efficiency and PID correction. Summed over the lepton momentum and D momentum bins. Red is $B \to D\ell\nu$, green is $B \to D^{*}\ell\nu$, blue is $B \to D^{**}\ell\nu$, yellow is non-resonant $B \to D^{(*)}\pi\ell\nu$, and the rest is background. Dark brown is DiffB, light brown is DBCascL, dark red is CascL, light grey is LMisID, blue-gray is RealD, grey is Comb, and dark grey is Cont.

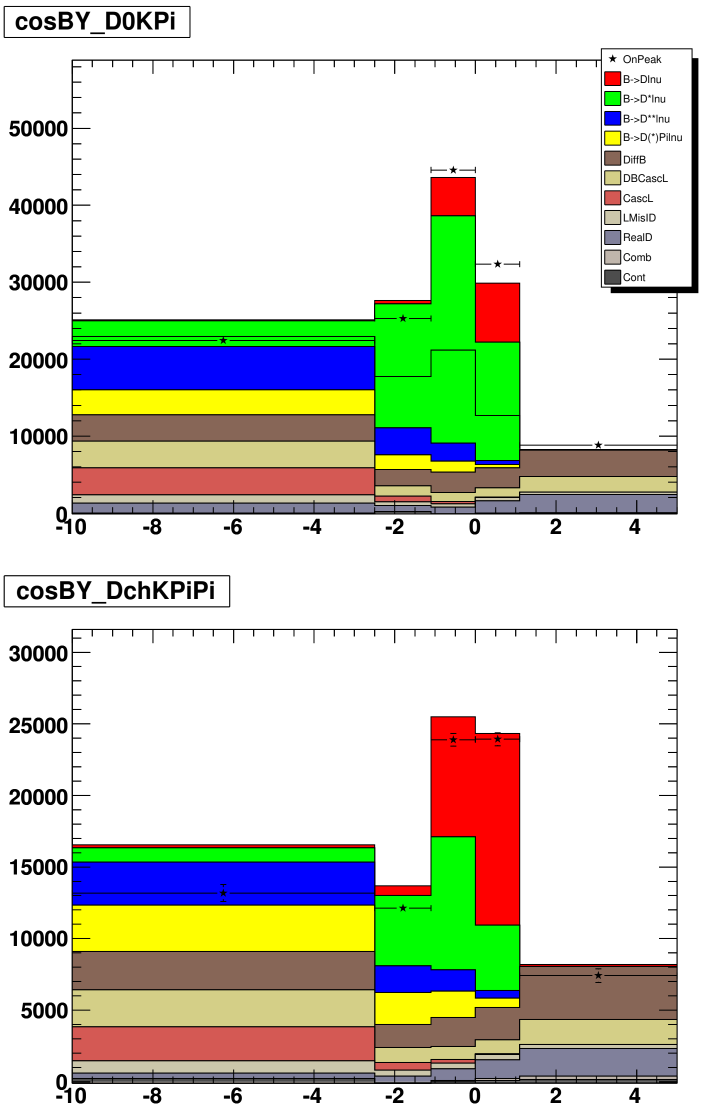

Figure 20: $cos\theta_{B-Dl}$ plot after applying tracking efficiency and PID correction. Summed over the lepton momentum and D momentum bins. Red is $B \to D\ell\nu$, green is $B \to D^{*}\ell\nu$, blue is $B \to D^{**}\ell\nu$, yellow is non-resonant $B \to D^{(*)}\pi\ell\nu$, and the rest is background. Dark brown is DiffB, light brown is DBCascL, dark red is CascL, light grey is LMisID, blue-gray is RealD, grey is Comb, and dark grey is Cont.

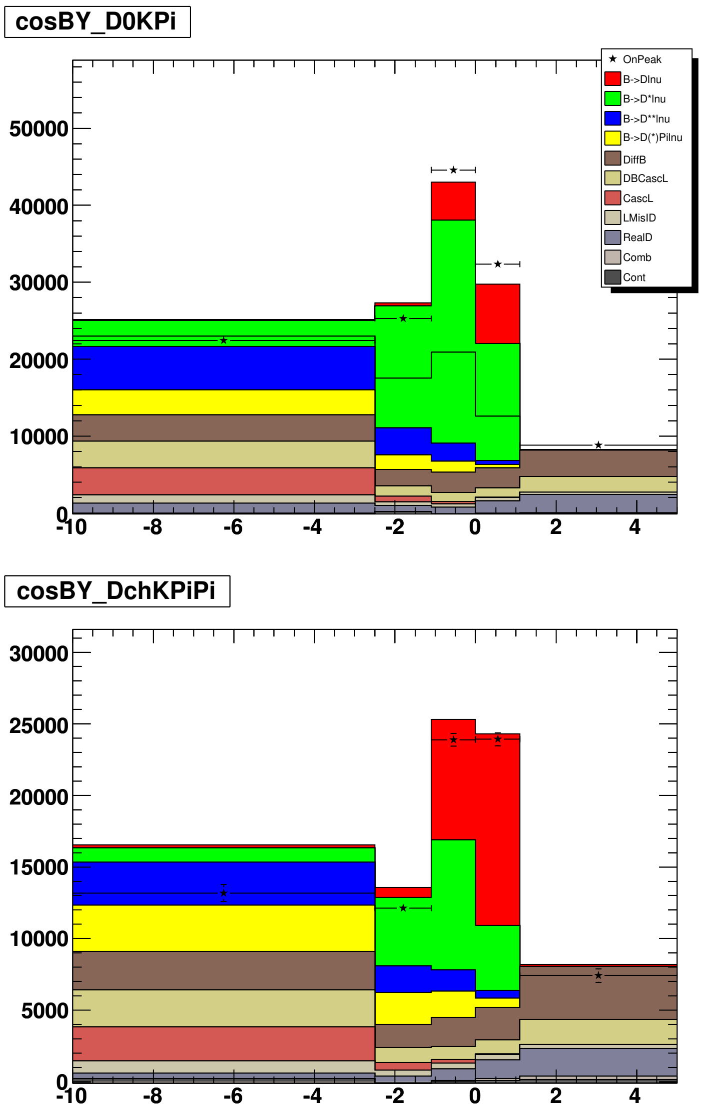

Figure 21: $cos\theta_{B-Dl}$ plot after applying new $B \to D^{*}\ell\nu$ form factor parameters. Summed over the lepton momentum and D momentum bins. Red is $B \to D\ell\nu$, green is $B \to D^{*}\ell\nu$, blue is $B \to D^{**}\ell\nu$, yellow is non-resonant $B \to D^{(*)}\pi\ell\nu$, and the rest is background. Dark brown is DiffB, light brown is DBCascL, dark red is CascL, light grey is LMisID, blue-gray is RealD, grey is Comb, and dark grey is Cont.

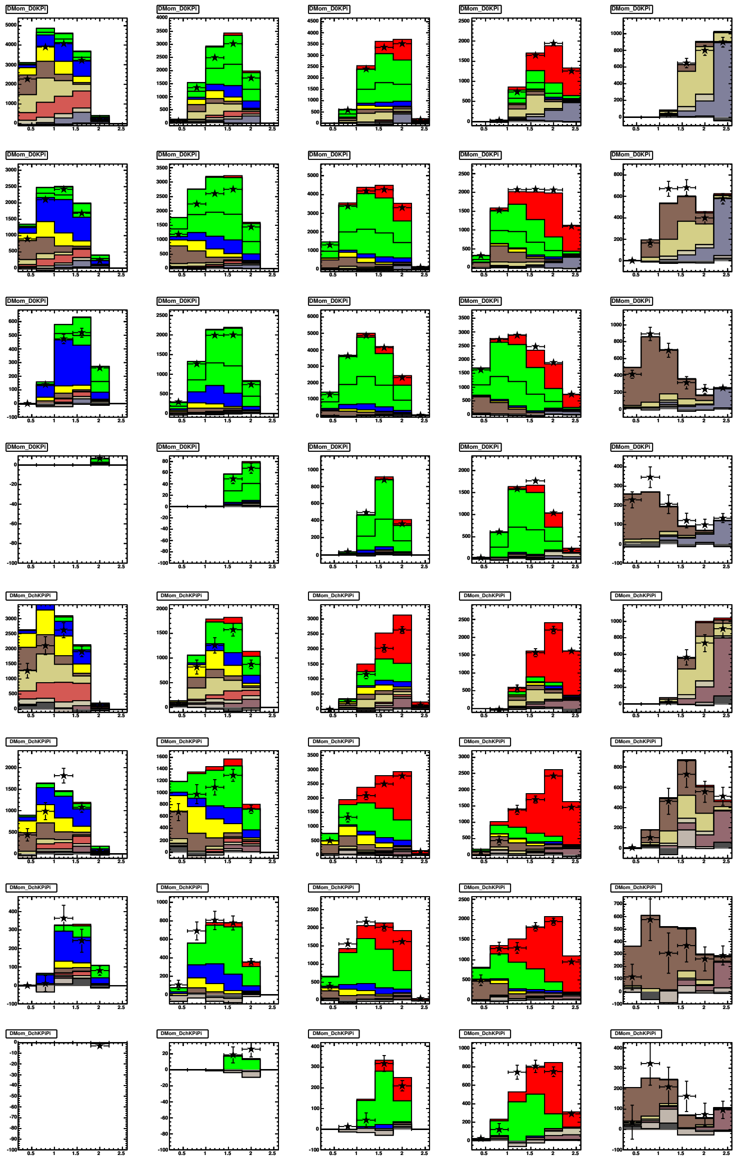

Figure 22: D momentum bin by bin plot before applying tracking efficiency and PID correction. The top half is for D^0 and the bottom half is for D^+. In each half, from top to bottom, the lepton momemtum increases. From left to right $cos\theta_{B-Dl}$ increases. Red is $B \to D\ell\nu$, green is $B \to D^{*}\ell\nu$, blue is $B \to D^{**}\ell\nu$, yellow is non-resonant $B \to D^{(*)}\pi\ell\nu$, and the rest is background. Dark brown is DiffB, light brown is DBCascL, dark red is CascL, light grey is LMisID, blue-gray is RealD, grey is Comb, and dark grey is Cont.

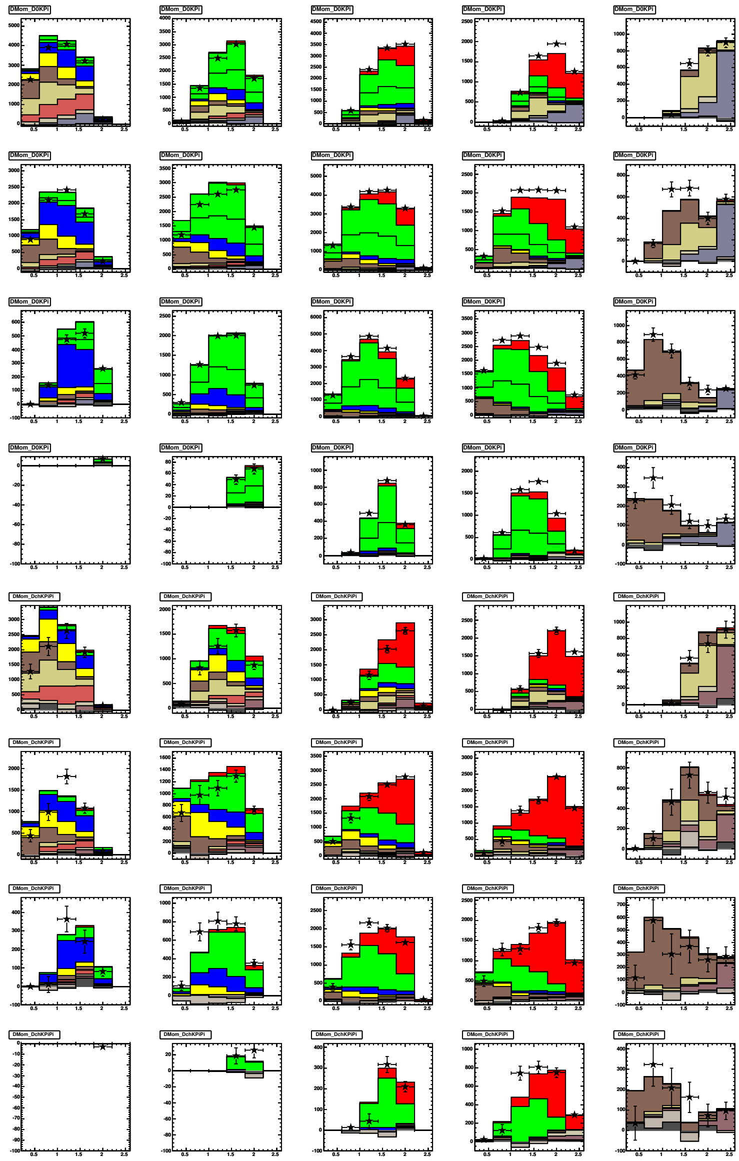

Figure 23: D momentum bin by bin plot after applying tracking efficiency and PID correction. The top half is for D^0 and the bottom half is for D^+. In each half, from top to bottom, the lepton momemtum increases. From left to right $cos\theta_{B-Dl}$ increases. Red is $B \to D\ell\nu$, green is $B \to D^*\ell\nu$, blue is $B \to D^{**}\ell\nu$, yellow is non-resonant $B \to D^{(*)}\pi\ell\nu$, and the rest is background. Dark brown is DiffB, light brown is DBCascL, dark red is CascL, light grey is LMisID, blue-gray is RealD, grey is Comb, and dark grey is Cont.

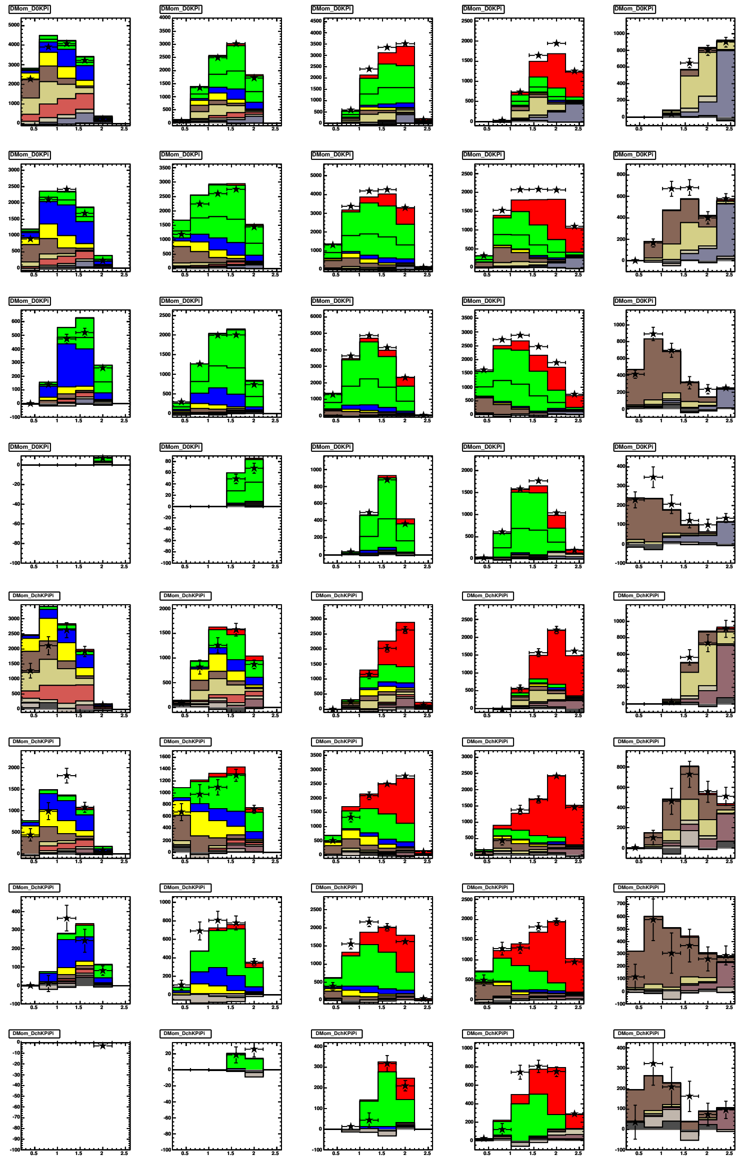

Figure 24: D momentum bin by bin plot after applying new $B \to D^* \ell \nu$ form factor parameters. The top half is for D^0 and the bottom half is for D^+. In each half, from top to bottom, the lepton momemtum increases. From left to right $cos\theta_{B-Dl}$ increases. Red is $B \to D\ell\nu$, green is $B \to D^*\ell\nu$, blue is $B \to D^{**}\ell\nu$, yellow is non-resonant $B \to D^{(*)}\pi\ell\nu$, and the rest is background. Dark brown is DiffB, light brown is DBCascL, dark red is CascL, light grey is LMisID, blue-gray is RealD, grey is Comb, and dark grey is Cont.

8 Constraints on variables in the fit

8.1 f_{+0}

We put constraint on f_{+0}, the B^+B^--$B^0\bar{B}^0$ production ratio (section 5.1). The measured value is [32]

$$f_{+0} = 1.006 \pm 0.036 \pm 0.031 = 1.006 \pm 0.0475 \tag{155}$$

Thus, we add the following term to the χ^2

$$\frac{(f_{+0} - 1.006)^2}{0.0475^2} \tag{156}$$

8.2 C_{+0}

This term is in χ^2 (section 4.3) to account for possible MC modelling difference between D^0 and D^+. Thus this is expected to be $C_{+0} = 1$. We put Gaussian constraint on this vale to avoid unnecessary correlation with branching fractions in the fit. As a size of deviation of C_{+0} from 1, we take the uncertainty of the ratio of $\mathcal{B}(D^0 \to K^-\pi^+)$ and $\mathcal{B}(D^+ \to K^-\pi^+\pi^+)$ measurements from CLEO-c [22]:

$$\begin{aligned} \mathcal{B}(D^0 \to K^-\pi^+) &= 0.0391 \pm 0.0007 \pm 0.0009 = 0.0391 \pm 0.00114 \\ \mathcal{B}(D^+ \to K^-\pi^+\pi^+) &= 0.095 \pm 0.002 \pm 0.003 = 0.095 \pm 0.0036 \end{aligned} \tag{157}$$

Hence, the uncertainty is

$$\sqrt{\left(\frac{0.00114}{0.0391}\right)^2 + \left(\frac{0.0036}{0.095}\right)^2} = 0.048 \tag{158}$$

Thus, we add the following term to the χ^2 to constrain C_{+0}

$$\frac{(C_{+0} - 1)^2}{0.048^2} \tag{159}$$

8.3 D^* decay branching fractions

We use CLEO-c values [22]

$$\begin{aligned} B_{Dp} &= 0.095 \pm 0.005 \\ B_{D0} &= 0.0391 \pm 0.0017 \end{aligned} \tag{160}$$

8.4 D^{**} decay branching fractions

For D_0^*, D_1 and D_1', based on isospin symmetry

$$\begin{aligned}
B_{DD0pDPp} &= 2B_{DD0pDP0} \\
B_{DD00DPp} &= 2B_{DD00DP0} \\
B_{DD1pDSPp} &= 2B_{DD1pDSP0} \\
B_{DD10DSPp} &= 2B_{DD10DSP0} \\
B_{DDP1pDSPp} &= 2B_{DDP1pDSP0} \\
B_{DDP10DSPp} &= 2B_{DDP10DSP0}
\end{aligned} \tag{161}$$

Thus, we use

$$\begin{aligned}
&B_{DD0pDPp} = B_{DD00DPp} = B_{DD1pDSPp} = B_{DD10DSPp} \\
&= B_{DDP1pDSPp} = B_{DDP10DSPp} = 0.6667
\end{aligned} \tag{162}$$

and

$$\begin{aligned}
&B_{DD0pDP0} = B_{DD00DP0} = B_{DD1pDSP0} = B_{DD10DSP0} \\
&= B_{DDP1pDSP0} = B_{DDP10DSP0} = 0.3333
\end{aligned} \tag{163}$$

For D_2^*, from isospin symmetry

$$\begin{aligned}
B_{DD2pDPp} &= 2B_{DD2pDP0} \\
B_{DD2pDSPp} &= 2B_{DD2pDSP0} \\
B_{DD20DPp} &= 2B_{DD20DP0} \\
B_{DD20DSPp} &= 2B_{DD20DSP0}
\end{aligned} \tag{164}$$

From PDG

$$\frac{B_{DD2pDPp}}{B_{DD2pDSPp}} = 1.9 \pm 1.1 \pm 0.3 \tag{165}$$

$$\frac{B_{DD20DPp}}{B_{DD20DSPp}} = 2.3 \pm 0.6 \tag{166}$$

By isospin symmetry, these two numbers are supposed to be same. Thus, we take an average and get

$$\begin{aligned}
f_{DD2} \equiv \frac{B_{DD2pDPp}}{B_{DD2pDSPp}} &= \frac{B_{DD20DPp}}{B_{DD20DSPp}} \\
&= 2.1 \pm 0.644
\end{aligned} \tag{167}$$

Hence, branching fractions are

$$B_{DD2pDPp} = B_{DD20DPp} = \frac{2f_{DD2}}{3(1+f_{DD2})} = 0.452 \pm 0.167 \tag{168}$$

$$B_{DD2pDP0} = B_{DD20DP0} = \frac{f_{DD2}}{3(1+f_{DD2})} = 0.226 \pm 0.084 \tag{169}$$

$$B_{DD2pDSPp} = B_{DD20DSPp} = \frac{2}{3(1+f_{DD2})} = 0.215 \pm 0.045 \tag{170}$$

$$B_{DD2pDSP0} = B_{DD20DSP0} = \frac{1}{3(1+f_{DD2})} = 0.107 \pm 0.022 \tag{171}$$

$$\tag{172}$$

8.5 $B \to D^{(*)}\ell\nu$ decay branching fractions

As described in Appendix D, decay ratios can be related by isospin symmetry. In order to apply the isospin symmetry to branching fractions, we need lifetime ratios. The ratio of B lifetimes τ_{B^+} and τ_{B^0} is [10]

$$t_{+0} \equiv \frac{\tau_{B^+}}{\tau_{B^0}} = 1.071 \pm 0.009 \tag{173}$$

Relations between B branching fractions are

$$B_{BpD} = t_{+0} B_{B0D} \tag{174}$$

$$B_{BpDS} = t_{+0} B_{B0DS} \tag{175}$$

We perform fitting with and without these constraints.

8.6 $B \to D^{**}\ell\nu$ and $B \to D^{(*)}\pi\ell\nu$ decay branching fractions

Our fitting method does not have the sensitivity to determine all 16 branching fractions of $B \to D^{**}\ell\nu$ and $B \to D^{(*)}\pi\ell\nu$ decays. Thus, we need constraints to reduce free parameters. Available measurements of these decay modes are very limited. Currently we have only three usable results. One is from PDG [10]

$$B_{BpDD1} = 0.0056 \pm 0.0013 \pm 0.0009 = 0.0056 \pm 0.00158 \tag{176}$$

Next is from the most recent Babar measurement [11]

$$\begin{aligned}
B_{BpDD1} &= 0.00448 \pm 0.00026 \pm 0.00035 = 0.00448 \pm 0.000436 \\
B_{BpDD2} &= 0.00354 \pm 0.00032 \pm 0.00054 = 0.00354 \pm 0.000627 \\
B_{B0DD1} &= 0.00364 \pm 0.00032 \pm 0.00049 = 0.00364 \pm 0.000585 \\
B_{B0DD2} &= 0.00270 \pm 0.00035 \pm 0.00043 = 0.00270 \pm 0.000554
\end{aligned} \tag{177}$$

The last one is also from PDG [10]

$$\begin{aligned}
&\mathcal{B}(B^+ \to D^-\pi^+\ell^+\nu) = 0.0053 \pm 0.0009 \pm 0.0005 = 0.0053 \pm 0.0010 \\
&\mathcal{B}(B^+ \to D^{*-}\pi^+\ell^+\nu) = 0.0064 \pm 0.0015 \pm 0.0002 = 0.0064 \pm 0.0015 \\
&\mathcal{B}(B^0 \to \bar{D}^0\pi^-\ell^+\nu) = 0.0032 \pm 0.0009 \pm 0.0003 = 0.0032 \pm 0.00095 \\
&\mathcal{B}(B^0 \to \bar{D}^{*0}\pi^-\ell^+\nu) = 0.0065 \pm 0.0015 \pm 0.0005 = 0.0065 \pm 0.0016
\end{aligned} \tag{178}$$

These values are based on a BELLE measurement [12] and $B \to D^{**}\ell\nu$ decays are included in those branching fractions. As we show in the following sections. It is convenient to divide $B \to D^{**}\ell\nu$ and $B \to D^{(*)}\pi\ell\nu$ decay branching fractions into three categories : $B \to D_1\ell\nu$ and $B \to D_2^*\ell\nu$, $B \to D_0^*\ell\nu$ and $B \to D\pi\ell\nu$, and $B \to D_1'\ell\nu$ and $B \to D^*\pi\ell\nu$.

8.6.1 $B \to D_1\ell\nu$ and $B \to D_2^*\ell\nu$

There are 4 branching fractions in these decay modes. We define a few parameters and relate the 4 branching fractions to those. Based on isospin symmetry

$$\begin{aligned}
B_{BpDD1} &= t_{+0}B_{B0DD1} \\
B_{BpDD2} &= t_{+0}B_{B0DD2}
\end{aligned} \tag{179}$$

The Babar results (Equation (177)) show that isospin symmetry holds. Thus, we take averages to get

$$\begin{aligned}
B_{BpDD1} &= \tfrac{1}{2}\left[(0.00448 \pm 0.000436) + (0.00364 \pm 0.000585) \times (1.071 \pm 0.009)\right] \\
&= 0.00419 \pm 0.000382
\end{aligned} \tag{180}$$

and

$$
\begin{aligned}
B_{BpDD2} &= \tfrac{1}{2}\left[(0.00354 \pm 0.000627) + (0.00270 \pm 0.000554) \times (1.071 \pm 0.009)\right] \\
&= 0.003215 \pm 0.000432
\end{aligned}
\tag{181}
$$

Thus, if we define a total branching fraction

$$
\begin{aligned}
B_{BpDD12T} &\equiv B_{BpDD1} + B_{BpDD2} \\
&= (0.00419 \pm 0.000382) + (0.003215 \pm 0.000432) \\
&= 0.007405 \pm 0.000577
\end{aligned}
\tag{182}
$$

We also define a ratio

$$
\begin{aligned}
f_{BpDD12} &\equiv \frac{B_{BpDD2}}{B_{BpDD1}} = \frac{0.003215 \pm 0.000432}{0.00419 \pm 0.000382} \\
&= 0.767 \pm 0.125
\end{aligned}
\tag{183}
$$

We can relate 4 branching fractions to f_{BpDD12} and $B_{BpDD12T}$

$$
B_{BpDD1} = \frac{1}{1 + f_{BpDD12}} B_{BpDD12T} \tag{184}
$$

$$
B_{B0DD1} = \frac{B_{BpDD1}}{t_{+0}} = \frac{1}{t_{+0}(1 + f_{BpDD12})} B_{BpDD12T} \tag{185}
$$

$$
B_{BpDD2} = f_{BpDD12} B_{BpDD1} = \frac{f_{BpDD12}}{1 + f_{BpDD12}} B_{BpDD12T} \tag{186}
$$

$$
B_{B0DD2} = \frac{B_{BpDD2}}{t_{+0}} = \frac{B_{BpDD2}}{t_{+0}(1 + f_{BpDD12})} B_{BpDD12T} \tag{187}
$$

8.6.2 $B \to D_0^* \ell\nu$ and non-resonant $B \to D\pi\ell\nu$

There are 6 branching fractions in this category. As in the previous section, we define a few parameters and relate the 6 branching fractions to those parameters. Isospin symmetry gives

$$
\begin{aligned}
&B_{BpDD0} = t_{+0} B_{B0DD0} \\
&B_{BpDPp} = 2B_{BpDP0} = t_{+0} B_{B0DPp} = 2t_{+0} B_{B0DP0} \\
&\mathcal{B}(B^+ \to D^- \pi^+ \ell^+ \nu) = t_{+0} \mathcal{B}(B^0 \to \bar{D}^0 \pi^- \ell^+ \nu)
\end{aligned}
\tag{188}
$$

Thus, we take an average to get

$$
\begin{aligned}
B_{BpDPiT} &\equiv \mathcal{B}(B^+ \to D^-\pi^+\ell^+\nu) \\
&= \frac{1}{2}\left[(0.0053 \pm 0.0010) + (0.00323 \pm 0.00095) \times (1.071 \pm 0.009)\right] \\
&= 0.00438 \pm 0.00071 \qquad (189)
\end{aligned}
$$

Since $B \to D^{**}\ell\nu$ decays are included in these branching fractions,

$$
\begin{aligned}
B_{BpDPiT} &= B_{BpDD0}B_{DD00DPp} + B_{BpDD2}B_{DD20DPp} + B_{BpDPp} \\
&= B_{BpDD0} \times \tfrac{2}{3} + B_{BpDD2}B_{DD2pDPp} + B_{BpDPp}
\end{aligned} \qquad (190)
$$

Using equations (168) and (181),

$$
\begin{aligned}
B_{BpDPp} + \tfrac{2}{3}B_{BpDD0} &= B_{BpDPiT} - B_{BpDD2}B_{DD2pDPp} \\
&= (0.00438 \pm 0.00071) - (0.003215 \pm 0.000432) \times (0.452 \pm 0.167) \\
&= 0.00293 \pm 0.00091
\end{aligned} \qquad (191)
$$

Thus, if we define a total branching fraction

$$
\begin{aligned}
B_{BpDPiDD0T} &\equiv B_{BpDD0} + B_{BpDPp} + B_{BpDP0} = B_{BpDD0} + \tfrac{3}{2}B_{BpDPp} \\
&= \tfrac{3}{2}(0.00293 \pm 0.00091) = 0.0044 \pm 0.0014
\end{aligned} \qquad (192)
$$

We also define a ratio

$$
f_{BpDPiDD0} \equiv \frac{B_{BpDPp}}{B_{BpDD0}} \qquad (193)
$$

Using these three raqtios, we can relate 6 branching fractions to $B_{BpDSPiDDP1T}$

$$
B_{BpDD0} = \frac{2}{2 + 3f_{BpDPiDD0}}B_{BpDPiDD0T} \qquad (194)
$$

$$
B_{BpDPp} = f_{BpDPiDD0}B_{BpDD0} = \frac{2f_{BpDPiDD0}}{2 + 3f_{BpDPiDD0}}B_{BpDPiDD0T} \qquad (195)
$$

$$
B_{BpDP0} = \frac{B_{BpDPp}}{2} = \frac{f_{BpDPiDD0}}{2 + 3f_{BpDPiDD0}}B_{BpDPiDD0T} \qquad (196)
$$

$$
B_{B0DD0} = \frac{B_{BpDD0}}{t_{+0}} = \frac{2}{t_{+0}(2 + 3f_{BpDPiDD0})}B_{BpDPiDD0T} \qquad (197)
$$

$$
B_{B0DPp} = \frac{B_{BpDPp}}{t_{+0}} = \frac{2f_{BpDPiDD0}}{t_{+0}(2 + 3f_{BpDPiDD0})}B_{BpDPiDD0T} \qquad (198)
$$

$$
B_{B0DP0} = \frac{B_{BpDP0}}{t_{+0}} = \frac{f_{BpDPiDD0}}{t_{+0}(2 + 3f_{BpDPiDD0})}B_{BpDPiDD0T} \qquad (199)
$$

8.6.3 $B \to D_1' \ell\nu$ and non-resonant $B \to D^*\pi\ell\nu$.

From isospin symmetry

$$\begin{aligned} B_{BpDDP1} &= t_{+0} B_{B0DDP1} \\ B_{BpDSPp} &= 2B_{BpDSP0} = t_{+0} B_{B0DSPp} = 2t_{+0} B_{B0DSP0} \\ \mathcal{B}(B^+ \to D^{*-}\pi^+\ell^+\nu) &= t_{+0}\mathcal{B}(B^0 \to \bar{D}^{*0}\pi^-\ell^+\nu) \end{aligned} \tag{200}$$

Thus, we take an average to get

$$\begin{aligned} B_{BpDSPiT} &\equiv \mathcal{B}(B^+ \to D^{*-}\pi^+\ell^+\nu) \\ &= \frac{1}{2}\left[(0.0064 \pm 0.0015) + (0.0065 \pm 0.0016) \times (1.071 \pm 0.009)\right] \\ &= 0.00668 \pm 0.00114 \end{aligned} \tag{201}$$

Since $B \to D^{**}\ell\nu$ decays are included in those branching fractions,

$$\begin{aligned} B_{BpDSPiT} &= B_{BpDD1} B_{DD10DSPp} + B_{BpDDP1} B_{DDP10DSPp} \\ &\quad + B_{BpDD2} B_{DD20DSPp} + B_{BpDSPp} \\ &= \tfrac{2}{3} B_{BpDD1} + \tfrac{2}{3} B_{BpDDP1} + B_{BpDD2} B_{DD2pDSPp} + B_{BpDSPp} \end{aligned} \tag{202}$$

Using equations (180), (170) and (181),

$$\begin{aligned} B_{BpDSPp} + \tfrac{2}{3} B_{BpDDP1} &= B_{BpDSPiT} - \tfrac{2}{3} B_{BpDD1} - B_{BpDD2} B_{DD2pDSPp} \\ &= (0.00668 \pm 0.00114) - \tfrac{2}{3} \times (0.00419 \pm 0.000382) \\ &\quad -(0.003215 \pm 0.000432) \times (0.215 \pm 0.045) \\ &= 0.00319 \pm 0.00118 \end{aligned} \tag{203}$$

Thus, if we define a total branching fraction

$$\begin{aligned} B_{BpDSPiDDP1T} &\equiv B_{BpDDP1} + B_{BpDSPp} + B_{BpDSP0} = B_{BpDDP1} + \tfrac{3}{2} B_{BpDSPp} \\ &= \tfrac{3}{2}(0.00319 \pm 0.00118) = 0.0048 \pm 0.0018 \end{aligned} \tag{204}$$

We also define a ratio

$$f_{BpDSPiDDP1} \equiv \frac{B_{BpDDP1}}{B_{BpDSPp}} \tag{205}$$

We can relate the 6 branching fractions to $B_{BpDSPiDDP1T}$ and $B_{BpDSPiDDP1T}$

$$B_{BpDDP1} = \frac{2}{2+3f_{BpDSPiDDP1}} B_{BpDSPiDDP1T} \tag{206}$$

$$\begin{aligned} B_{BpDSPp} &= f_{BpDSPiDDP1} B_{BpDDP1} \\ &= \frac{2f_{BpDSPiDDP1}}{2+3f_{BpDSPiDDP1}} B_{BpDSPiDDP1T} \end{aligned} \tag{207}$$

$$\begin{aligned} B_{BpDSP0} &= \frac{B_{BpDSPp}}{2} \\ &= \frac{f_{BpDSPiDDP1}}{2+3f_{BpDSPiDDP1}} B_{BpDSPiDDP1T} \end{aligned} \tag{208}$$

$$\begin{aligned} B_{B0DDP1} &= \frac{B_{BpDDP1}}{t_{+0}} \\ &= \frac{2}{t_{+0}(2+3f_{BpDSPiDDP1})} B_{BpDSPiDDP1T} \end{aligned} \tag{209}$$

$$\begin{aligned} B_{B0DSPp} &= \frac{B_{BpDSPp}}{t_{+0}} \\ &= \frac{2f_{BpDSPiDDP1}}{t_{+0}(2+3f_{BpDSPiDDP1})} B_{BpDSPiDDP1T} \end{aligned} \tag{210}$$

$$\begin{aligned} B_{B0DSP0} &= \frac{B_{BpDSP0}}{t_{+0}} \\ &= \frac{f_{BpDSPiDDP1}}{t_{+0}(2+3f_{BpDSPiDDP1})} B_{BpDSPiDDP1T} \end{aligned} \tag{211}$$

8.6.4 $B \to D^{**}\ell\nu$ and non-resonant $B \to D^{(*)}\pi\ell\nu$

We define a total branching fraction

$$B_{BpDDPiT} \equiv B_{BpDD12T} + B_{BpDPiDD0T} + B_{BpDSPiDDP1T} \tag{212}$$

We also define two ratios

$$\begin{aligned} f_{BpDPiDD12} \equiv \frac{B_{BpDPiDD0T}}{B_{BpDD12T}} &= \frac{3}{2}\frac{0.00293 \pm 0.00091}{0.007405 \pm 0.000577} \\ &= 0.59 \pm 0.19 \end{aligned} \tag{213}$$

and

$$\begin{aligned} f_{BpDSPiDD12} \equiv \frac{B_{BpDSPiDDP1T}}{B_{BpDD12T}} &= \frac{3}{2}\frac{0.00319 \pm 0.00118}{0.007405 \pm 0.000577} \\ &= 0.65 \pm 0.24 \end{aligned} \tag{214}$$

Then

$$B_{BpDD12T} = \frac{B_{BpDDPiT}}{1 + f_{BpDPiDD12} + f_{BpDSPiDD12}} \tag{215}$$

$$\begin{aligned} B_{BpDPiDD0T} &= f_{BpDPiDD12} B_{BpDD12T} \\ &= \frac{f_{BpDPiDD12} B_{BpDDPiT}}{1 + f_{BpDPiDD12} + f_{BpDSPiDD12}} \end{aligned} \tag{216}$$

$$\begin{aligned} B_{BpDSPiDDP1T} &= f_{BpDSPiDD12} B_{BpDD12T} \\ &= \frac{f_{BpDSPiDD12} B_{BpDDPiT}}{1 + f_{BpDPiDD12} + f_{BpDSPiDD12}} \end{aligned} \tag{217}$$

Substituting these into equations (184)-(187), (194)-(199) and (206)-(211),

$$B_{BpDD1} = \frac{B_{BpDDPiT}}{(1 + f_{BpDD12})(1 + f_{BpDPiDD12} + f_{BpDSPiDD12})} \tag{218}$$

$$B_{BpDD2} = f_{BpDD12} B_{BpDD1} \tag{219}$$

$$B_{BpDD0} = \frac{2 f_{BpDPiDD12} B_{BpDDPiT}}{(2 + 3 f_{BpDPiDD0})(1 + f_{BpDPiDD12} + f_{BpDSPiDD12})} \tag{220}$$

$$B_{BpDDP1} = \frac{2 f_{BpDSPiDD12} B_{BpDDPiT}}{(2 + 3 f_{BpDSPiDDP1})(1 + f_{BpDPiDD12} + f_{BpDSPiDD12})} \tag{221}$$

$$B_{BpDPp} = f_{BpDPiDD0} B_{BpDD0} \tag{222}$$

$$B_{BpDP0} = \frac{B_{BpDPp}}{2} \tag{223}$$

$$B_{BpDSPp} = f_{BpDSPiDDP1} B_{BpDDP1} \tag{224}$$

$$B_{BpDSP0} = \frac{B_{BpDSPp}}{2} \tag{225}$$

and

$$B_{B0DD1} = \frac{B_{BpDD1}}{t_{+0}} \tag{226}$$

$$B_{B0DD2} = \frac{B_{BpDD2}}{t_{+0}} \tag{227}$$

$$B_{B0DD0} = \frac{B_{BpDD0}}{t_{+0}} \tag{228}$$

$$B_{B0DDP1} = \frac{B_{BpDDP1}}{t_{+0}} \tag{229}$$

$$B_{B0DPp} = \frac{B_{BpDPp}}{t_{+0}} \tag{230}$$

$$B_{B0DP0} = \frac{B_{BpDP0}}{t_{+0}} \tag{231}$$

$$B_{B0DSPp} = \frac{B_{BpDSPp}}{t_{+0}} \tag{232}$$

$$B_{B0DSP0} = \frac{B_{BpDSP0}}{t_{+0}} \tag{233}$$

Thus, we bave only one branching fraction, $B_{BpDDPiT}$, to be determined by the fit. We also have five ratios. Three of them are

$$f_{BpDD12} = 0.767 \pm 0.125 \tag{234}$$

$$f_{BpDPiDD12} = 0.911 \pm 0.308 \tag{235}$$

$$f_{BpDSPiDD12} = 0.992 \pm 0.390 \tag{236}$$

These ratios may be floated in the fit with Gaussian constraints. No usuful measurement to determine the ratios $f_{BpDPiDD0}$ and $f_{BpDSPiDDP1}$. Only values available are from MC. SP5/SP6 uses

$$\begin{aligned} B_{BpDD0} = 0.0020, \quad & B_{BpDPp} = 0.0060 \\ B_{BpDDP1} = 0.0037, \quad & B_{BpDSPp} = 0.0020 \end{aligned} \tag{237}$$

Thus,

$$f_{BpDPiDD0} = 60/20 = 3.0, \quad f_{BpDSPiDDP1} = 20/37 = 0.54 \tag{238}$$

We cannot rely on these values. Hence, we need either to float or to determine them in the fitting procedure. Details are in section 10.

9 Validation of fit

To validate our fitting method, we use Run3 MC. We split Run3 MC into two halves. We use the first half as a fake data. We create MC histograms from the second half, and fit the fake data by the MC histograms. We then perform fitting in a few different settings

9.1 Case 1 : FF slope fixed

First case of validation fitting is

- Use original ISGW2 model for $B \to D\ell\nu$

9.2 Case 2 : FF slope with standard parametrization

Second case of validation fitting is

- Use HQEF model for $B \to D\ell\nu$ with standard parametrization:

$$h_+(w) = h_+(1)[1 - \rho_D^2(w-1)] \tag{239}$$

9.3 Case 3 : FF slope with new parametrization

Third case of validation fitting is

- Use HQEF model for $B \to D\ell\nu$ with new parametrization:

$$h_+(w) = h_+(1)[1 - 8\rho_D^2 z + (51\rho_D^2 - 10)z^2 - (252\rho_D^2 - 84)z^3] \tag{240}$$

9.4 Case 4 : float all ratios

Third case of validation fitting is

- Use HQEF model for $B \to D\ell\nu$ with new parametrization:
- Float all five ratios : f_{BpDD12}, $f_{BpDPiDD0}$, $f_{BpDSPiDDP1}$, $f_{BpDPiDD12}$ and $f_{BpDSPiDD12}$.

10 Fit results

10.1 Constraints on $f_{BpDPiDD0}$ and $f_{BpDSPiDDP1}$

We performed the fit by floating two ratios $f_{BpDPiDD0}$ and $f_{BpDSPiDDP1}$ (see section 8.6). $f_{BpDPiDD0}$ settled at around 0.5 and $f_{BpDSPiDDP1}$ tend to go to infinity. $f_{BpDSPiDDP1} = \infty$ is not realistic. We think $f_{BpDSPiDDP1}$ goes to infinity because the MC shape of $B \to D_1^* \ell\nu$ and/or $B \to D^* \pi \ell\nu$ histograms is not really reflect the data. Thus, in order to avoid infinity we assume

$$\begin{aligned} f_{BpDPiDD0} &= 1 \pm 2 \\ f_{BpDSPiDDP1} &= 5 \pm 10 \end{aligned} \tag{241}$$

and put Gaussian constraints on $f_{BpDPiDD0}$ and $f_{BpDSPiDDP1}$ in the fit. The effect of this assumption is examined in the systematic uncertainty section (section 11).

10.2 Fit result

11 Systematic Uncertainties

12 Conclusion

13 Acknowledgements

A Decay modes to consider

A.1 Semileptonic $B \to D^{(*,**)}\ell\nu$ decays

A.1.1 Semileptonic B^+ decays

There are three types of decay modes (Figure 25).

- $B^+ \to \bar{D}^{(*,**)0}\ell^+\nu_\ell$
- $B^+ \to \bar{D}^{(*)0}\pi^0\ell^+\nu_\ell$
- $B^+ \to D^{(*)-}\pi^+\ell^+\nu_\ell$

A.1.2 Semileptonic B^0 decays

There are three types of decay modes (Figure 26).

- $B^0 \to D^{(*,**)-}\ell^+\nu_\ell$
- $B^0 \to D^{(*)-}\pi^0\ell^+\nu_\ell$
- $B^0 \to \bar{D}^{(*)0}\pi^-\ell^+\nu_\ell$

A.2 D^* and D^{**} decays

A.2.1 $D^{*,**+}$ decays

There are three types of decay modes (Figure 27).

- $D^{*,**+} \to D^{(*)0}\pi^+$
- $D^{*,**+} \to D^{(*)+}\pi^0$
- $D^{*,**+} \to D^{(*)+}\gamma$

Note that $D^{**+} \to D^{*+}\gamma$ is an electromagnetic process. Thus, it is negligible compared to strong processes. In case of $D^{*+} \to D^{*+}\gamma$, becasue strong processes are suppressed by phase space, the EM process ampritude has comparable size to strong processes.

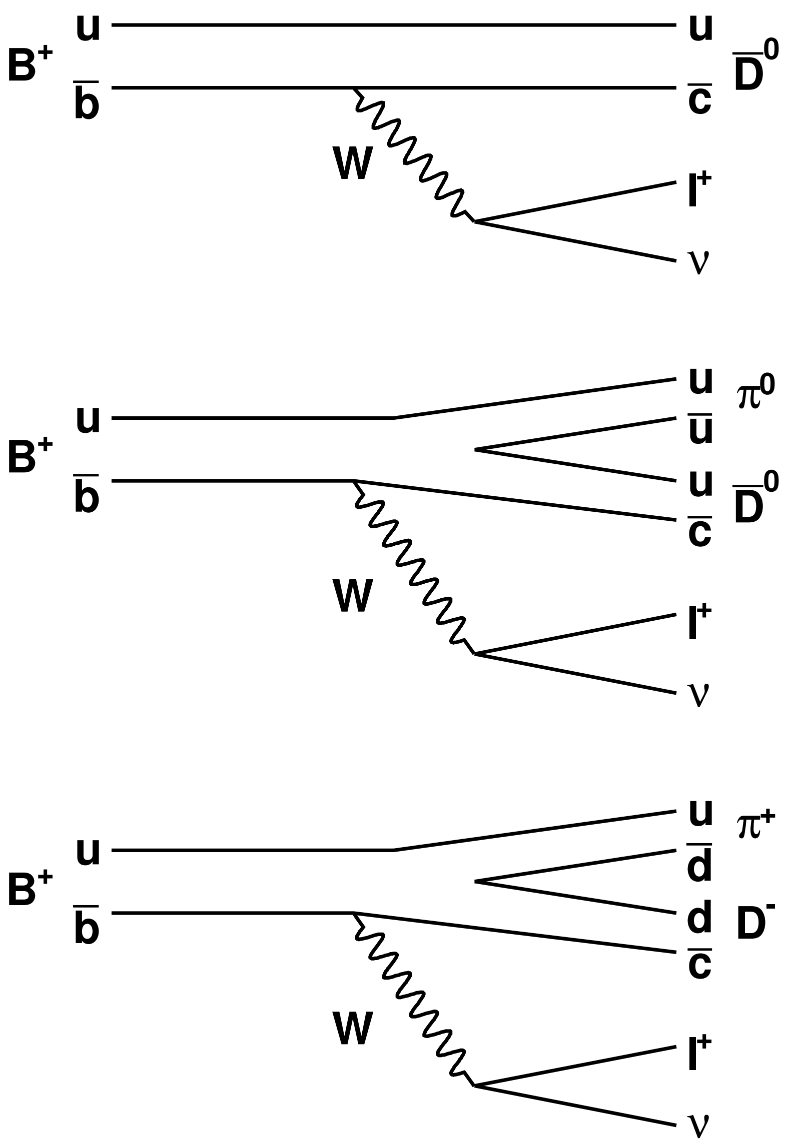

Figure 25: Feynman diagrams of semileptonic $B^+ \to D^{(*,**)}\ell\nu$ decays

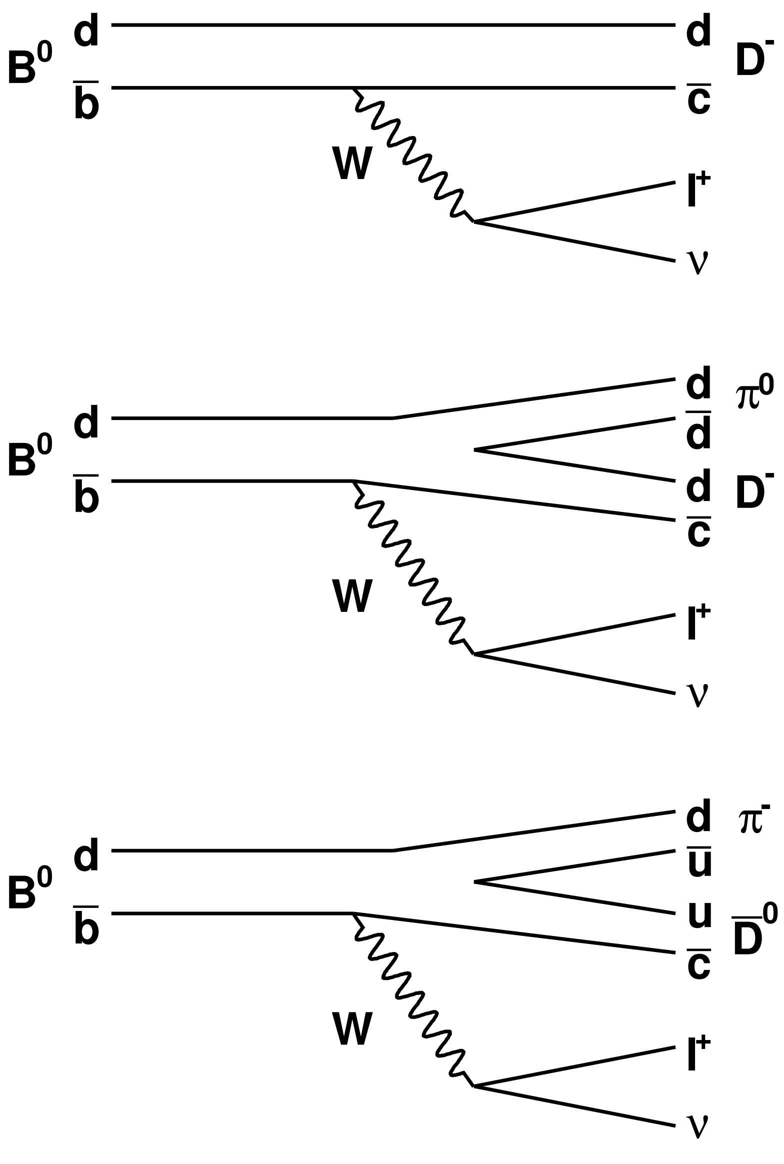

Figure 26: Feynman diagrams of semileptonic $B^0 \to D^{(*,**)}\ell\nu$ decays

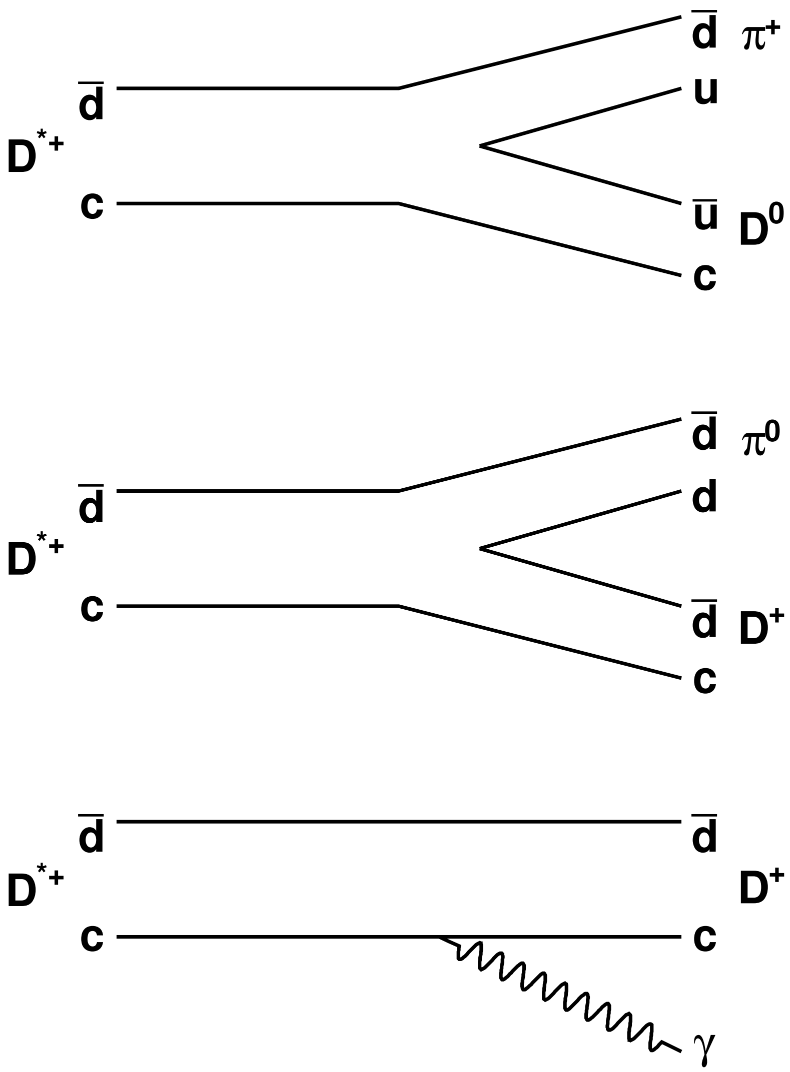

Figure 27: Feynman diagrams of $D^{*,**+}$ decays

A.2.2 $D^{*,**0}$ decays

There are three types of decay modes (Figure 28).

- $D^{*,**0} \to D^{(*)+}\pi^-$
- $D^{*,**0} \to D^{(*)0}\pi^0$
- $D^{*,**0} \to D^{(*)0}\gamma$

Note that

- $D^{*0} \to D^+\pi^-$ is not allowed
  because $m_{D^{*0}} < m_{D^+} + m_{\pi^-}$
- $D^{**0} \to D^{*0}\gamma$ is negligible

A.3 D^0 and D^+ decays

A.3.1 D^0 decays

There are four decay modes used in the reconstruction of D^0 (Figure 29).

- $D^0 \to K^-\pi^+$
- $D^0 \to K^-\pi^+\pi^+\pi^-$
- $D^0 \to K^-\pi^+\pi^0$
- $D^0 \to K_s^0\pi^+\pi^-$

A.3.2 D^+ decays

There are two decay modes used in the reconstruction of D^+ (Figure 30).

- $D^+ \to K^-\pi^+\pi^+$
- $D^+ \to \bar{K}_s^0\pi^+$

A.3.3 π^0 and K_s^0

π^0 is reconstructed from 2γ.
K_s^0 is reconstructed from $\pi^0\pi^0$ or $\pi^+\pi^-$.

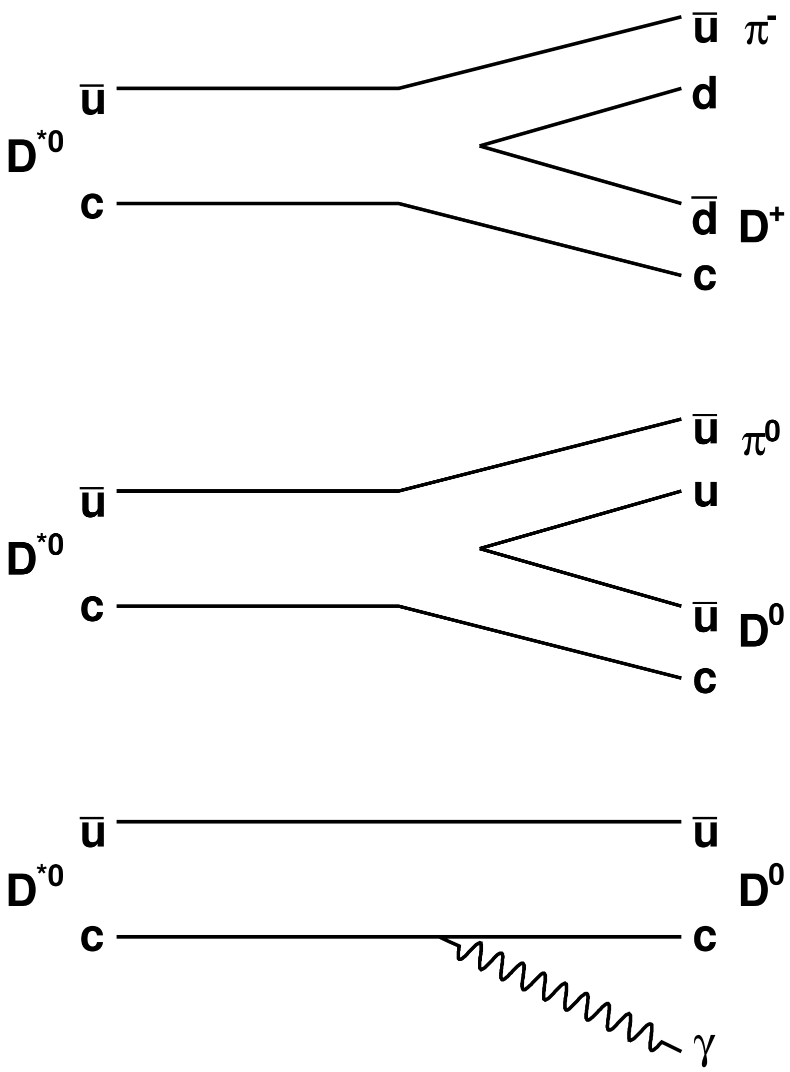

Figure 28: Feynman diagrams of $D^{*,**0}$ decays

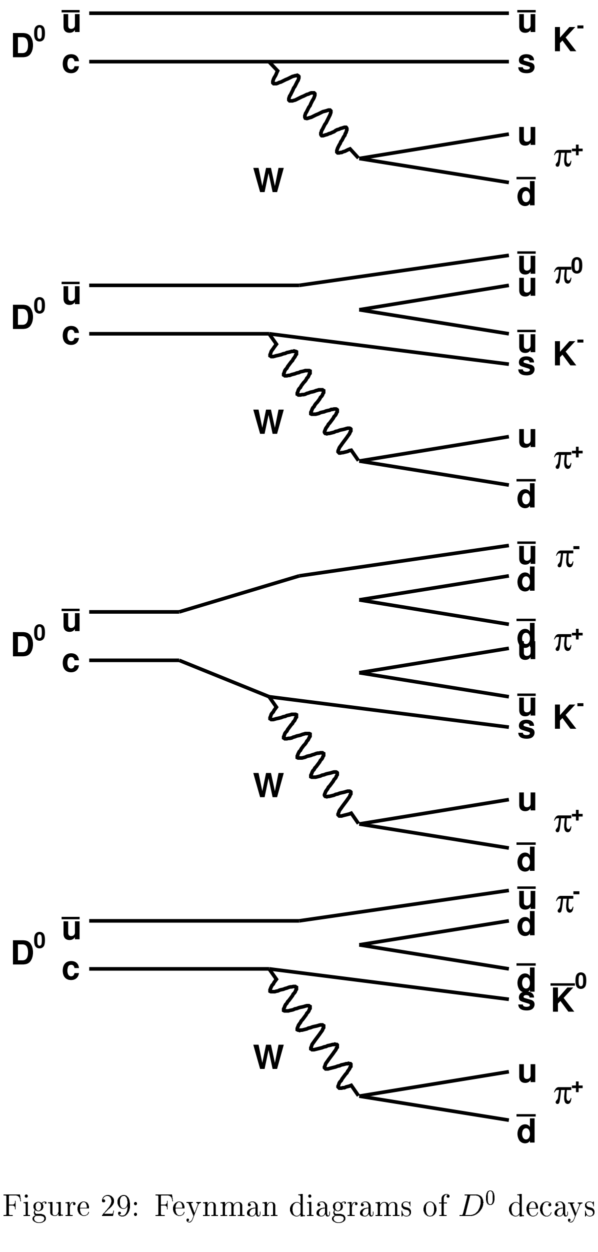

Figure 29: Feynman diagrams of D^0 decays

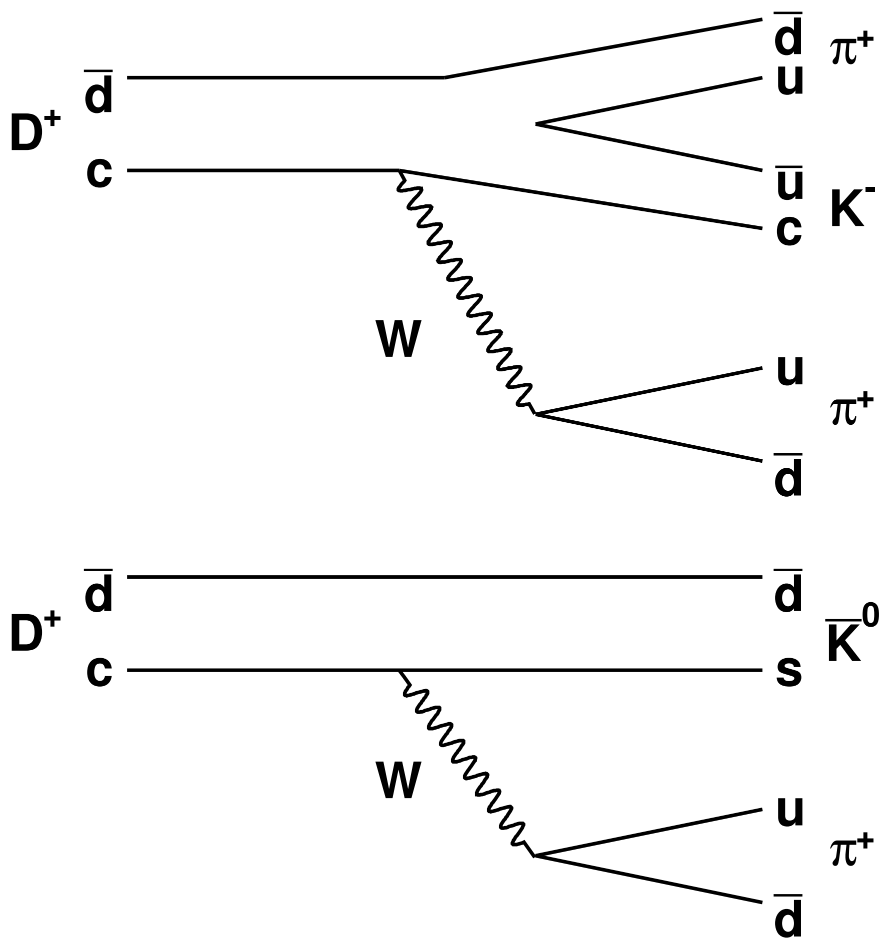

Figure 30: Feynman diagrams of D^+ decays

A.4 Decay chain

A.4.1 B^+ decay chain

1. $B^+ \to \bar{D}^0 \ell^+ \nu_\ell$ (D^0)
2. $B^+ \to \bar{D}^{*0} \ell^+ \nu_\ell$
   - $D^- \pi^+$ (not possible)
   - $\bar{D}^0 \pi^0$ (D^0)
   - $\bar{D}^0 \gamma$ (D^0)
3. $B^+ \to \bar{D}^{**0} \ell^+ \nu_\ell$
   - $D^- \pi^+$ (D^+)
   - $\bar{D}^0 \pi^0$ (D^0)
   - $\bar{D}^0 \gamma$ (D^0)
   - $D^{*-} \pi^+$
     - $\bar{D}^0 \pi^-$ (D^0)
     - $D^- \pi^0$ (D^+)
     - $D^- \gamma$ (D^+)
   - $\bar{D}^{*0} \pi^0$
     - $D^- \pi^+$ (D^+)
     - $\bar{D}^0 \pi^0$ (D^0)
     - $\bar{D}^0 \gamma$ (D^0)
   - $\bar{D}^{*0} \gamma$ (negligible)

4. $B^+ \to \bar{D}^0 \pi^0 \ell^+ \nu_\ell$ (D^0)
5. $B^+ \to D^- \pi^+ \ell^+ \nu_\ell$ (D^+)
6. $B^+ \to \bar{D}^{*0} \pi^0 \ell^+ \nu_\ell$
   - $\to D^- \pi^+$ (not possible)
   - $\to \bar{D}^0 \pi^0$ (D^0)
   - $\to \bar{D}^0 \gamma$ (D^0)
7. $B^+ \to D^{*-} \pi^+ \ell^+ \nu_\ell$
   - $\to \bar{D}^0 \pi^-$ (D^0)
   - $\to D^- \pi^0$ (D^+)
   - $\to D^- \gamma$ (D^+)

A.4.2 B^0 decay chain

1. $B^0 \to D^- \ell^+ \nu_\ell$ (D^0)
2. $B^0 \to D^{*-} \ell^+ \nu_\ell$
   - $\to \bar{D}^0 \pi^-$ (D^0)
   - $\to D^- \pi^0$ (D^+)
   - $\to D^- \gamma$ (D^+)

3. $B^0 \to D^{**-}\ell^+\nu_\ell$
   - $\to \bar{D}^0\pi^-$ (D^0)
   - $\to D^-\pi^0$ (D^+)
   - $\to D^-\gamma$ (D^+)
   - $\to D^{*-}\pi^0$
     - $\to \bar{D}^0\pi^-$ (D^0)
     - $\to D^-\pi^0$ (D^+)
     - $\to D^-\gamma$ (D^+)
   - $\to \bar{D}^{*0}\pi^-$
     - $\to D^-\pi^+$ (not possible)
     - $\to \bar{D}^0\pi^0$ (D^0)
     - $\to \bar{D}^0\gamma$ (D^0)
   - $\to \bar{D}^{*-}\gamma$ (negligible)
4. $B^0 \to D^-\pi^0\ell^+\nu_\ell$ (D^+)
5. $B^0 \to \bar{D}^0\pi^-\ell^+\nu_\ell$ (D^0)
6. $B^0 \to D^{*-}\pi^0\ell^+\nu_\ell$
   - $\to \bar{D}^0\pi^-$ (D^0)
   - $\to D^-\pi^0$ (D^+)
   - $\to D^-\gamma$ (D^+)

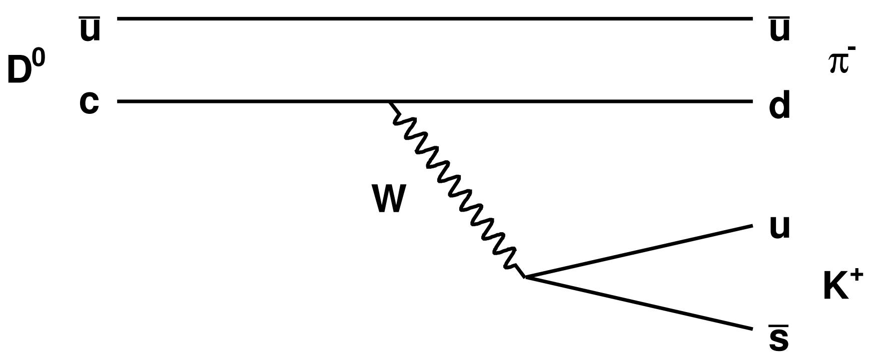

Figure 31: Feynman diagram of a doubly Cabbibo suppressed D^+ decay.

7. $B^0 \to \bar{D}^{*0}\pi^-\ell^+\nu_\ell$

$\to D^-\pi^+$	(not possible)
$\to \bar{D}^0\pi^0$	(D^0)
$\to \bar{D}^0\gamma$	(D^0)

A.5 Background

A.5.1 $B \to D^{(*)}\bar{D}^{(*)}(K)$

The typical decay modes and branching fractions are given in Table 9.

A.5.2 Doubly Cabbibo suppressed D decay

The decay $D^0 \to K^+\pi^-$ is shown in Figure 31 as an example of this type of decay

Decay mode	Branching fraction ($\times 10^{-3}$)
$B^+ \to \bar{D}^0 D^{*+}$	0.46 ± 0.09
$B^+ \to \bar{D}^0 D^+$	0.48 ± 0.10
$B^+ \to \bar{D}^0 D^{*+} K^0$	5.2 ± 1.2
$B^+ \to \bar{D}^{*0} D^{*+} K^0$	7.8 ± 2.6
$B^+ \to \bar{D}^0 D^0 K^+$	1.37 ± 0.32
$B^+ \to \bar{D}^0 D^{*0} K^+$	4.7 ± 1.0
$B^+ \to \bar{D}^{*0} D^{*0} K^+$	5.3 ± 1.6
$B^+ \to D^{*-} D^+ K^+$	1.5 ± 0.4
$B^0 \to D^{*+} D^{*-}$	8.3 ± 1.1
$B^0 \to D^{*-} D^+$ or $D^- D^{*+}$	9.3 ± 1.5
$B^0 \to D^- D^0 K^+$	1.7 ± 0.4
$B^0 \to D^- D^{*0} K^+$	4.6 ± 1.0
$B^0 \to D^{*-} D^0 K^+$	$3.1^{+0.6}_{-0.5}$
$B^0 \to D^{*-} D^{*0} K^+$	11.8 ± 2.0
$B^0 \to D^{*-} D^+ K^0$ or $D^- D^{*+} K^0$	6.5 ± 1.6
$B^0 \to D^{*-} D^{*+} K^0$	8.8 ± 1.9

Table 9: Branching fractions of typical $B \to D^{(*)} \bar{D}^{(*)} (K)$ decays [10].

B Numerical values used in MC and fitting

The values used in SP5/SP6 MC are given in Tables 10-18. Used values in the fit are given in relevant sections in the text.

B.1 Measured $B \to D^{(*)}\pi^+\ell^+\nu$ branching fractions

$B \to D^{(*)}\pi^+\ell^+\nu$ branching fractions given in Table 10 and 11 includes not only non-resonant contribution but also $B \to D^{(*)}\pi^+\ell^+\nu$ contributions. Thus,

$$\begin{aligned}\mathcal{B}(B^+ \to D^-\pi^+\ell^+\nu) \\ = B_{BpDD0}B_{DD00DPp} + B_{BpDD2}B_{DD20DPp} + B_{BpDPp}\end{aligned} \tag{242}$$

$$\begin{aligned}\mathcal{B}(B^+ \to D^{*-}\pi^+\ell^+\nu) = B_{BpDD1}B_{DD10DSPp} + B_{BpDDP1}B_{DDP10DSPp} \\ +B_{BpDD2}B_{DD20DSPp} + B_{BpDSPp}\end{aligned} \tag{243}$$

$$\begin{aligned}\mathcal{B}(B^0 \to \bar{D}^0\pi^-\ell^+\nu) \\ = B_{B0DD0}B_{DD0pDPp} + B_{B0DD2}B_{DD2pDPp} + B_{B0DPp}\end{aligned} \tag{244}$$

$$\begin{aligned}\mathcal{B}(B^0 \to \bar{D}^{*0}\pi^-\ell^+\nu) = B_{B0DD1}B_{DD1pDSPp} + B_{B0DDP1}B_{DDP1pDSPp} \\ +B_{B0DD2}B_{DD2pDSPp} + B_{B0DSPp}\end{aligned} \tag{245}$$

Thus, using SP5/SP6 MC values

$$\begin{aligned}\mathcal{B}(B^+ \to D^-\pi^+\ell^+\nu) &= 0.0020 \times 0.6667 + 0.0037 \times 0.459 + 0.0060 \\ &= 0.00903\end{aligned} \tag{246}$$

$$\begin{aligned}\mathcal{B}(B^+ \to D^{*-}\pi^+\ell^+\nu) &= 0.0056 \times 0.6667 + 0.0037 \times 0.6667 \\ &\quad +0.0037 \times 0.209 + 0.0020 \\ &= 0.00897\end{aligned} \tag{247}$$

$$\begin{aligned}\mathcal{B}(B^0 \to \bar{D}^0\pi^-\ell^+\nu) &= 0.0020 \times 0.6667 + 0.0037 \times 0.459 + 0.0060 \\ &= 0.00903\end{aligned} \tag{248}$$

$$\begin{aligned}\mathcal{B}(B^0 \to \bar{D}^{*0}\pi^-\ell^+\nu) &= 0.0056 \times 0.6667 + 0.0037 \times 0.6667 \\ &\quad +0.0037 \times 0.209 + 0.0020 \\ &= 0.00897\end{aligned} \tag{249}$$

Branching fraction	SP5/SP6	Measurement [reference]
B_{BpD}	0.0210	0.0215 ± 0.0022 [10]
B_{BpDS}	0.0560	0.065 ± 0.005 [10]
B_{BpDD0}	0.0020	
B_{BpDD1}	0.0056	$0.0056 \pm 0.0013 \pm 0.0009$ [10]
		$0.00448 \pm 0.00026 \pm 0.00035$ [11]
B_{BpDDP1}	0.0037	
B_{BpDD2}	0.0037	$0.00354 \pm 0.00032 \pm 0.00054$ [11]
B_{BpDPp}	0.0060	
B_{BpDP0}	0.0030	
B_{BpDSPp}	0.0020	
B_{BpDSP0}	0.0010	
$\mathcal{B}(B^+ \to D^- \pi^+ \ell^+ \nu)$	0.00903	$0.0053 \pm 0.0009 \pm 0.0005$ [10]
$\mathcal{B}(B^+ \to D^{*-} \pi^+ \ell^+ \nu)$	0.00897	$0.0064 \pm 0.0015 \pm 0.0002$ [10]

Table 10: B^+ decay branching fractions. "Measurement" is the most recent mesured vlue. Definitions of these notations are given in section 2.3

Branching fraction	SP5/SP6	Measurement [reference]
B_{B0D}	0.0210	0.0213 ± 0.0018 [10]
B_{B0DS}	0.0560	0.0520 ± 0.0024 [10]
B_{B0DD0}	0.0020	
B_{B0DD1}	0.0056	$0.00364 \pm 0.00032 \pm 0.00049$ [11]
B_{B0DDP1}	0.0037	
B_{B0DD2}	0.0037	$0.00270 \pm 0.00035 \pm 0.00043$ [11]
B_{B0DPp}	0.0060	
B_{B0DP0}	0.0030	
B_{B0DSPp}	0.0020	
B_{B0DSP0}	0.0010	
$\mathcal{B}(B^0 \to \bar{D}^0\pi^-\ell^+\nu)$	0.00903	$0.0032 \pm 0.0009 \pm 0.0003$ [10]
$\mathcal{B}(B^0 \to \bar{D}^{*0}\pi^-\ell^+\nu)$	0.00897	$0.0065 \pm 0.0015 \pm 0.0005$ [10]

Table 11: B^0 decay branching fractions. "Measurement" is the most recent mesured vlue. Definitions of these notations are given in section 2.3

Branching fraction	SP5/SP6	Calculated	Used
B_{BpDD1}	0.0056	0.00419 ± 0.000382	
B_{BpDD2}	0.0037	0.003215 ± 0.000432	
$B_{BpDD12T}$	0.0093	0.007405 ± 0.000577	
B_{BpDD0}	0.0020		
B_{BpDPp}	0.0060		
B_{BpDP0}	0.0030		
$B_{BpDPiDD0T}$	0.0110	0.0044 ± 0.0014	
B_{BpDDP1}	0.0037		
B_{BpDSPp}	0.0020		
B_{BpDSP0}	0.0010		
$B_{BpDSPiDDP1T}$	0.0067	0.0048 ± 0.0018	
$B_{BpDDPiT}$	0.0270	0.0166 ± 0.0024	
f_{BpDD12}	$37/56 = 0.66$	0.767 ± 0.125	0.767
$f_{BpDPiDD0}$	$60/20 = 3.0$		
$f_{BpDSPiDDP1}$	$20/37 = 0.54$		
$f_{BpDPiDD12}$	$110/93 = 1.18$	0.59 ± 0.19	0.59
$f_{BpDSPiDD12}$	$67/93 = 0.72$	0.65 ± 0.24	0.65

Table 12: $B^+ \to D^{**}\ell\nu$ and $B^+ \to D^{(*)}\pi\ell\nu$ decay branching fractions and ratios defeined in section 8. The "Calculated" branching fractions are also given in section 8. "Used" is the used values in the fit. Definitions of these notations are given in section 2.3 and 8

Branching fraction	SP5/SP6	Mesurement [reference]	Used
$\mathcal{B}(B^+ \to X\ell^+\nu)$		0.109 ± 0.004 [10]	
$\mathcal{B}(B^0 \to X\ell^+\nu)$		0.104 ± 0.004 [10]	
$\mathcal{B}(B \to X\ell^+\nu)$		0.1081 ± 0.0014 [10]	
$\mathcal{B}(B \to X_c\ell\nu)$	0.1040	$0.1061 \pm 0.0016 \pm 0.0060$ [20]	
$\mathcal{B}(B \to X_u\ell\nu)$	0.001365	0.00233 ± 0.00022 [10]	
		$0.00224 \pm 0.00027 \pm 0.00026 \pm 0.00039$ [21]	
$\mathcal{B}(B^+ \to \bar{X}_c^0\ell^+\nu)$	0.1040		0.1094
$\mathcal{B}(B^0 \to X_c^-\ell^+\nu)$	0.1040		0.1021

Table 13: Inclusive B decay branching fractions. "Measurement" is the most recent mesured vlue and "Used" is the used value in the fit.

Branching fraction	SP5/SP6	Used
$B_{DD0pDPp}$	0.6667	0.6667
$B_{DD0pDP0}$	0.3333	0.3333
$B_{DD00DPp}$	0.6667	0.6667
$B_{DD00DP0}$	0.3333	0.3333
$B_{DD1pDSPp}$	0.6667	0.6667
$B_{DD1pDSP0}$	0.3333	0.3333
$B_{DD10DSPp}$	0.6667	0.6667
$B_{DD10DSP0}$	0.3333	0.3333
$B_{DDP1pDSPp}$	0.6667	0.6667
$B_{DDP1pDSP0}$	0.3333	0.3333
$B_{DDP10DSPp}$	0.6667	0.6667
$B_{DDP10DSP0}$	0.3333	0.3333
$B_{DD2pDPp}$	0.4590	0.452
$B_{DD2pDP0}$	0.2290	0.226
$B_{DD2pDSPp}$	0.2090	0.215
$B_{DD2pDSP0}$	0.1030	0.107
$B_{DD20DPp}$	0.4590	0.452
$B_{DD20DP0}$	0.2290	0.226
$B_{DD20DSPp}$	0.2090	0.215
$B_{DD20DSP0}$	0.1030	0.107

Table 14: D^{**} decay branching fractions. "Used" is the used values in the fit. Definitions of these notations are given in section 2.3

Branching fraction	SP5/SP6	Mesurement [reference]	Used
B_{DSpDPp}	0.6830	0.677 ± 0.006 [10]	0.677
B_{DSpDP0}	0.3060	0.307 ± 0.005 [10]	0.307
B_{DSpDG}	0.0110	0.016 ± 0.005 [10]	0.016
B_{DS0DP0}	0.6190	0.619 ± 0.029 [10]	0.619
B_{DS0DG}	0.3810	0.381 ± 0.029 [10]	0.381
B_{Dp}	0.0900	$0.095 \pm 0.002 \pm 0.003$ [22]	0.095
B_{D0}	0.0383	$0.0391 \pm 0.0008 \pm 0.0009$ [22]	0.0391

Table 15: $D^{(*)}$ decay branching fractions. "Measurement" is the most recent mesured vlue and "Used" is the used value in the fit. Definitions of these notations are given in section 2.3

Constant	SP5/SP6	Mesurement [reference]	Used
t_{+0}	1	1.071 ± 0.009 [10]	1.071
f_{+0}	1	$1.006 \pm 0.036 \pm 0.031$ [32]	
C_{+0}	1		
$\frac{B_{DD2pDPp}}{B_{DD2pDSPp}}$	$459/209 = 2.2$	1.9 ± 1.4 [10]	
$\frac{B_{DD20DPp}}{B_{DD20DSPp}}$	$459/209 = 2.2$	2.3 ± 0.6 [10]	
f_{DD2}	2.2		2.1

Table 16: Constants. "Measurement" is the most recent mesured vlue and "Used" is the used value in the fit. Definition of these constants are given in sections 8, 5.1, 4.3

Branching fraction	SP5/SP6	Mesurement [reference]	Used
$\mathcal{B}(D^+ \to \bar{K}^0 e\nu)$	0.0670	$0.0871 \pm 0.0038 \pm 0.0037$ [18]	0.0871
$\mathcal{B}(D^+ \to \bar{K}^{*0} e\nu)$	0.0480	$0.0556 \pm 0.0027 \pm 0.0023$ [18]	0.0556
$\mathcal{B}(D^+ \to X e\nu)$	0.1372	$0.1613 \pm 0.0020 \pm 0.0033$ [19]	

Table 17: Semileptonic D decay branching fractions. "Measurement" is the most recent mesured vlue and "Used" is the used value in the fit. Definitions of these notations are given in section 2.3

Parameter	SP5/SP6	Mesurement [reference]	Used
R_1	1.18	$1.396 \pm 0.060 \pm 0.035 \pm 0.027$ [31]	1.396
R_2	0.72	$0.885 \pm 0.040 \pm 0.022 \pm 0.013$ [31]	0.885
ρ^2	0.92	$1.145 \pm 0.059 \pm 0.030 \pm 0.035$ [31]	1.145

Table 18: $B \to D^* \ell \nu$ FF parameters. "Measurement" is the most recent mesured vlue and "Used" is the used value in the fit. Definition of these parameters are given in Appendix H. Note that different parametrizations of ρ^2 was used in SP5/SP6 MC and [31]. See details in section 6

Type of MC	Cross section (nb)
B^+B^-	0.525
$B^0\bar{B}^0$	0.525
$c\bar{c}$	1.30
uds	2.09
$\tau^+\tau^-$	0.94

Table 19: Cross sections used to calculate MC luminosities.

C BToDlnu skim rates and luminosities

The event selection rates and luminosities of R16b BToDlnu skims of data and MC is summarized in Table 20 and 21. The luminosity of MC is calculated by the generated number of events and its cross section. Cross sections are taken from the Babar Physics Book [33] and given in Table 19. The luminosities are calculated based on the cross sections and the number of events before skimming. For example, in case of ccbar Run4 MC, as the number of events before skimming is 188718626, its luminosity is

$$\frac{188718626}{1.30 \times 10^3} = 1.452 \times 10^5 \text{pb}^{-1} = 145.2\text{fb}^{-1}$$

Data set	Selection rate	Luminosity
OnPeak Run1	8792976/245552690	17.801201
Run2	31374579/852649140	59.417877
Run3	17527801/438622047	30.648255
Run4	57952809/1448776065	99.356858
Total		207.224191
OffPeak Run1	515760/28946433	2.329883
Run2	1674989/90665305	6.835803
Run3	659867/31451100	2.396283
Run4	2878531/132941301	9.923230
Total		21.485199

Table 20: BToDlnu Data skims event selection rates and luminosities.

Data set	Selection rate	Luminosity
BpBm Run1	6920906/27176000	51.764
Run2	39029539/146536000	279.12
Run3	23854196/86492000	164.75
Run4	89759580/323822000	616.80
Total		1112.43
B0B0bar Run1	7421839/28762000	54.785
Run2	30164526/111924000	213.19
Run3	17081965/61158000	116.49
Run4	90093404/321150000	611.71
Total		996.18
ccbar Run1	1897239/21346000	16.420
Run2	9838664/99972000	76.708
Run3	6127861/57700000	44.385
Run4	25956105/246602000	189.69
Total		327.20
uds Run1	948025/30168000	14.434
Run2	6799899/176242000	84.326
Run3	5639210/124040000	59.349
Run4	15259514/346551000	165.81
Total		323.919
tautau Run1	135022/22098000	23.509
Run2	695973/99806000	106.18
Run3	544465/69852000	74.311
Run4	1472037/154900000	164.79
Total		368.79

Table 21: BToDlnu MC skims event selection rates and luminosities.

D Isospin Symmetry

D.1 Semileptonic B decays

From isospin symmetry, these B decay rates are identical

$$\begin{aligned}
\Gamma(B^+ \to \bar{D}^0 \ell^+ \nu) &= \Gamma(B^0 \to D^- \ell^+ \nu) \\
\Gamma(B^+ \to \bar{D}^{*0} \ell^+ \nu) &= \Gamma(B^0 \to D^{*-} \ell^+ \nu) \\
\Gamma(B^+ \to \bar{D}^{**0} \ell^+ \nu) &= \Gamma(B^0 \to D^{**-} \ell^+ \nu)
\end{aligned} \tag{250}$$

Isospin symmetry may be applied to non-resonant $B \to D^{(*)} \pi \ell \nu$ decays.

$$\begin{aligned}
\Gamma(B^+ \to D^- \pi^+ \ell^+ \nu) &= \Gamma(B^0 \to \bar{D}^0 \pi^- \ell^+ \nu) \\
\Gamma(B^+ \to D^{*-} \pi^+ \ell^+ \nu) &= \Gamma(B^0 \to \bar{D}^{*0} \pi^- \ell^+ \nu)
\end{aligned} \tag{251}$$

$$\begin{aligned}
\Gamma(B^+ \to D^- \pi^+ \ell^+ \nu) &= 2\Gamma(B^+ \to \bar{D}^0 \pi^0 \ell^+ \nu) \\
\Gamma(B^0 \to \bar{D}^0 \pi^- \ell^+ \nu) &= 2\Gamma(B^0 \to D^- \pi^0 \ell^+ \nu) \\
\Gamma(B^+ \to D^{*-} \pi^+ \ell^+ \nu) &= 2\Gamma(B^+ \to \bar{D}^{*0} \pi^0 \ell^+ \nu) \\
\Gamma(B^0 \to \bar{D}^{*0} \pi^- \ell^+ \nu) &= 2\Gamma(B^0 \to D^{*-} \pi^0 \ell^+ \nu)
\end{aligned} \tag{252}$$

The origin of the factor 2 is, for example,

$$\begin{aligned}
& B^+(u\bar{b}) : |1/2, 1/2> \\
& D^-(d\bar{c}) : |1/2, -1/2> \\
& \pi^+(u\bar{d}) : |1, 1> \\
& D^-\pi^+ : |1, 1> \times |1/2, -1/2> = \sqrt{\tfrac{1}{3}} |3/2, 1/2> + \sqrt{\tfrac{2}{3}} |1/2, 1/2> \\
& \bar{D}^0(u\bar{c}) : |1/2, 1/2> \\
& \pi^0(u\bar{u} \text{ or } d\bar{d}) : |1, 0> \\
& \bar{D}^0\pi^0 : |1, 0> \times |1/2, 1/2> = \sqrt{\tfrac{2}{3}} |3/2, 1/2> - \sqrt{\tfrac{1}{3}} |1/2, 1/2>
\end{aligned} \tag{253}$$

hence

$$\Gamma(B^+ \to D^- \pi^+ \ell^+ \nu) : \Gamma(B^+ \to \bar{D}^0 \pi^0 \ell^+ \nu) = \frac{2}{3} : \frac{1}{3} = 2 : 1 \tag{254}$$

Branching fractions are not same because of the difference in total rate (Γ) or life time (τ) of B^+ and B^0. We define

$$t_{+0} \equiv \frac{\tau_{B^+}}{\tau_{B^0}} = \frac{\Gamma_{B^0}}{\Gamma_{B^+}} \tag{255}$$

and

$$t_{0+} \equiv \frac{\tau_{B^0}}{\tau_{B^+}} = \frac{\Gamma_{B^+}}{\Gamma_{B^0}} \tag{256}$$

So branching fractions are, for example,

$$\frac{\mathcal{B}(B^+ \to \bar{D}^{*0}\ell^+\nu)}{\mathcal{B}(B^0 \to D^{*-}\ell^+\nu)} = \frac{\Gamma(B^+ \to D^*\ell\nu)}{\Gamma(B^0 \to D^*\ell\nu)}\frac{\Gamma_{B^0}}{\Gamma_{B^+}} = t_{+0} \tag{257}$$

Thus, due to isospin symmetry, we have the following relations between branching fractions of semileptonic B decays.

$$\begin{aligned}
&\mathcal{B}(B^+ \to \bar{D}^0\ell^+\nu) = t_{+0}\mathcal{B}(B^0 \to D^-\ell^+\nu)\\
&\mathcal{B}(B^+ \to \bar{D}^{*0}\ell^+\nu) = t_{+0}\mathcal{B}(B^0 \to D^{*-}\ell^+\nu)\\
&\mathcal{B}(B^+ \to \bar{D}^{**0}\ell^+\nu) = t_{+0}\mathcal{B}(B^0 \to D^{**-}\ell^+\nu)\\
&\mathcal{B}(B^+ \to D^-\pi^+\ell^+\nu) = 2\mathcal{B}(B^+ \to \bar{D}^0\pi^0\ell^+\nu)\\
&= t_{+0}\mathcal{B}(B^0 \to \bar{D}^0\pi^-\ell^+\nu) = 2t_{+0}\mathcal{B}(B^0 \to D^-\pi^0\ell^+\nu)\\
&\mathcal{B}(B^+ \to D^{*-}\pi^+\ell^+\nu) = 2\mathcal{B}(B^+ \to \bar{D}^{*0}\pi^0\ell^+\nu)\\
&= t_{+0}\mathcal{B}(B^0 \to \bar{D}^{*0}\pi^-\ell^+\nu) = 2t_{+0}\mathcal{B}(B^0 \to D^{*-}\pi^0\ell^+\nu)
\end{aligned} \tag{258}$$

D.2 D^{**} decays

Isospin symmetry may be applied to D^{**} decays as well.

$$\begin{aligned}
&\Gamma(D^{**0} \to D^+\pi^-) = \Gamma(D^{**+} \to D^0\pi^+)\\
&\Gamma(D^{**0} \to D^0\pi^0) = \Gamma(D^{**+} \to D^+\pi^0)\\
&\Gamma(D^{**0} \to D^{*+}\pi^-) = \Gamma(D^{**+} \to D^{*0}\pi^+)\\
&\Gamma(D^{**0} \to D^{*0}\pi^0) = \Gamma(D^{**+} \to D^{*+}\pi^0)
\end{aligned} \tag{259}$$

And also

$$\begin{aligned}
&\Gamma(D^{**0} \to D^+\pi^-) = 2\Gamma(D^{**0} \to D^0\pi^0)\\
&\Gamma(D^{**+} \to D^0\pi^+) = 2\Gamma(D^{**+} \to D^+\pi^0)\\
&\Gamma(D^{**0} \to D^{*+}\pi^-) = 2\Gamma(D^{**0} \to D^{*0}\pi^0)\\
&\Gamma(D^{**+} \to D^{*0}\pi^+) = 2\Gamma(D^{**+} \to D^{*+}\pi^0)
\end{aligned} \tag{260}$$

This factor 2 has the same origin as B decay case. For example,

$$
\begin{aligned}
&D^{**+} : |1/2, 1/2 > \\
&D^0 : |1/2, -1/2 > \\
&\pi^+ : |1, 1 > \\
&D^0\pi^+ : |1, 1 > \times |1/2, -1/2 >= \sqrt{\tfrac{1}{3}}|3/2, 1/2 > + \sqrt{\tfrac{2}{3}}|1/2, 1/2 > \\
&D^+ : |1/2, 1/2 > \\
&\pi^0 : |1, 0 > \\
&D^+\pi^0 : |1, 0 > \times |1/2, 1/2 >= \sqrt{\tfrac{2}{3}}|3/2, 1/2 > - \sqrt{\tfrac{1}{3}}|1/2, 1/2 >
\end{aligned}
\tag{261}
$$

hence

$$\Gamma(D^{**+} \to D^0\pi^+) : \Gamma(D^{**+} \to D^+\pi^0) = \frac{2}{3} : \frac{1}{3} = 2 : 1 \tag{262}$$

Supposing total rates or lifetimes of D^{**0} and D^{**+} are same, branching fractions for D^{**} decays are

$$
\begin{aligned}
&\mathcal{B}(D^{**0} \to D^+\pi^-) = 2\mathcal{B}(D^{**0} \to D^0\pi^0) = \mathcal{B}(D^{**+} \to D^0\pi^+) = 2\mathcal{B}(D^{**+} \to D^+\pi^0) \\
&\mathcal{B}(D^{**0} \to D^{*+}\pi^-) = 2\mathcal{B}(D^{**0} \to D^{*0}\pi^0) = \mathcal{B}(D^{**+} \to D^{*0}\pi^+) = 2\mathcal{B}(D^{**+} \to D^{*+}\pi^0)
\end{aligned}
\tag{263}
$$

E Classification of D^{**}

E.1 Angular momentum of mesons

In atomic spectroscopy, there are two useful schemes to add angular momentums: LS-coupling and jj-coupling.

- LS-coupling

$$\begin{aligned}\vec{S} &= \vec{s}_1 + \vec{s}_2 \\ \vec{J} &= \vec{L} + \vec{S}\end{aligned} \tag{264}$$

- jj-coupling

$$\begin{aligned}\vec{j}_1 &= \vec{L} + \vec{s}_1 \\ \vec{J} &= \vec{j}_1 + \vec{s}_2\end{aligned} \tag{265}$$

where s, l and j are the spin, orbital angular momentum and total angular momentum of individual particles, and S, L and J are the spin, orbital angular momentum and total angular momentum of the system.

E.2 Standard classification of mesons

For equal-mass meson system, it is traditional to couple the orbital angular momentum, $\vec{L}$, with the total spin of the quark and anti-quark, $\vec{S}$ (LS-coupling scheme).

$$\begin{aligned}\vec{S} &= \vec{s}_1 + \vec{s}_2 \\ \vec{J} &= \vec{L} + \vec{S}\end{aligned} \tag{266}$$

This is the standard practise for light mesons and heavy quarkonium ($c\bar{c}$ and $b\bar{b}$). The good quantum numbers are then S, L and J.
There are spin-singlet and spin-triplet levels because S is always $S = 0$ or $S = 1$.

- For $L = 0$ and $S = 0$, $J = 0$: ${}^1S_0$
- For $L = 0$ and $S = 1$, $J = 1$: ${}^3S_1$
- For $L = 1$ and $S = 0$, $J = 1$: ${}^1P_1$
- For $L = 1$ and $S = 1$, $J = 0, 1, 2$: ${}^3P_0$, ${}^3P_1$ or ${}^3P_2$

	Particle	J^P
$^1S_0$	D	0^-
$^3S_1$	D^*	1^-
$^1P_1$	D_1	1^+
$^3P_0$	D_0^*	0^+
$^3P_1$	D_1^*	1^+
$^3P_2$	D_2^*	2^+

Table 22: Traditional spectroscopic notation of D, D^* and D^{**} mesons.

In general, for $S = 0$ and $S = 1$

$$^1L_L \quad \text{and} \quad ^3L_{L-1,L,L+1} \tag{267}$$

We may apply this classification to D, D^* and D^{**} mesons. It is summarized in Table 22. In this classification D^{**} consists of one singlet (D_1) and a triplet (D_0^*, D_1^* and D_2^*).
Parity of mesons is given by $(-1)^L$. Thus, $P = (+)$ for $L = 0$ and $P = (-)$ for $L = 1$.

E.3 Heavy Quark Effective Theory (HQET) and D, D^* and D^{**} mesons

In HQET, the spin symmetry suggests that the spin of heavy quark is conserved. Thus, for the mesons consist of heavy and light quarks, we can apply jj coupling scheme. First, we can add the angular momentum (L) and the spin of the light quark (s_l) to get the angular momentum of light constituent (j_l). Then we can add the spin of the heavy quark (s_h) to j_l.

$$\begin{aligned} \vec{j_l} &= \vec{L} + \vec{s_l} \\ \vec{J} &= \vec{j_l} + \vec{s_h} \end{aligned} \tag{268}$$

For $L = 0$ and $s_l = 1/2$, $j_l = 1/2$ only, and for $L = 1$ and $s_l = 1/2$, $j_l = 1/2$ or $j_l = 3/2$. Hence,

- $L = 0$, $j_l = 1/2 \rightarrow J = 0$ (D) or 1 (D^*)

j_l^P	Particles	J^P	mass (GeV)
$\frac{1}{2}^+$	D, D^*	0^-, 1^-	1.971
$\frac{1}{2}^+$	D_0^*, D_1'	0^+, 1^+	2.40
$\frac{3}{2}^+$	D_1, D_2^*	1^+, 2^+	2.445

Table 23: Spin parity of charmed meson doublets

- $L = 1$, $j_l = 1/2 \to J = 0$ (D_0^*) or 1 (D_1')
- $L = 1$, $j_l = 3/2 \to J = 1$ (D_1) or 2 (D_2^*)

Parity of mesons is $(-1)^L$. Thus, $P = (+)$ for $L = 0$ and $P = (-)$ for $L = 1$. These are summarized in Table 23. In this classification, D^{**} consists of two doublets : (D_0^*, D_1') and (D_1, D_2^*).

E.4 Decay modes of D^{**}

The HQET based classification implies that the $j = 3/2$ states will decay only through the d-wave ($D_1 \to D^*$ and $D_2^* \to D$) and so will be narrow. The $j = 1/2$ states can decay through the s-wave ($D_0^* \to D$ and $D_1' \to D^*$) and, in general, will be broad. This is shown in Figure 32 and summarized in Table 24. We consider this in detail.

Spin-parity of $D\pi$ system is

- Since $D : S = 0, P = (-)$ and $\pi : S = 0, P = (-)$
- if $L = 0$, $J = 0$ and $P = (-)(-)(-)^0 = (+)$, then $J^P = 0^+$
- if $L = 1$, $J = 1$ and $P = (-)(-)(-)^1 = (-)$, then $J^P = 1^-$
- if $L = 2$, $J = 2$ and $P = (-)(-)(-)^2 = (+)$, then $J^P = 2^+$

Note that $P = (-)^L$. Spin-parity of $D^*\pi$ system is

- Since $D : S = 1, P = (-)$ and $\pi : S = 0, P = (-)$
- if $L = 0$, $J = 1$ and $P = (-)(-)(-)^0 = (+)$, then $J^P = 1^+$

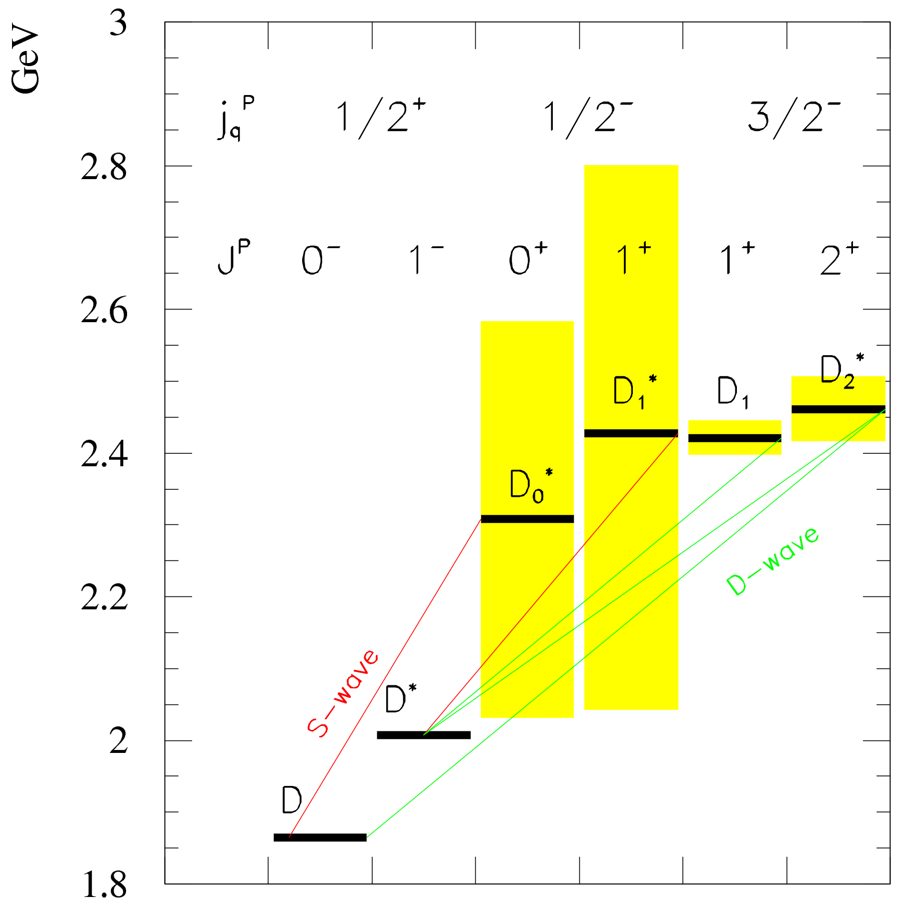

Figure 32: Charmed meson levels and transitions. $j_q = j_l$ in the text. The yellow bands show the width of each D^{**} state [11]

.

Initial state	Final state	ΔL	description
D_0^*	$D\pi$	0	broad S-wave transition
	$D^*\pi$	1	parity violation
D_1'	$D\pi$	1	parity violation
	$D^*\pi$	0	broad S-wave transition
		2	heavy quark spin symmetry violation
D_1	$D\pi$	1	parity violation
	$D^*\pi$	0	heavy quark spin symmetry violation
		2	narrow D-wave transition
D_2^*	$D\pi$	2	narrow D-wave transition
	$D^*\pi$	2	narrow D-wave transition

Table 24: D^{**} decay modes.

- if $L = 1$, $J = 2, 1, 0$ and $P = (-)(-)(-)^1 = (-)$, then $J^P = 0^-, 1^-, 2^-$
- if $L = 2$, $J = 3, 2, 1$ and $P = (-)(-)(-)^2 = (+)$, then $J^P = 1^+, 2^+, 3^+$

Thus,

- $J^P = 0^+$ state (D_0^*) can decay only to $D\pi$ and $\Delta L = 0$
- $J^P = 1^+$ state (D_1 and D_1') can decay only to $D^*\pi$ and $\Delta L = 0, 2$
- $J^P = 2^+$ state (D_2^*) can decay both to $D\pi$ and to $D^*\pi$ and $\Delta L = 2$

Next, we consider angular momentum of D_1 and D_1' decays.

- $D_1(L = +1, s_l = +1/2, j_l = +3/2; s_h = -1/2, J = +1)$
  $\to D^*(s_l = +1/2, s_h = +1/2, j_D = +1) + \pi(j_\pi = 0) + (L = 0); J = +1$
  This violates heavy quark spin symmetry ($s_h = -1/2 \to s_h = +1/2$)
- $D_1(L = +1, s_l = +1/2, j_l = +3/2; s_h = -1/2, J = +1)$
  $\to D^*(s_l = -1/2, s_h = -1/2, j_D = -1) + \pi(j_\pi = 0) + (L = +2); J = +1$
  This conserves heavy quark spin symmetry ($s_h = -1/2 \to s_h = -1/2$)

- $D_1'(L = +1, s_l = -1/2, j_l = +1/2; s_h = +1/2, J = +1)$
  $\to D^*(s_l = +1/2, s_h = +1/2, j_D = +1) + \pi(j_\pi = 0) + (L = 0); J = +1$
  This conserves heavy quark spin symmetry ($s_h = +1/2 \to s_h = +1/2$)

- $D_1'(L = +1, s_l = -1/2, j_l = +1/2; s_h = +1/2, J = +1)$
  $\to D^*(s_l = -1/2, s_h = -1/2, j_D = -1) + \pi(j_\pi = 0) + (L = +2); J = +1$
  This violates heavy quark spin symmetry ($s_h = +1/2 \to s_h = -1/2$)

F $\cos\theta_{BY}$

F.1 $B \to D\ell\nu$ decays

In the decay of $B \to Dl + \nu$, 4-momentum conservation gives

$$p_B = p_{Dl} + p_\nu \tag{269}$$

As the mass of neutrino is equal to zero

$$0 = p_\nu^2 = (p_B - p_{Dl})^2 = p_B^2 + p_{Dl}^2 - 2p_B \cdot p_{Dl} = m_B^2 + m_{Dl}^2 - 2p_B \cdot p_{Dl} \tag{270}$$

Here,

$$p_B \cdot p_{Dl} = E_B E_{Dl} - \vec{p}_B \cdot \vec{p}_{Dl} = E_B E_{Dl} - |\vec{p}_B||\vec{p}_{Dl}| \cos\Theta_{B-Dl} \tag{271}$$

Hence

$$\begin{aligned} 0 &= m_B^2 + m_{Dl}^2 - 2(E_B E_{Dl} - |\vec{p}_B||\vec{p}_{Dl}| \cos\Theta_{B-Dl}) \\ \Rightarrow m_B^2 + m_{Dl}^2 &= 2E_B E_{Dl} - 2|\vec{p}_B||\vec{p}_{Dl}| \cos\Theta_{B-Dl} \end{aligned} \tag{272}$$

Therefore

$$\cos\Theta_{B-Dl} = \frac{2E_B E_{Dl} - m_B^2 - m_{Dl}^2}{2|\vec{p}_B||\vec{p}_{Dl}|} \tag{273}$$

In practise, E_B is given by the half of the beam energy in the CM frame. $|\vec{p}_B|$ is given by

$$|\vec{p}_B| = \sqrt{E_B^2 - m_B^2} \tag{274}$$

F.2 With an additional pion

If there are additional particles, $\cos\Theta_{B-Dl} < -1$ is possible. Let us consider an additional pion, for example, from D^*. Conservation of 4-momentum is

$$p_B = p_{Dl} + p_\pi + p_\nu \tag{275}$$

Then,

$$\begin{aligned} &(p_\nu + p_\pi)^2 = (p_B - p_{Dl})^2 \\ &\Rightarrow p_\nu^2 + p_\pi^2 + 2p_\nu \cdot p_\pi = p_B^2 + p_{Dl}^2 - 2p_B \cdot p_{Dl} \\ &\Rightarrow 0 + m_\pi^2 + 2p_\nu \cdot p_\pi = m_B^2 + m_{Dl}^2 - 2p_B \cdot p_{Dl} \end{aligned} \tag{276}$$

Since $m_\pi \ll m_B$,

$$0 + 0 + 2p_\nu \cdot p_\pi = m_B^2 + m_{Dl}^2 - 2p_B \cdot p_{Dl} \tag{277}$$

and also

$$\begin{aligned} p_\nu \cdot p_\pi &= E_\nu E_\pi - \vec{p}_\nu \cdot \vec{p}_\pi = E_\nu E_\pi - |\vec{p}_\nu||\vec{p}_\pi| \cos\Theta_{\nu-\pi} \\ &= E_\nu E_\pi - E_\nu E_\pi \cos\Theta_{\nu-\pi} = E_\nu E_\pi \left(1 - \cos\Theta_{\nu-\pi}\right) \geq 0 \end{aligned} \tag{278}$$

Let the angle between B and Dl be Θ'_{B-Dl}. Then,

$$p_B \cdot p_{Dl} = E_B E_{Dl} - \vec{p}_B \cdot \vec{p}_{Dl} = E_B E_{Dl} - |\vec{p}_B||\vec{p}_{Dl}| \cos\Theta'_{B-Dl} \tag{279}$$

Hence,

$$\begin{aligned} \cos\Theta'_{B-Dl} &= \tfrac{2E_B E_{Dl} - m_B^2 - m_{Dl}^2}{2|\vec{p}_B||\vec{p}_{Dl}|} + \tfrac{2p_\nu \cdot p_\pi}{2|\vec{p}_B||\vec{p}_{Dl}|} \\ &= \cos\Theta_{B-Dl} + \alpha \end{aligned} \tag{280}$$

where

$$\alpha = \frac{2p_\nu \cdot p_\pi}{2|\vec{p}_B||\vec{p}_{Dl}|} \geq 0 \tag{281}$$

Considering

$$-1 \leq \cos\Theta'_{B-Dl} \leq 1 \tag{282}$$

$\cos\Theta_{B-Dl} = \cos\Theta'_{B-Dl} - \alpha$ is

$$-1 - \alpha \leq \cos\Theta_{B-Dl} \leq 1 - \alpha \leq 1 \tag{283}$$

Since $\alpha \geq 0$, the lower end of $\cos\Theta_{B-Dl}$ can be smaller than -1, whereas the upper end remains to 1.

F.3 If D and l come from different B

In the case that D and l came from different B, $\cos\Theta_{B-Dl} > 1$ is possible. The p_{Dl} is

$$p_{Dl} = p_D + p_l = (E_D + E_l, -\vec{p}_D - \vec{p}_l) = (E_{Dl}, -\vec{p}_{Dl}) \tag{284}$$

Hence

$$\begin{aligned} &E_{Dl} = E_D + E_l = \sqrt{m_D^2 + |\vec{p}_D|^2} + \sqrt{m_l^2 + |\vec{p}_l|^2} = \sqrt{m_D^2 + |\vec{p}_D|^2} + |\vec{p}_l| \\ &|\vec{p}_{Dl}|^2 = |\vec{p}_D + \vec{p}_l|^2 = |\vec{p}_D|^2 + |\vec{p}_l|^2 + 2|\vec{p}_D||\vec{p}_l| \cos\theta \end{aligned} \tag{285}$$

and

$$
\begin{aligned}
m_{Dl}^2 &= p_{Dl}^2 = E_{Dl}^2 - |\vec{p}_{Dl}|^2 \\
&= m_D^2 + |\vec{p}_D|^2 + |\vec{p}_l|^2 + 2|\vec{p}_l|\sqrt{m_D^2 + |\vec{p}_D|^2} - |\vec{p}_D|^2 - |\vec{p}_l|^2 - 2|\vec{p}_D||\vec{p}_l|\cos\theta \\
&= m_D^2 + 2|\vec{p}_l|\sqrt{m_D^2 + |\vec{p}_D|^2} - 2|\vec{p}_D||\vec{p}_l|\cos\theta \\
&= m_D^2 + |\vec{p}_l|(2\sqrt{m_D^2 + |\vec{p}_D|^2} - 2|\vec{p}_D|\cos\theta)
\end{aligned} \tag{286}
$$

If D and l come from different B, p_D and p_l are not restricted by energy momentum conservation. The $|\vec{p}_D|$ and $|\vec{p}_l|$ can be any value. If $|\vec{p}_l|$ is very large, E_{Dl} is very large but m_{Dl}^2 can be as small as m_D^2 if

$$2\sqrt{m_D^2 + |\vec{p}_D|^2} \simeq 2|\vec{p}_D|\cos\theta \tag{287}$$

Hence

$$\cos\Theta_{B-Dl} = \frac{2E_B E_{Dl} - m_B^2 - m_{Dl}^2}{2|\vec{p}_B||\vec{p}_{Dl}|} \tag{288}$$

can be larger than 1.

G Velocity transfer w

G.1 w and q^2

In the framework of Heavy Quark Effective Theory (HQET) it is convenient to use the velocity transfer w instead of momentum transfer q^2. In semileptonic $B \to D^{(*)}\ell\nu$ decays, w is defined as the product of 4-velocities of B and $D^{(*)}$

$$w \equiv v_B \cdot v_{D^{(*)}} = \frac{p_B \cdot p_{D^{(*)}}}{m_B m_{D^{(*)}}} \tag{289}$$

The momentum transfer q from B to $D^{(*)}$ (or the invariant mass of the virtual W) is given by

$$q = p_\ell + p_\nu = p_B - p_{D^{(*)}} \tag{290}$$

Thus

$$\begin{aligned} & q^2 = (p_B - p_{D^{(*)}})^2 = p_B^2 + p_{D^{(*)}}^2 - 2p_B \cdot p_{D^{(*)}} = m_B^2 + m_{D^{(*)}}^2 - 2p_B \cdot p_{D^{(*)}} \\ & \Rightarrow p_B \cdot p_{D^{(*)}} = \tfrac{m_B^2 + m_{D^{(*)}}^2 - q^2}{2} \end{aligned} \tag{291}$$

Hence

$$w = \frac{m_B^2 + m_{D^{(*)}}^2 - q^2}{2m_B m_{D^{(*)}}} \tag{292}$$

w is a Lorentz invariant and linearly related to q^2.
w corresponds to the relativistic boost γ of the D in the B rest frame.

$$\gamma_{D^{(*)}} = \frac{E_{D^{(*)}}}{m_{D^{(*)}}} \tag{293}$$

G.2 $1 \le w \lesssim 1.5$

The range of w and q^2 are restricted by kinematics of the decay. When $q^2 = 0$, w is maximum

$$w\mathrm{max} = \frac{m_B^2 + m_{D^{(*)}}^2}{2m_B m_{D^{(*)}}} \tag{294}$$

where, using $2m_B = 5279$, $m_D = 1867$ and $m_{D^*} = 2008$ MeV,

$$\frac{m_B^2 + m_D^2}{2m_B m_D} = 1.590, \quad \frac{m_B^2 + m_{D^*}^2}{2m_B m_{D^*}} = 1.504 \tag{295}$$

The minimum of the w is

$$w_{\text{min}} = 1 \tag{296}$$

which corresponds to

$$q^2_{\text{max}} = (m_B - m_{D^{(*)}})^2 \tag{297}$$

where

$$(m_B - m_D)^2 = 11.64, \quad (m_B - m_{D^*})^2 = 10.69 \ \ (\text{GeV}/c^2)^2 \tag{298}$$

G.3 Practical calculation of w

We can calculate w by the following formula

$$w = \frac{p_B \cdot p_{D^{(*)}}}{m_B m_{D^{(*)}}} = \frac{E_B E_{D^{(*)}} - |\vec{P}_B||\vec{P}_{D^{(*)}}| \cos\theta_{B-D}}{m_B m_{D^{(*)}}} \tag{299}$$

In practise, E_B is the half of the beam energy, and $|\vec{P}_B|$ is given by

$$|\vec{P}_B| = \sqrt{E_B^2 - m_B^2} \tag{300}$$

$\cos\theta_{B-D}$ can be calculated from $\cos\theta_{B-Dl}$ (see Appendix F and Figure 12).

H Form Factors (FF) of $B \to D^{(*,**)} X \ell\nu$ decays

H.1 Matrix elements, form factors and decay rates

The amplitude of $B \to D^{(*,**)}\ell\nu$ is given by

$$\mathcal{M} = -i\frac{G_F}{\sqrt{2}} V_{cb} L^\mu H_\mu \tag{301}$$

where the leptonic current can be written in terms of Dirac spinors u_l and v_ν

$$L^\mu = \bar{u}_l \gamma^\mu (1-\gamma_5) v_\nu \tag{302}$$

The hadronic current H_μ can be written in terms of quark spinors b and c

$$H^\mu =< D|\bar{c}\gamma^\mu(1-\gamma_5)b|B >=< D|V^\mu|B > + < D|A^\mu|B > \tag{303}$$

where

$$\begin{aligned} V^\mu &= \bar{c}\gamma^\mu b \quad \text{(vector current)} \\ A^\mu &= \bar{c}\gamma^\mu\gamma_5 b \quad \text{(axial-vector current)} \end{aligned} \tag{304}$$

H.1.1 $B \to D\ell\nu$

In this case

$$< D|A^\mu|B >= 0 \tag{305}$$

and

$$\begin{aligned} &< D(p')|V^\mu|B(p) > \\ &= F_1(q^2)\left[(p+p')^\mu - \tfrac{m_B^2-m_D^2}{q^2}q^\mu\right] + F_0(q^2)\tfrac{m_B^2-m_D^2}{q^2}q^\mu \end{aligned} \tag{306}$$

or

$$< D(p')|V^\mu|B(p) >= f_+(q^2)(p+p')^\mu + f_-(q^2)(p-p')^\mu \tag{307}$$

where

$$\begin{aligned} F_1(q^2) &= f_+(q^2) \\ F_0(q^2) &= f_+(q^2) + \tfrac{q^2}{m_B^2-m_D^2} f_-(q^2) \\ q^\mu &= p^\mu - p'^\mu \end{aligned} \tag{308}$$

The form factors $F_1(q^2)$ and $F_0(q^2)$ can be associated with the exchange of particles with quantum numbers $J^P = 1^-$ and $J^P = 0^+$, respectively. There is no singular behaviour at $q^2 = 0$ because $F_1(0) = F_0(0)$. In practise the terms proportional to q^μ are nearly always negligible. Thus

$$< D(p')|V^\mu|B(p) >= F_1(q^2)(p+p')^\mu \tag{309}$$

or

$$< D(p')|V^\mu|B(p) >= f_+(q^2)(p+p')^\mu \tag{310}$$

The differential decay rate is given by

$$\begin{aligned} \frac{d\Gamma(B \to D\ell\nu)}{dq^2} &= \frac{G_F^2|V_{cb}|^2}{24\pi^3}|\vec{P}_D|^3|f_+(q^2)|^2 \\ = \frac{G_F^2|V_{cb}|^2}{192\pi^3 m_B^3}&\left[(q^2 - m_B^2 - m_D^2)^2 - 4m_B^2 m_D^2\right]^{3/2}|f_+(q^2)|^2 \end{aligned} \tag{311}$$

where we used the following calculation. In the B rest frame,

$$p = (m_B, \vec{0}), \quad p' = (\sqrt{m_D^2 + |\vec{P}_D|^2}, \vec{p}') \tag{312}$$

Thus

$$\begin{aligned} & q^2 = (p-p')^2 = p^2 + p'^2 - 2p\cdot p' = m_B^2 + m_D^2 - 2m_B\sqrt{m_D^2 + |\vec{P}_D|^2} \\ & \Rightarrow 4m_B^2\left(m_D^2 + |\vec{P}_D|^2\right) = (q^2 - m_B^2 - m_D^2)^2 \\ & \Rightarrow |\vec{P}_D| = \tfrac{1}{2m_B}\left[(q^2 - m_B^2 - m_D^2)^2 - 4m_B^2 m_D^2\right]^{1/2} \end{aligned} \tag{313}$$

H.1.2 $B \to D^*\ell\nu$

In this case

$$< D^*(p',\varepsilon)|V^\mu|B(p) >= \frac{2i\epsilon^{\mu\nu\alpha\beta}}{m_B + m_{D^*}}\varepsilon_\nu^* p'_\alpha p_\beta V(q^2) \tag{314}$$

and

$$\begin{aligned} < D^*(p',\varepsilon)|A^\mu|B(p) >= &-(m_B + m_{D^*})\varepsilon^{*\mu}A_1(q^2) \\ &+\frac{\varepsilon^*\cdot q}{m_B + m_{D^*}}(p+p')^\mu A_2(q^2) \\ &+2m_{D^*}\frac{\varepsilon^*\cdot q}{q^2}q^\mu A_3(q^2) \\ &-2m_{D^*}\frac{\varepsilon^*\cdot q}{q^2}q^\mu A_0(q^2) \end{aligned} \tag{315}$$

where

$$A_3(q^2) = \frac{m_B + m_{D^*}}{2m_{D^*}} A_1(q^2) - \frac{m_B - m_{D^*}}{2m_{D^*}} A_2(q^2) \tag{316}$$

with $A_0(0) = A_3(0)$. Or

$$< D^*(p', \varepsilon)|V^\mu|B(p) >= i\epsilon^{\mu\nu\alpha\beta} \varepsilon^*_\nu (p + p')_\alpha (p - p')_\beta g(q^2) \tag{317}$$

and

$$\begin{aligned} &< D^*(p', \varepsilon)|A^\mu|B(p) > \\ &= \varepsilon^{*\mu} f(q^2) + \varepsilon^* \cdot q(p + p')^\mu a_+(q^2) + \varepsilon^* \cdot q(p - p')^\mu a_-(q^2) \end{aligned} \tag{318}$$

where

$$\begin{aligned} V(q^2) &= (m_B - m_{D^*}) g(q^2) \\ A_1(q^2) &= \tfrac{1}{m_B - m_{D^*}} f(q^2) \\ A_2(q^2) &= (m_B - m_{D^*}) a_+(q^2) \\ A_3(q^2) - A_0(q^2) &= \tfrac{q^2}{2m_{D^*}} a_-(q^2) \end{aligned} \tag{319}$$

Here, we used

$$\begin{aligned} \epsilon^{\mu\nu\alpha\beta} p_\alpha p_\beta &= \epsilon^{\mu\nu\alpha\beta} p'_\alpha p'_\beta = 0 \\ \epsilon^{\mu\nu\alpha\beta} p_\alpha p'_\beta &= -\epsilon^{\mu\nu\alpha\beta} p'_\alpha p_\beta \end{aligned} \tag{320}$$

Again, terms proportional to q^μ only play an important role for the case $l = \tau$. Thus those are negligible in our case

$$\begin{aligned} < D^*(p', \varepsilon)|A^\mu|B(p) > &= -(m_B + m_{D^*}) \varepsilon^{*\mu} A_1(q^2) \\ &+ \frac{\varepsilon^* \cdot q}{m_B + m_{D^*}} (p + p')^\mu A_2(q^2) \end{aligned} \tag{321}$$

or

$$< D^*(p', \varepsilon)|A^\mu|B(p) >= \varepsilon^{*\mu} f(q^2) + \varepsilon^* \cdot q(p + p')^\mu a_+(q^2) \tag{322}$$

The form factors $A_1(q^2)$ and $A_2(q^2)$ can be associated with the exchange of particles with quantum numbers $J^P = 1^+$, whereas $V(q^2)$ is associated with $J^P = 1^-$.

H.1.3 $B \to D_0^* \ell\nu$

In this case

$$< D_0^*(p', \varepsilon)|V^\mu|B(p) >= 0 \tag{323}$$

and

$$< D_0^*(p', \varepsilon)|A^\mu|B(p) >= u_+(q^2)(p + p')^\mu + u_-(q^2)(p - p')^\mu \tag{324}$$

H.1.4 $B \to D_1'\ell\nu$

In this case

$$< D_1'(p',\varepsilon)|V^\mu|B(p) >= \varepsilon^{*\mu} l_{1/2}(q^2) + \varepsilon^* \cdot q(p+p')^\mu c_{1/2+}(q^2) + \varepsilon^* \cdot q(p-p')^\mu c_{1/2-}(q^2) \quad (325)$$

and

$$< D_1'(p',\varepsilon)|A^\mu|B(p) >= i\epsilon^{\mu\nu\alpha\beta}\varepsilon^*_\nu (p+p')_\alpha (p-p')_\beta q_{1/2}(q^2) \quad (326)$$

H.1.5 $B \to D_1\ell\nu$

In this case

$$< D_1(p',\varepsilon)|V^\mu|B(p) >= \varepsilon^{*\mu} l_{3/2}(q^2) + \varepsilon^* \cdot q(p+p')^\mu c_{3/2+}(q^2) + \varepsilon^* \cdot q(p-p')^\mu c_{3/2-}(q^2) \quad (327)$$

and

$$< D_1(p',\varepsilon)|A^\mu|B(p) >= i\epsilon^{\mu\nu\alpha\beta}\varepsilon^*_\nu (p+p')_\alpha (p-p')_\beta q_{3/2}(q^2) \quad (328)$$

H.1.6 $B \to D_2^*\ell\nu$

In this case

$$< D_2^*(p',\varepsilon)|V^\mu|B(p) >= i\epsilon^{\mu\nu\alpha\beta}\varepsilon^*_\nu (p+p')_\alpha (p-p')_\beta h(q^2) \quad (329)$$

and

$$< D_2^*(p',\varepsilon)|A^\mu|B(p) >= \varepsilon^{*\mu} k(q^2) + \varepsilon^* \cdot q(p+p')^\mu b_+(q^2) + \varepsilon^* \cdot q(p-p')^\mu b_-(q^2) \quad (330)$$

H.2 ISGW2 model

The quark-model B and D masses are

$$\begin{aligned} \tilde{m}_B &= m_b + m_u = m_b + m_d \\ \tilde{m}_D &= m_c + m_u = m_c + m_d \end{aligned} \quad (331)$$

where m_u, m_d, m_c and m_b are u, d, c and b quark masses, respectively. In ISGW2 model,

$$\begin{aligned} m_d &= m_u = 0.33\text{GeV} \\ m_c &= 1.82\text{GeV} \\ m_b &= 5.20\text{GeV} \end{aligned} \quad (332)$$

Using, these quark masses, ISGW2 define

$$\mu_{\pm} = \left(\frac{1}{m_c} \pm \frac{1}{m_b}\right)^{-1} \tag{333}$$

The hyperfine-averaged physical mass of a HQS multiplet with light degrees of freedom having angular momentum j_l

$$\bar{m}_{j_l} = \frac{j_l + 1}{2j_l + 1} m_{J=j_l+\frac{1}{2}} + \frac{j_l}{2j_l + 1} m_{J=j_l-\frac{1}{2}} \tag{334}$$

For example

$$\begin{aligned} \bar{m}_B &= \tfrac{3}{4} m_B + \tfrac{1}{4} m_{B^*} = 5.31 \\ \bar{m}_D &= \bar{m}_{D^*} = \tfrac{3}{4} m_D + \tfrac{1}{4} m_{D^*} \\ \bar{m}_{D_0^*} &= \bar{m}_{D_1{}'} = \tfrac{3}{4} m_{D_1'} + \tfrac{1}{4} m_{D_0^*} \\ \bar{m}_{D_1} &= \bar{m}_{D_2^*} = \tfrac{5}{8} m_{D_2^*} + \tfrac{3}{8} m_{D_1} \end{aligned} \tag{335}$$

where

$$\begin{aligned} m_B &= 5.27\text{GeV}, \quad m_{B^*} = 5.33\text{GeV} \\ m_D &= 1.87\text{GeV}, \quad m_{D^*} = 2.01\text{GeV} \\ m_{D_0^*} &= 2.40\text{GeV}, \quad m_{D_1'} = 2.49\text{GeV} \\ m_{D_1} &= 2.42\text{GeV}, \quad m_{D_2^*} = 2.46\text{GeV} \end{aligned} \tag{336}$$

There are also parameters β in the wave functions, and those values in the ISGW2 model are

$$\begin{aligned} \beta_B &= 0.431\text{GeV} \\ \beta_D &= 0.45\text{GeV} \\ \beta_{D^*} &= 0.38\text{GeV} \\ \beta_{D^{**}} &= 0.33\text{GeV} \end{aligned} \tag{337}$$

Also, β_{BX}^2 ($X = D$, D^* or D^{**}) is defined as

$$\beta_{BX}^2 \equiv \frac{1}{2}(\beta_B^2 + \beta_X^2) \tag{338}$$

The momentum transfer is

$$t = (p_B - p_D)^2 = q^2 \tag{339}$$

and the maximum momentum transfer is

$$t_m = (m_B - m_D)^2 \tag{340}$$

where m_D can be m_{D^*} or $m_{D^{**}}$.
In ISGW2 model, the factor $F_n^{(\alpha)}$ is defined as

$$F_n^{(\alpha)} = \left(\frac{\bar{m}_B}{\tilde{m}_B}\right)^{n_B(\alpha)} \left(\frac{\bar{m}_D}{\tilde{m}_D}\right)^{n_X(\alpha)} \left(\frac{\tilde{m}_D}{\tilde{m}_B}\right)^{1/2} \left(\frac{\beta_B \beta_D}{\beta_{BD}^2}\right)^{n/2} \left[1 + \frac{1}{6N} r^2 (t_m - t)\right]^{-N} \tag{341}$$

where $N = 2+n+n'$. n and n' are the harmonic oscillator quantum numbers of the initial and final wave-functions. Therefore, $N = 2$ for S wave to S wave ($B \to D$ or D^*), and $N = 3$ for S wave to P wave ($B \to D^{**}$). $n_B(\alpha)$ and $n_X(\alpha)$ is given in the table

Form factors (α)	$n_B(\alpha)$	$n_X(\alpha)$
$f_+ + f_-$	-1/2	+1/2
$f_+ - f_-$	+1/2	-1/2
g	-1/2	-1/2
f	+1/2	+1/2
$a_+ + a_-$	-3/2	+1/2
$a_+ - a_-$	-1/2	-1/2
$u_+ + u_-$	-1/2	+1/2
$u_+ - u_-$	+1/2	-1/2
l	+1/2	+1/2
$c_+ + c_-$	-3/2	+1/2
$c_+ - c_-$	-1/2	-1/2
q	-1/2	-1/2
h	-3/2	-1/2
k	-1/2	+1/2
$b_+ + b_-$	-5/2	+1/2
$b_+ - b_-$	-3/2	-1/2

and r^2 is

$$r^2 = \frac{3}{4m_b m_c} + \frac{3m_d^2}{2\bar{m}_B \bar{m}_D \beta_{BD}^2} + \frac{1}{\bar{m}_B \bar{m}_D}\left(\frac{16}{33-2N_f}\right)\ln\left[\frac{\alpha_s(\mu_{QM})}{\alpha_s(m_c)}\right] \quad (342)$$

where, if a scale $\mu < 0.6$ GeV,

$$\alpha_s(\mu) = 0.6 \quad (343)$$

and if $\mu > 0.6$ GeV,

$$\alpha_s(\mu) = \frac{12\pi}{33-2N_f}\left[\ln\left(\frac{\mu^2}{\Lambda_{QCD}^2}\right)\right]^{-1} \quad (344)$$

where N_f is the number of active flavors below the scale μ. For $\mu = m_c$, $N_f = 3$, and for $\mu = m_b$, $N_f = 4$. Thus, $N_f = 3$ for $b \to c$ decays. The constants in the above equations are

$$\begin{aligned} \mu_{QM} &= 0.1\text{GeV} \\ \Lambda_{QCD}^2 &= 0.04\text{GeV}^2 \end{aligned} \quad (345)$$

The factor $R^{(\alpha)}$ is defined as

$$R^{(\alpha)} = C_{cb}\left[f^{(\alpha)} + \tilde{\beta}_{cb}^{(\alpha)}(w)\frac{\alpha_s\left(\sqrt{m_b m_c}\right)}{\pi}\right] \quad (346)$$

where $f^{(\alpha)} = 0$ for $a_+ + a_-$ and $f^{(\alpha)} = 1$ for others.
Here

$$C_{cb} = \left[\frac{\alpha_s(m_b)}{\alpha_s(m_c)}\right]^{a_I}\left[\frac{\alpha_s(m_c)}{\alpha_s(\mu_{QM})}\right]^{a_L(w)} \quad (347)$$

is independent of α and has

$$a_I = -\frac{6}{33-2N_f} \quad (348)$$

and

$$a_L(w) = -\frac{8}{33-2N_f'}[wr(w)-1] \quad (349)$$

with

$$r(w) = \frac{1}{\sqrt{w^2-1}}\ln\left(w+\sqrt{w^2-1}\right) \quad (350)$$

and

$$w = 1 + \frac{t_m - t}{2m_B m_D} \tag{351}$$

where m_D may be m_D^* or m_D^{**} depending on the decay modes. N_f is the number of active flavours below the scale m_b and N_f' is the number of active flavours below the scale m_c. Thus, $N_f = 4$ and $N_f' = 3$. In ISGW2, $\tilde{w}$ is defined as

$$\tilde{w} = 1 + \frac{t_m - t}{2\bar{m}_B \bar{m}_D} \tag{352}$$

For w near 1

$$\left[\frac{\alpha_s(m_c)}{\alpha_s(\mu_{QM})}\right]^{a_L(w)} = 1 - \frac{2}{3}\left(\frac{8}{33 - 2N_f'}\right) \ln\left[\frac{\alpha_s(\mu_{QM})}{\alpha_s(m_c)}\right](w-1) \tag{353}$$

In SP5/SP6, $\left[\frac{\alpha_s(m_c)}{\alpha_s(\mu_{QM})}\right]^{a_L(w)} = 1$ was used.

At $w = 1$, $\tilde{\beta}_{cb}$ are

$$\begin{array}{l}
\tilde{\beta}_{cb}^{(f_+ + f_-)}(1) = \gamma_{cb} - \frac{2}{3}\chi_{cb} \\
\tilde{\beta}_{cb}^{(f_+ - f_-)}(1) = \gamma_{cb} + \frac{2}{3}\chi_{cb} \\
\tilde{\beta}_{cb}^{(g)}(1) = \gamma_{cb} + \frac{2}{3} \\
\tilde{\beta}_{cb}^{(f)}(1) = \gamma_{cb} - \frac{2}{3} \\
\tilde{\beta}_{cb}^{(a_+ + a_-)}(1) = -1 - \chi_{cb} + \frac{4}{3}\frac{1}{(1-z_{cb})} + \frac{2}{3}\frac{1+z_{cb}}{(1-z_{cb})^2}\gamma_{cb} \\
\tilde{\beta}_{cb}^{(a_+ - a_-)}(1) = -\frac{1}{3} - \chi_{cb} + \frac{4}{3}\frac{1}{(1-z_{cb})} + \left[1 - \frac{2}{3}\frac{1+z_{cb}}{(1-z_{cb})^2}\right]\gamma_{cb}
\end{array} \tag{354}$$

where

$$\gamma_{cb} = \frac{2z_{cb}}{1 - z_{cb}} \ln\left(\frac{1}{z_{cb}}\right) - 2 \tag{355}$$

and

$$\chi_{cb} = -1 - \frac{\gamma_{cb}}{1 - z_{cb}} \tag{356}$$

with

$$z_{cb} = \frac{m_c}{m_b} \tag{357}$$

w dependence of $\tilde{\beta}$ is weak and negligible.

In ISGW, LL-coupling was used, and ISGW2 also follows the convention. But, ISGW2 aware that jj-coupling is a better representation of heavy-light mesons. Thus, ISGW2 gives jj-coupling type of form factors for D_1 and D_1'.

H.2.1 $B \to D\ell\nu$ (1^2S_0)

Matrix element is

$$< D(p')|V^\mu|B(p) >= f_+(q^2)(p+p')^\mu + f_-(q^2)(p-p')^\mu \tag{358}$$

The differential decay rate is given by

$$\frac{d\Gamma(B \to D\ell\nu)}{dq^2} = \frac{G_F^2|V_{cb}|^2}{192\pi^3 m_B^3}\left[(q^2 - m_B^2 - m_D^2)^2 - 4m_B^2 m_D^2\right]^{3/2}|f_+(q^2)|^2 \tag{359}$$

where f_+ is the form factor.

$$f_+ + f_- = \left[2 - \frac{\tilde{m}_D}{m_c}\left(1 - \frac{m_d m_c}{2\mu_+ \tilde{m}_D}\frac{\beta_B^2}{\beta_{BD}^2}\right)\right] F_3^{(f_+ + f_-)} R^{(f_+ + f_-)} \tag{360}$$

and

$$f_+ - f_- = \frac{\tilde{m}_B}{m_c}\left(1 - \frac{m_d m_c}{2\mu_+ \tilde{m}_D}\frac{\beta_B^2}{\beta_{BD}^2}\right) F_3^{(f_+ - f_-)} R^{(f_+ - f_-)} \tag{361}$$

Thus, we get f_+

$$f_+ = \frac{(f_+ + f_-) + (f_+ - f_-)}{2} \tag{362}$$

Form factors for the differential decay rate below is given by

$$\alpha = \gamma = 0, \quad \beta_{++} = f_+^2 \tag{363}$$

H.2.2 $B \to D^*\ell\nu$ (1^3S_0)

Matrix element is

$$< D^*(p',\varepsilon)|V^\mu|B(p) >= i\epsilon^{\mu\nu\alpha\beta}\varepsilon_\nu^*(p+p')_\alpha(p-p')_\beta g(q^2) \tag{364}$$

and

$$< D^*(p',\varepsilon)|A^\mu|B(p) >= \varepsilon^{*\mu} f(q^2) + \varepsilon^* \cdot q(p+p')^\mu a_+(q^2) + \varepsilon^* \cdot q(p-p')^\mu a_-(q^2) \tag{365}$$

Form factors are

$$f = C_f \tilde{m}_B\left[(1 + tildew) + \frac{m_d(\tilde{w} - 1)}{2\mu_+}\right] F_3^{(f)} R^{(f)} \tag{366}$$

where $C_f = 0.989$ for $B \to D^*$.

$$g = \frac{1}{2}\left[\frac{1}{m_c} - \frac{m_d \beta_B^2}{2\mu_- \tilde{m}_D \beta_{BD}^2}\right] F_3^{(g)} R^{(g)} \tag{367}$$

$$a_+ + a_- = C_{cb}\left[\frac{m_d}{(1+\tilde{w})m_c m_b}\frac{\beta_D^2}{\beta_{BD}^2}\left(1 - \frac{m_d}{2\tilde{m}_B}\frac{\beta_D^2}{\beta_{BD}^2}\right) + \tilde{\beta}^{(a_+ + a_-)}\frac{\alpha_s}{\pi}\tilde{m}_B\right] F_3^{(a_+ + a_-)} \tag{368}$$

$$a_+ - a_- = -\frac{1}{\tilde{m}_D}\left[\frac{\tilde{m}_B}{m_b} - \frac{m_d}{2\mu_+}\frac{\beta_D^2}{\beta_{BD}^2} + \frac{\tilde{w} m_d \tilde{m}_B}{(1+\tilde{w})m_c m_b}\frac{\beta_D^2}{\beta_{BD}^2}\left(1 - \frac{m_d}{2\tilde{m}_B}\frac{\beta_D^2}{\beta_{BD}^2}\right)\right] F_3^{(a_+ - a_-)} R^{(a_+ - a_-)} \tag{369}$$

Form factors for the differential decay rate below is given by

$$\begin{aligned} \alpha &= f^2 + 4m_B^2 g^2 p_D^2 \\ \beta_{++} &= \tfrac{f^2}{4m_D^2} - m_B^2 g^2 y + \tfrac{1}{2}\left[(1-y)\tfrac{m_B^2}{m_D^2} - 1\right] f a_+ + \tfrac{m_B^2 p_D^2}{m_D^2} a_+^2 \\ \gamma &= 2gf \end{aligned} \tag{370}$$

where

$$p_D^2 = \frac{[m_B^2(1-y) + m_D^2]^2}{4m_B^2} - m_D^2 \tag{371}$$

is the square of the recoil three-momentum of the D.

H.2.3 $B \to D_0^* \ell \nu$ (1^3P_0)

Matrix element is

$$< D_0^*(p', \varepsilon)|V^\mu|B(p) >= 0 \tag{372}$$

and

$$< D_0^*(p', \varepsilon)|A^\mu|B(p) >= u_+(q^2)(p+p')^\mu + u_-(q^2)(p-p')^\mu \tag{373}$$

Form factors are

$$u_+ + u_- = -\sqrt{\frac{2}{3}}\frac{m_d}{\beta_B} F_5^{(u_+ + u_-)} \tag{374}$$

$$u_+ - u_- = \sqrt{\frac{2}{3}}\frac{m_d \tilde{m}_B}{\beta_B \tilde{m}_D} F_5^{(u_+ - u_-)} \tag{375}$$

Form factors for the differential decay rate below is given by

$$\alpha = \gamma = 0, \quad \beta_{++} = u_+^2 \tag{376}$$

H.2.4 $B \to D_1' \ell \nu$ (1^3P_1)

Matrix element is

$$< D_1'(p', \varepsilon)|V^\mu|B(p) >= \varepsilon^{*\mu} l(q^2) + \varepsilon^* \cdot q(p+p')^\mu c_+(q^2) + \varepsilon^* \cdot q(p-p')^\mu c_-(q^2) \tag{377}$$

and

$$< D_1'(p', \varepsilon)|A^\mu|B(p) >= i\epsilon^{\mu\nu\alpha\beta}\varepsilon^*_\nu (p+p')_\alpha (p-p')_\beta q(q^2) \tag{378}$$

Form factors are

$$q = -\frac{m_d}{2\tilde{m}_D \beta_B}\left(\frac{5+\tilde{w}}{6}\right) F_5^{(q)} \tag{379}$$

$$l = -\tilde{m}_B \beta_B \left[\frac{1}{\mu_-} + \frac{m_d \tilde{m}_D(\tilde{w}-1)}{\beta_B^2}\left(\frac{5+\tilde{w}}{6m_c} - \frac{1}{2\mu_-}\frac{m_d}{\tilde{m}_D}\frac{\beta_B^2}{\beta_{BD}^2}\right)\right] F_5^{(l)} \tag{380}$$

$$c_+ + c_- = -\frac{m_d \tilde{m}_D}{2m_c \tilde{m}_B \beta_B}\left(1 - \frac{m_d m_c}{2\tilde{m}_D \mu_-}\frac{\beta_B^2}{\beta_{BD}^2}\right) F_5^{(c_+ + c_-)} \tag{381}$$

$$c_+ - c_- = -\frac{m_d \tilde{m}_D}{2m_c \tilde{m}_B \beta_B}\left(\frac{\tilde{w}+2}{3} - \frac{m_d m_c}{2\tilde{m}_D \mu_-}\frac{\beta_B^2}{\beta_{BD}^2}\right) F_5^{(c_+ - c_-)} \tag{382}$$

Form factors for the differential decay rate below is given by

$$\begin{aligned}
&\alpha = l^2 + 4m_B^2 q^2 p_D^2 \\
&\beta_{++} = \tfrac{l^2}{4m_D^2} - m_B^2 q^2 y + \tfrac{1}{2}\left[(1-y)\tfrac{m_B^2}{m_D^2} - 1\right] l c_+ + \tfrac{m_B^2 p_D^2}{m_D^2} c_+^2 \\
&\gamma = 2lq
\end{aligned} \tag{383}$$

H.2.5 $B \to D_1 \ell \nu$ (1^1P_1)

Matrix element is Matrix element is

$$< D_1'(p', \varepsilon)|V^\mu|B(p) >= \varepsilon^{*\mu} r(q^2) + \varepsilon^* \cdot q(p+p')^\mu s_+(q^2) + \varepsilon^* \cdot q(p-p')^\mu s_-(q^2) \tag{384}$$

and

$$< D_1'(p', \varepsilon)|A^\mu|B(p) >= i\epsilon^{\mu\nu\alpha\beta}\varepsilon^*_\nu (p+p')_\alpha (p-p')_\beta v(q^2) \tag{385}$$

Form factors are

$$v = \left[\frac{\tilde{m}_B \beta_B}{4\sqrt{2} m_b m_c \tilde{m}_D} + \frac{(\tilde{w}-1)}{6\sqrt{2}}\frac{m_d}{\tilde{m}_D \beta_B}\right] F_5^{(v)} \tag{386}$$

$$r = \frac{\tilde{m}_B \beta_B}{\sqrt{2}} \left[\frac{1}{\mu_+} + \frac{m_d \tilde{m}_D}{3 m_c \beta_B^2} (\tilde{w} - 1)^2 \right] F_5^{(r)} \tag{387}$$

$$s_+ + s_- = \frac{m_d}{\sqrt{2} \tilde{m}_B \beta_B} \left(1 - \frac{m_d}{m_c} + \frac{m_d}{2\mu_+} \frac{\beta_B^2}{\beta_{BD}^2} \right) F_5^{(s_+ + s_-)} \tag{388}$$

$$s_+ - s_- = \frac{m_d}{\sqrt{2} m_c \beta_B} \left(\frac{4 - \tilde{w}}{3} - \frac{m_d m_c}{2 \tilde{m}_D \mu_+} \frac{\beta_B^2}{\beta_{BD}^2} \right) F_5^{(s_+ - s_-)} \tag{389}$$

Form factors for the differential decay rate below is given by

$$\begin{aligned} &\alpha = r^2 + 4 m_B^2 v^2 p_D^2 \\ &\beta_{++} = \tfrac{r^2}{4 m_D^2} - m_B^2 v^2 y + \tfrac{1}{2} \left[(1 - y) \tfrac{m_B^2}{m_D^2} - 1 \right] r s_+ + \tfrac{m_B^2 p_D^2}{m_D^2} s_+^2 \\ &\gamma = 2 r v \end{aligned} \tag{390}$$

H.2.6 $B \to D_2^* \ell \nu$ $(1^3 P_2)$

Matrix element is

$$< D_2^*(p', \varepsilon) | V^\mu | B(p) > = i \epsilon^{\mu\nu\alpha\beta} \varepsilon_\nu^* (p + p')_\alpha (p - p')_\beta h(q^2) \tag{391}$$

and

$$< D_2^*(p', \varepsilon) | A^\mu | B(p) > = \varepsilon^{*\mu} k(q^2) + \varepsilon^* \cdot q (p + p')^\mu b_+(q^2) + \varepsilon^* \cdot q (p - p')^\mu b_-(q^2) \tag{392}$$

Form factors are

$$h = \frac{m_d}{2\sqrt{2} \tilde{m}_B \beta_B} \left[\frac{1}{m_c} - \frac{m_d \beta_B^2}{2 \mu_- \tilde{m}_D \beta_{BD}^2} \right] F_5^{(h)} \tag{393}$$

$$k = \frac{m_d}{\sqrt{2} \beta_B} (1 + \tilde{w}) F_5^{(k)} \tag{394}$$

$$b_+ + b_- = \frac{m_d^2}{4\sqrt{2} m_c m_b \tilde{m}_B \beta_B} \frac{\beta_D^2}{\beta_{BD}^2} \left(1 - \frac{m_d}{2 \tilde{m}_B} \frac{\beta_D^2}{\beta_{BD}^2} \right) F_5^{(b_+ + b_-)} \tag{395}$$

$$b_+ - b_- = -\frac{m_d}{\sqrt{2} m_b \tilde{m}_D \beta_B} \left[1 - \frac{m_d m_b}{2 \mu_+ \tilde{m}_B} \frac{\beta_D^2}{\beta_{BD}^2} + \frac{m_d}{4 m_c} \frac{\beta_D^2}{\beta_{BD}^2} \left(1 - \frac{m_d}{2 \tilde{m}_B} \frac{\beta_D^2}{\beta_{BD}^2} \right) \right] F_5^{(b_+ - b_-)} \tag{396}$$

Form factors for the differential decay rate below is given by

$$
\begin{aligned}
&\alpha = \tfrac{m_B^2 p_D^2}{2m_D^2}(k^2 + 4m_B^2 h^2 p_D^2) \\
&\beta_{++} = -\tfrac{1}{2} y \tfrac{m_B^4 p_D^2}{m_D^2} h^2 + \tfrac{m_B^2}{24 m_D^2}\left(y + \tfrac{4p_D^2}{m_D^2}\right) k^2 + \tfrac{1}{3}\tfrac{m_B^2 p_D^2}{m_D^2}\left[(1-y)\tfrac{m_B^2}{m_D^2} - 1\right] k b_+ + \tfrac{2}{3}\left(\tfrac{m_B^2 p_D^2}{m_D^2}\right)^2 b_+^2 \\
&\gamma = \tfrac{m_B^2 p_D^2}{m_D^2} k h
\end{aligned}
\tag{397}
$$

H.2.7 $B \to D_1^* \ell\nu$ $(\frac{1}{2}^+)$

Form factors are

$$q_{1/2} = \sqrt{\frac{1}{6}} \frac{m_d}{\tilde{m}_D \beta_B} \left(1 - \frac{\beta_B^2 \tilde{m}_B}{4 m_d m_c m_b}\right) F_5^{(q_{1/2})} \tag{398}$$

$$l_{1/2} = \sqrt{\frac{2}{3}} \tilde{m}_B \beta_B \left[\frac{1}{2m_c} - \frac{3}{2m_b} + \frac{m_d \tilde{m}_D (\tilde{w}-1)}{\beta_B^2}\left(\frac{1}{m_c} - \frac{1}{2\mu_-}\frac{m_d}{\tilde{m}_D}\frac{\beta_B^2}{\beta_{BD}^2}\right)\right] F_5^{(l_{1/2})} \tag{399}$$

$$c_{1/2+} + c_{1/2-} = \frac{m_d^2 \beta_D^2}{\sqrt{6} m_c \tilde{m}_B \beta_B \beta_{BD}^2} F_5^{(c_{1/2+} + c_{1/2-})} \tag{400}$$

$$c_{1/2+} - c_{1/2-} = -\sqrt{\frac{2}{3}} \frac{m_d}{2\tilde{m}_D \beta_B}\left(1 + \frac{m_d}{2m_c}\frac{\beta_D^2}{\beta_{BD}^2}\right) F_5^{(c_{1/2+} - c_{1/2-})} \tag{401}$$

H.2.8 $B \to D_1 \ell\nu$ $(\frac{3}{2}^+)$

Form factors are

$$q_{3/2} = -\frac{1}{2\sqrt{3}} \frac{m_d}{\tilde{m}_D \beta_B}\left(\frac{1+\tilde{w}}{2} + \frac{\beta_B^2 \tilde{m}_B}{2 m_d m_c m_b}\right) F_5^{(q_{3/2})} \tag{402}$$

$$l_{3/2} = -\frac{2}{\sqrt{3}} \tilde{m}_B \beta_B \left[\frac{1}{m_c} + \frac{m_d \tilde{m}_D (\tilde{w}-1)}{2\beta_B^2}\left(\frac{\tilde{w}+1}{2m_c} - \frac{1}{2\mu_-}\frac{m_d}{\tilde{m}_D}\frac{\beta_B^2}{\beta_{BD}^2}\right)\right] F_5^{(l_{3/2})} \tag{403}$$

$$c_{3/2+} + c_{3/2-} = -\frac{\sqrt{3} m_d}{2\tilde{m}_B \beta_B}\left[1 - \frac{m_d}{2m_c} - \frac{m_d}{3}\frac{\beta_B^2}{\beta_{BD}^2}\left(\frac{1}{2\mu_-} - \frac{1}{\mu_+}\right)\right] F_5^{(c_{3/2+} + c_{3/2-})} \tag{404}$$

$$c_{3/2+} - c_{3/2-} = -\frac{m_d}{2\sqrt{3}\tilde{m}_D \beta_B}\left[\frac{(2-\tilde{w})\tilde{m}_D}{m_c} + \frac{m_d \beta_B^2}{\beta_{BD}^2}\left(\frac{1}{2\mu_-} - \frac{1}{\mu_+}\right)\right] F_5^{(c_{3/2+} - c_{3/2-})} \tag{405}$$

H.2.9 Differential decay rate

Differential decay rate is given by

$$\frac{d^2\Gamma}{dxdy} = \Gamma_0\left[\frac{y}{m_B^2}\alpha + 2\left(2x\left(1+y-\frac{m_D^2}{m_B^2}\right)-4x^2-y\right)\beta_{++} - y\left(1-4x+y-\frac{m_D^2}{m_B^2}\right)\gamma\right] \tag{406}$$

where

$$\Gamma_0 = \frac{G_F^2|V_{cb}|^2 m_B^5}{32\pi^3} \tag{407}$$

and

$$x = \frac{E_e}{m_B}, \quad y = \frac{t}{m_B^2} = \frac{(p_B - p_D)^2}{m_B^2} \tag{408}$$

H.3 LLSW model

Kinematic variables are w and θ. This θ is the angle between the charged lepton and the charmed meson in the rest frame of the virtual W boson. Thus $\theta = \pi - \chi$,

$$\cos\theta = \cos(\pi - \chi) = -\cos\chi \tag{409}$$

H.3.1 $B \to D_1 \ell\nu$

The matrix elements are

$$\frac{< D_1(v',\varepsilon)|V^\mu|B(v) >}{\sqrt{m_{D_1} m_B}} = f_{V_1}\varepsilon^{*\mu} + (f_{V_2}v^\mu + f_{V_3}v'^\mu)(\varepsilon^* \cdot v) \tag{410}$$

$$\frac{< D_1(v',\varepsilon)|A^\mu|B(v) >}{\sqrt{m_{D_1} m_B}} = i f_A \epsilon^{\mu\alpha\beta\gamma}\varepsilon^*_\alpha v_\beta v'_\gamma \tag{411}$$

The differential decay rate is

$$\begin{aligned}\frac{d^2\Gamma_{D_1}}{dw\,d\cos\theta} \;=\; & 3\Gamma_0 r_1^3\sqrt{w^2-1}\{\sin^2\theta[(w-r_1)f_{V_1} + (w^2-1)(f_{V_3}+r_1 f_{V_2})]^2 \\ & +(1-2r_1 w + r_1^2)[(1+\cos^2\theta)(f_{V_1}^2 + (w^2-1)f_A^2) - 4\cos\theta\sqrt{w^2-1}f_{V_1}f_A]\}\end{aligned} \tag{412}$$

where

$$\Gamma_0 = \frac{G_F^2|V_{cb}|^2 m_B^5}{192\pi^3} \tag{413}$$

and

$$r_1 = \frac{m_{D_1}}{m_B} \tag{414}$$

The form factors are

$$
\begin{aligned}
\sqrt{6}f_A &= -(w+1)\tau - \varepsilon_b\{(w-1)[(\bar{\Lambda}' + \bar{\Lambda})\tau - (2w+1)\tau_1 - \tau_2] + (w+1)\eta_b\} \\
&\quad -\varepsilon_c[4(w\bar{\Lambda}' - \bar{\Lambda})\tau - 3(w-1)(\tau_1 - \tau_2) + (w+1)(\eta_{\rm ke} - 2\eta_1 - 3\eta_3)] \\
\sqrt{6}f_{V_1} &= (1-w^2)\tau - \varepsilon_b(w^2-1)[(\bar{\Lambda}' + \bar{\Lambda})\tau - (2w+1)\tau_1 - \tau_2 + \eta_b] \\
&\quad -\varepsilon_c[4(w+1)(w\bar{\Lambda}' - \bar{\Lambda})\tau - (w^2-1)(3\tau_1 - 3\tau_2 - \eta_{\rm ke} + 2\eta_1 + 3\eta_3)] \\
\sqrt{6}f_{V_2} &= -3\tau - 3\varepsilon_b[(\bar{\Lambda}' + \bar{\Lambda})\tau - (2w+1)\tau_1 - \tau_2 + \eta_b] \\
&\quad -\varepsilon_c[(4w-1)\tau_1 + 5\tau_2 + 3\eta_{\rm ke} + 10\eta_1 + 4(w-1)\eta_2 - 5\eta_3)] \\
\sqrt{6}f_{V_3} &= (w-2)\tau + \varepsilon_b\{(2+w)[(\bar{\Lambda}' + \bar{\Lambda})\tau - (2w+1)\tau_1 - \tau_2] - (2-w)\eta_b\} \\
&\quad +\varepsilon_c[4(w\bar{\Lambda}' - \bar{\Lambda})\tau + (2+w)\tau_1 + (2+3w)\tau_2 \\
&\quad +(w-2)\eta_{\rm ke} - 2(6+w)\eta_1 - 4(w-1)\eta_2 - (3w-2)\eta_3]
\end{aligned}
\tag{415}
$$

The differential decay rate can be expanded in powers of $w-1$

$$
\begin{aligned}
\tfrac{d^2\Gamma_{D_1}}{dw\,d\cos\theta} &= \Gamma_0\tau^2(1)r_1^3\sqrt{w^2-1}\textstyle\sum_n(w-1)^n \\
&\quad \{\sin^2\theta s_1^{(n)} + (1 - 2r_1w + r_1^2)[(1+\cos^2\theta)t_1^{(n)} - 4\cos\theta\sqrt{w^2-1}u_1^{(n)}]\}
\end{aligned}
\tag{416}
$$

where

$$
\begin{aligned}
& s_1^{(0)} = 32\varepsilon_c^2(1-r_1)^2(\bar{\Lambda}' - \bar{\Lambda})^2 + ... \\
& s_1^{(1)} = 32\varepsilon_c(1-r_1^2)(\bar{\Lambda}' - \bar{\Lambda}) + ... \\
& s_1^{(2)} = 8(1+r_1)^2 + ... \\
& t_1^{(0)} = 32\varepsilon_c^2(\bar{\Lambda}' - \bar{\Lambda})^2 + ... \\
& t_1^{(1)} = 4 + 8\varepsilon_c[4(\bar{\Lambda}' - \bar{\Lambda}) + \hat{\eta}_{\rm ke} - 2\hat{\eta}_1 - 3\hat{\eta}_3] + 8\varepsilon_b\hat{\eta}_b + ... \\
& t_1^{(2)} = 8(1 + \hat{\tau}') + ... \\
& u_1^{(0)} = 8\varepsilon_c(\bar{\Lambda}' - \bar{\Lambda}) + ... \\
& u_1^{(1)} = 2 + ...
\end{aligned}
\tag{417}
$$

where

$$
\varepsilon_c = \frac{1}{2m_c}, \quad \varepsilon_b = \frac{1}{2m_b} \tag{418}
$$

and

$$
\hat{\eta}_i = \frac{\eta_i}{\tau(1)}, \quad \tau' = \frac{d\tau}{dt}, \quad \hat{\tau}' = \frac{\tau'}{\tau(1)} \tag{419}
$$

are all evaluated at $w = 1$.

$$\begin{aligned}
\bar{\Lambda}' - \bar{\Lambda} &= 0.39\mathrm{GeV} \\
\bar{\Lambda} &= 0.4\mathrm{GeV} \\
m_c &= 1.4\mathrm{GeV} \\
m_b &= 4.8\mathrm{GeV} \\
\tau_B &= 1.6\mathrm{ps} \\
\hat{\tau}' &= -1.5 \\
|V_{cb}|^2 & 0.04
\end{aligned} \tag{420}$$

H.3.2 $B \to D_2^* \ell\nu$

The matrix elements are

$$\frac{< D_2^*(v',\varepsilon)|V^\mu|B(v) >}{\sqrt{m_{D_2^*} m_B}} = ik_V \epsilon^{\mu\alpha\beta\gamma} \varepsilon^*_{\alpha\sigma} v^\sigma v_\beta v'_\gamma \tag{421}$$

$$\frac{< D_2^*(v',\varepsilon)|A^\mu|B(v) >}{\sqrt{m_{D_2^*} m_B}} = k_{A_1} \varepsilon^{*\mu\alpha} v_\alpha + (k_{A_2} v^\mu + k_{A_3} v'^\mu) \varepsilon^*_{\alpha\beta} v^\alpha v^\beta \tag{422}$$

The differential decay rate is

$$\begin{aligned}
\frac{d^2\Gamma_{D_2^*}}{dw\, d\cos\theta} &= \tfrac{3}{2}\Gamma_0 r_2^3 (w^2-1)^{3/2} \{ \tfrac{4}{3} \sin^2\theta [(w-r_2)k_{A_1} + (w^2-1)(k_{A_3} + r_2 k_{A_2})]^2 \\
&\quad + (1 - 2r_2 w + r_2^2)[(1+\cos^2\theta)(k_{A_1}^2 + (w^2-1)k_V^2) - 4\cos\theta\sqrt{w^2-1}\, k_{A_1} k_V] \}
\end{aligned} \tag{423}$$

where

$$r_2 = \frac{m_{D_2^*}}{m_B} \tag{424}$$

Form factors are

$$\begin{aligned}
k_V &= -\tau - \varepsilon_b[(\bar{\Lambda}' + \bar{\Lambda})\tau - (2w+1)\tau_1 - \tau_2 + \eta_b] - \varepsilon_c(\tau_1 - \tau_2 + \eta_{\mathrm{ke}} - 2\eta_1 + \eta_3) \\
k_{A_1} &= -(1+w)\tau - \varepsilon_b\{(w-1)[(\bar{\Lambda}' + \bar{\Lambda})\tau - (2w+1)\tau_1 - \tau_2] + (1+w)\eta_b\} \\
&\quad - \varepsilon_c[(w-1)(\tau_1 - \tau_2) + (w+1)(\eta_{\mathrm{ke}} - 2\eta_1 + \eta_3)] \\
k_{A_2} &= -2\varepsilon_c(\tau_1 + \eta_2) \\
k_{A_3} &= \tau + \varepsilon_b[(\bar{\Lambda}' + \bar{\Lambda})\tau - (2w+1)\tau_1 - \tau_2 + \eta_b] - \varepsilon_c(\tau_1 + \tau_2 - \eta_{\mathrm{ke}} + 2\eta_1 - 2\eta_2 - \eta_3)
\end{aligned} \tag{425}$$

The differential decay rate can be expanded in powers of $w-1$

$$\begin{aligned}\frac{d^2\Gamma_{D_2^*}}{dw\,d\cos\theta} &= \tfrac{3}{2}\Gamma_0\tau^2(1)r_2^3(w^2-1)^{3/2}\textstyle\sum_n(w-1)^n \\ &\quad \{\tfrac{4}{3}\sin^2\theta s_2^{(n)}+(1-2r_2w+r_2^2)[(1+\cos^2\theta)t_2^{(n)}-4\cos\theta\sqrt{w^2-1}u_2^{(n)}]\}\end{aligned} \tag{426}$$

where

$$\begin{aligned}s_2^{(0)} &= 4(1-r_2)^2[1+2\varepsilon_b\hat\eta_b+2\varepsilon_c(\hat\eta_{\rm ke}-2\hat\eta_1+\hat\eta_3)]+... \\ s_2^{(1)} &= 4(1-r_2)^2(1+2\hat\tau')+... \\ t_2^{(0)} &= 4+8\varepsilon_b\hat\eta_b+8\varepsilon_c(\hat\eta_{\rm ke}-2\hat\eta_1+\hat\eta_3)+... \\ t_2^{(1)} &= 2(3+4\hat\tau')+... \\ u_2^{(0)} &= 2+...\end{aligned} \tag{427}$$

H.3.3 $B\to D_0^*\ell\nu$

The matrix elements are

$$\frac{<D_0^*(v',\varepsilon)|V^\mu|B(v)>}{\sqrt{m_{D_0^*}m_B}}=0 \tag{428}$$

$$\frac{<D_0^*(v',\varepsilon)|A^\mu|B(v)>}{\sqrt{m_{D_0^*}m_B}}=g_+(v^\mu+v'^\mu)+g_-(v^\mu-v'^\mu) \tag{429}$$

The differential decay rate is

$$\frac{d^2\Gamma_{D_0^*}}{dw\,d\cos\theta}=3\Gamma_0r_0^{*3}(w^2-1)^{3/2}\sin^2\theta[(1+r_0^*)g_+-(1-r_0^*)g_-]^2 \tag{430}$$

where

$$r_0^*=\frac{m_{D_0^*}}{m_B} \tag{431}$$

Form factors are

$$\begin{aligned}g_+ &= \varepsilon_c\left[2(w-1)\zeta_1-3\zeta\tfrac{w\bar\Lambda^*-\bar\Lambda}{w+1}\right]-\varepsilon_b\left[\tfrac{\bar\Lambda^*(2w+1)-\bar\Lambda(w+2)}{w+1}\zeta-2(w-1)\zeta_1\right] \\ g_- &= \zeta+\varepsilon_c[\chi_{\rm ke}+6\chi_1-2(w+1)\chi_2]+\varepsilon_b\chi_b\end{aligned} \tag{432}$$

The differential decay rate can be expanded in powers of $w-1$

$$\frac{d^2\Gamma_{D_0^*}}{dw\,d\cos\theta}=3\Gamma_0\zeta^2(1)r_0^{*3}(w^2-1)^{3/2}\sin^2\theta\sum_n(w-1)^ns_0^{(n)} \tag{433}$$

where where

$$s_0^{(0)} = (1-r_0^*)^2[1+2\varepsilon_c(\hat{\chi}_{\rm ke}+6\hat{\chi}_1-4\hat{\chi}_2)+4\varepsilon_b\hat{\chi}_b]+3(\varepsilon_c+\varepsilon_b)(1-r_0^{*2})(\bar{\Lambda}^*-\bar{\Lambda})+...$$
$$s_0^{(1)} = 2(1-r_0^*)^2\hat{\zeta}'+... \tag{434}$$

H.3.4 $B \to D_1^* \ell\nu$

The matrix elements are

$$\frac{< D_1^*(v',\varepsilon)|V^\mu|B(v) >}{\sqrt{m_{D_1^*}m_B}} = g_{V_1}\varepsilon^{*\mu}+(g_{V_2}v^\mu+g_{V_3}v'^\mu)(\varepsilon^*\cdot v) \tag{435}$$

$$\frac{< D_1^*(v',\varepsilon)|A^\mu|B(v) >}{\sqrt{m_{D_1^*}m_B}} = ig_A\epsilon^{\mu\alpha\beta\gamma}\varepsilon^*_\alpha v_\beta v'_\gamma \tag{436}$$

The differential decay rate is

$$\begin{aligned}\frac{d^2\Gamma_{D_1^*}}{dw\,d\cos\theta} &= 3\Gamma_0 r_1^{*3}\sqrt{w^2-1}\{\sin^2\theta[(w-r_1^*)g_{V_1}+(w^2-1)(g_{V_3}+r_1^*g_{V_2})]^2 \\ &\quad +(1-2r_1^*w+r_1^{*2})[(1+\cos^2\theta)(g_{V_1}^2+(w^2-1)g_A^2)-4\cos\theta\sqrt{w^2-1}g_{V_1}g_A]\}\end{aligned} \tag{437}$$

where

$$r_1^* = \frac{m_{D_1^*}}{m_B} \tag{438}$$

Form factors are

$$\begin{aligned}g_A &= \zeta+\varepsilon_c\left[\tfrac{w\bar{\Lambda}^*-\bar{\Lambda}}{w+1}\zeta+\chi_{\rm ke}-2\chi_1\right]-\varepsilon_b\left[\tfrac{\bar{\Lambda}^*(2w+1)-\bar{\Lambda}(w+2)}{w+1}\zeta-2(w-1)\zeta_1-\chi_b\right] \\ g_{V_1} &= (w-1)\zeta+\varepsilon_c\left[(w\bar{\Lambda}^*-\bar{\Lambda})\zeta+(w-1)(\chi_{\rm ke}-2\chi_1)\right] \\ &\quad -\varepsilon_b\left[(\bar{\Lambda}^*(2w+1)-\bar{\Lambda}(w+2))\zeta-2(w^2-1)\zeta_1-(w-1)\chi_b\right] \\ g_{V_2} &= 2\varepsilon_c(\zeta_1-\chi_2) \\ g_{V_3} &= -\zeta-\varepsilon_c\left[\tfrac{w\bar{\Lambda}^*-\bar{\Lambda}}{w+1}\zeta+2\zeta_1+\chi_{\rm ke}-2\chi_1+2\chi_2\right]+\varepsilon_b\left[\tfrac{\bar{\Lambda}^*(2w+1)-\bar{\Lambda}(w+2)}{w+1}\zeta-2(w-1)\zeta_1-\chi_b\right]\end{aligned} \tag{439}$$

The differential decay rate can be expanded in powers of $w-1$

$$\begin{aligned}\frac{d^2\Gamma_{D_1^*}}{dw\,d\cos\theta} &= 3\Gamma_0\zeta^2(1)r_1^{*3}\sqrt{w^2-1}\sum_n(w-1)^n \\ &\quad \{\sin^2\theta s_1^{(n)}+(1-2r_1^*w+r_1^{*2})[(1+\cos^2\theta)t_1^{(n)}-4\cos\theta\sqrt{w^2-1}u_1^{(n)}]\}\end{aligned} \tag{440}$$

where

$$\begin{aligned}
s_1^{(0)} &= (\varepsilon_c - 3\varepsilon_b)^2(1 - r_1^*)^2(\bar{\Lambda}^* - \bar{\Lambda})^2 + ... \\
s_1^{(1)} &= -2(\varepsilon_c - 3\varepsilon_b)(1 - r_1^{*2})(\bar{\Lambda}^* - \bar{\Lambda}) + ... \\
s_1^{(2)} &= (1 + r_1^{*2}) + ... \\
t_1^{(0)} &= (\varepsilon_c - 3\varepsilon_b)^2(\bar{\Lambda}^* - \bar{\Lambda})^2 + ... \\
t_1^{(1)} &= 2 + 4(\varepsilon_c - 3\varepsilon_b)(\bar{\Lambda}^* - \bar{\Lambda}) + 4\varepsilon_c(\hat{\chi}_{\mathrm{ke}} - 2\hat{\chi}_1) + 4\varepsilon_b\hat{\chi}_b + ... \\
t_1^{(2)} &= 2(1 + 2\hat{\zeta}') + ... \\
u_1^{(0)} &= (\varepsilon_c - 3\varepsilon_b)(\bar{\Lambda}^* - \bar{\Lambda}) + ... \\
u_1^{(1)} &= 1 + ...
\end{aligned} \tag{441}$$

where

$$\zeta(1) = \frac{2}{\sqrt{3}}\tau(1), \qquad \hat{\zeta}' = \frac{1}{2} + \hat{\tau}' \tag{442}$$

H.3.5 Differential decay rate using x, y

In ISGW2 model differential decay rate of the form $\frac{d^2\Gamma}{dxdy}$ is used. Here $x = \frac{E_e}{m_B}$ and $y = \frac{q^2}{m_B^2}$. Using

$$w = \frac{m_B^2 + m_D^2 - q^2}{2m_B m_D} = \frac{m_B^2 + m_D^2 - m_B^2 y}{2m_B m_D} \tag{443}$$

The rescaled lepton energy is given by

$$2x = \frac{2E_e}{m_B} = 1 - rw - r\sqrt{w^2 - 1}\cos\theta \tag{444}$$

Hence

$$\frac{\partial x}{\partial w} = -\frac{r}{2}\left(1 - \frac{2w}{\sqrt{w^2 - 1}}\right), \qquad \frac{\partial y}{\partial w} = -\frac{2m_D}{m_B} = -2r \tag{445}$$

and

$$\frac{\partial x}{\partial \cos\theta} = -\frac{r}{2}\sqrt{w^2 - 1}, \qquad \frac{\partial y}{\partial \cos\theta} = 0 \tag{446}$$

Thus

$$dxdy = \left(\frac{\partial x}{\partial w}\frac{\partial y}{\partial \cos\theta} - \frac{\partial y}{\partial w}\frac{\partial x}{\partial \cos\theta}\right) dwd\cos\theta \tag{447}$$

$$\Rightarrow \qquad dxdy = -r^2\sqrt{w^2 - 1}dwd\cos\theta \tag{448}$$

H.4 HQET model

H.4.1 Velocity transfer w

The velocity transfer is related to q^2

$$w = \frac{M_B^2 + M_D^2 - q^2}{2M_B M_D} = v_B \cdot v_D = \frac{p_B \cdot p_D}{M_B M_D} \tag{449}$$

where, D may be D^* or D^{**}. In the context of HQET, it is more natural to use w instead of q^2

H.4.2 $B \to D\ell\nu$

The differential decay rate is given by

$$\frac{d\Gamma(B \to D\ell\nu)}{dq^2} = \frac{G_F^2 |V_{cb}|^2}{192\pi^3 m_B^3} \left[(q^2 - m_B^2 - m_D^2)^2 - 4m_B^2 m_D^2\right]^{3/2} |F_1(q^2)|^2 \tag{450}$$

where F_1 is the form factor. In HQET, the form factor is related to heavy quark form factors $h_+(w)$ and $h_-(w)$

$$RF_1(q^2) = h_+(w) - \frac{m_B - m_D}{m_B + m_D} h_-(w) \tag{451}$$

where R is

$$R = \frac{\sqrt{m_B M_D}}{m_B + m_D} \simeq 0.88 \tag{452}$$

Hence

$$\frac{d\Gamma(B \to D\ell\nu)}{dw} = \frac{G_F^2 |V_{cb}|^2}{48\pi^3} (m_B + m_D)^2 m_D^3 (w^2 - 1)^{3/2} \left| h_+(w) - \frac{m_B - m_D}{m_B + m_D} h_-(w) \right|^2 \tag{453}$$

In heavy quark limit, the form factors $h_+(w)$ and $h_-(w)$ are

$$h_+(w) = \xi(w), \;\; h_-(w) = 0 \tag{454}$$

where $\xi(w)$ is the Isgur-Wise Function.

$$\xi(w) = 1 - \rho_D^2 (w - 1) \tag{455}$$

H.4.3 $B \to D^* \ell \nu$

The kinematic variables in $B \to D^* \ell \nu$ decays are shown in Figure 12.

- θ_ℓ : Angle between the directions of "the ℓ in the W rest frame" and "the W in the B rest frame".
- θ_V : Angle between the directions of "the D in the D^* rest frame" and "the D^* in the B rest frame".
- χ : Azimuthal angle between the planes formed by "W-ℓ system" and "$D^* - D$ system".

Form factors $V(q^2)$, $A_1(q^2)$ and $A_2(q^2)$ are related to helicity form factors $H_0(q^2)$, $H_+(q^2)$ and $H_-(q^2)$, which correspond to the three allowed polarization state of D^* (one longitudinal and two transverse). A_1 contributes to all three helicity components, A_2 contributes only to the helicity-zero component and V contributes only to the helicity ± 1 components

$$
\begin{aligned}
H_+(q^2) &= (m_B + m_{D^*})A_1(q^2) - \tfrac{\sqrt{(q^2 - m_B^2 - m_{D^*}^2)^2 - 4m_B^2 m_{D^*}^2}}{m_B + m_{D^*}} V(q^2) \\
H_-(q^2) &= (m_B + m_{D^*})A_1(q^2) + \tfrac{\sqrt{(q^2 - m_B^2 - m_{D^*}^2)^2 - 4m_B^2 m_{D^*}^2}}{m_B + m_{D^*}} V(q^2) \\
H_0(q^2) &= \tfrac{1}{2m_{D^*}\sqrt{q^2}} \left[(m_B^2 - m_{D^*}^2 - q^2)(m_B + m_{D^*})A_1(q^2) - \tfrac{(q^2 - m_B^2 - m_{D^*}^2)^2 - 4m_B^2 m_{D^*}^2}{m_B + m_{D^*}} A_2(q^2) \right]
\end{aligned}
\tag{456}
$$

Differential decay rate is given in terms of the helicity form factors,

$$
\begin{aligned}
\tfrac{d\Gamma(B \to D^* \ell \nu)}{dw d\cos\theta_V d\cos\theta_\ell d\chi} \quad = \quad & \tfrac{3G_F^2}{4(4\pi)^4} |V_{cb}|^2 m_B m_{D^*}^2 r \sqrt{w^2 - 1} (1 - 2wr + r^2) \times \\
& [(1 - \cos\theta_\ell)^2 \sin^2\theta_V |H_+(w)|^2 \\
& + (1 + \cos\theta_\ell)^2 \sin^2\theta_V |H_-(w)|^2 \\
& + 4\sin^2\theta_\ell \cos^2\theta_V |H_0(w)|^2 \\
& - 4\sin\theta_\ell (1 - \cos\theta_\ell) \sin\theta_V \cos\theta_V \cos\chi H_+(w) H_0(w) \\
& + 4\sin\theta_\ell (1 + \cos\theta_\ell) \sin\theta_V \cos\theta_V \cos\chi H_-(w) H_0(w) \\
& - 2\sin^2\theta_\ell \sin^2\theta_V \cos 2\chi H_+(w) H_-(w)]
\end{aligned}
\tag{457}
$$

where r is the mass ratio

$$
r = \frac{m_{D^*}}{m_B} \tag{458}
$$

$H_i(w)$ are

$$H_i = -m_B \frac{R^*(1-r^2)(w+1)}{2\sqrt{1-2wr+r^2}} h_{A_1}(w) \widetilde{H}_i(w) \tag{459}$$

where R^* is

$$R^* = \frac{2\sqrt{m_B m_{D^*}}}{m_B + m_D} \tag{460}$$

$h_{A_1}(w)$ is

$$h_{A_1}(w) = h_{A_1}(0)\left(1 - \rho^2(w-1)\right) \tag{461}$$

where ρ^2 is the form factor slope, and $\widetilde{H}_i(w)$ are

$$\begin{aligned} \widetilde{H}_{\pm}(w) &= \tfrac{\sqrt{1-2wr+r^2}}{1-r}\left(1 \mp \sqrt{\tfrac{w-1}{w+1}} R_1(w)\right) \\ \widetilde{H}_0(w) &= 1 + \tfrac{w-1}{1-r}\left(1 - R_2(w)\right) \end{aligned} \tag{462}$$

where R_1 and R_2 are the form factor ratios.

H.5 GoityRoberts model

In GoiryRoberts model, the "soft-pion" domain was studied in the framework of the chiral Lagrangian approach combined with the $1/m_Q$ expansion.

H.5.1 $B \to D\pi\ell\nu$

The amplitude for this process has the general form

$$T = \kappa j_\mu \Omega^\mu \tag{463}$$

Here j_μ is the V-A charged leptonic current and the Ω^μ is the hadronic part of the amplitude. To evaluate Ω^μ, these six diagrams are considered to get the amplitude (matrix element)

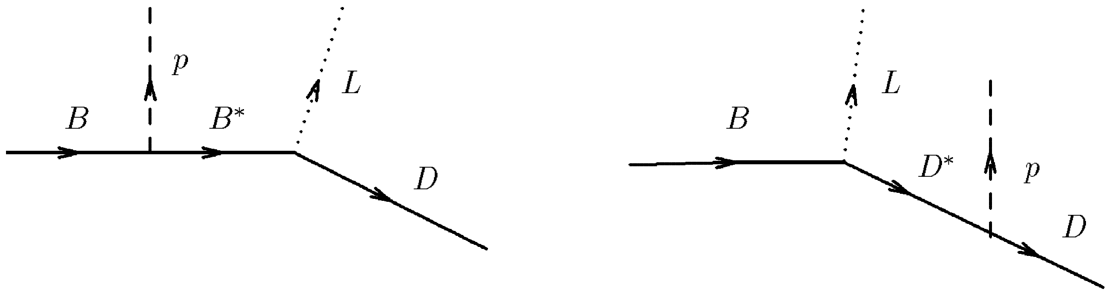

(a)

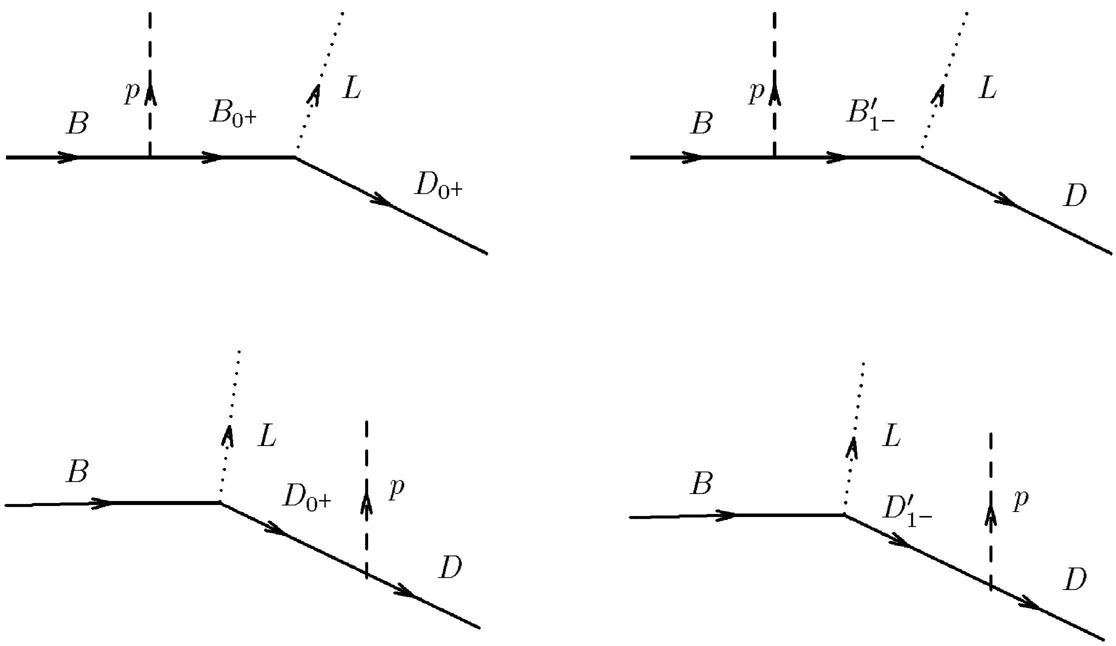

(b)

(a) shows two non-resonant decays , (b) shows four resonant decays. The non-resonant portion of Ω^μ is

$$\begin{aligned}\Omega_\mu^{NR} &= \tfrac{g}{F_0}\xi(\nu)p_\nu\Big\{\tfrac{\Theta^{\nu\rho}(v)}{-2(p\cdot v-\delta m_B)+i\varepsilon}\left[iv^\alpha v'^\beta\epsilon_{\mu\alpha\beta\rho}+g_{\mu\rho}(1+\nu)-v_\mu v'_\rho\right] \\ &\quad +\tfrac{\Theta^{\nu\rho}(v')}{2(p\cdot v'-\delta m_D)+i\varepsilon}\left[iv^\alpha v'^\beta\epsilon_{\mu\alpha\beta\rho}+g_{\mu\rho}(1+\nu)-v_\rho v'_\mu\right]\Big\}\end{aligned} \tag{464}$$

where $\delta m_D = m_{D^*} - m_D$ and $\delta m_B = m_{B^*} - m_B$, and

$$\Theta^{\mu\nu}(v) = g^{\mu\nu} - v^\mu v^\nu \tag{465}$$

The resonant portion of Ω^μ is

$$\begin{aligned}\Omega_\mu^{R} &= \tfrac{\alpha_1}{F_0}\rho_1(\nu)(v-v')_\mu\left[-\tfrac{p\cdot v}{2(-p\cdot v-\delta\tilde m_1)}+\tfrac{p\cdot v'}{2(p\cdot v'-\delta\tilde m_1)}\right] \\ &\quad +\tfrac{\alpha_2}{3F_0}\rho_2(\nu)p_\rho\Big\{\tfrac{\Theta^{\nu\rho}(v)}{2(-p\cdot v-\delta\tilde m_2)}\left[i\epsilon_{\mu\nu\alpha\beta}v^\alpha v'^\beta(\nu-1)+g_{\mu\nu}(\nu^2-1)-v'_\nu\left(v_\mu(2+\nu)-3v'_\mu\right)\right] \\ &\quad +\tfrac{\Theta^{\nu\rho}(v')}{2(p\cdot v'-\delta\tilde m_2)}\left[i\epsilon_{\mu\nu\alpha\beta}v^\alpha v'^\beta(\nu-1)+g_{\mu\nu}(\nu^2-1)-v_\nu\left(v'_\mu(2+\nu)-3v_\mu\right)\right]\Big\} \\ &\quad +\tfrac{\alpha_3}{F_0}\xi^{(1)}(\nu)p_\nu\Big\{\tfrac{\Theta^{\nu\rho}(v)}{-2p\cdot v-\delta\tilde m_3}\left[i\epsilon_{\mu\alpha\beta\rho}v^\alpha v'^\beta+g_{\mu\rho}(\nu+1)-v_\mu v'_\rho\right] \\ &\quad +\tfrac{\Theta^{\nu\rho}(v')}{2p\cdot v'-\delta\tilde m_3}\left[i\epsilon_{\mu\alpha\beta\rho}v^\alpha v'^\beta+g_{\mu\rho}(\nu+1)-v_\rho v'_\mu\right]\Big\}\end{aligned} \tag{466}$$

Here we denote $\delta\tilde m - j = \delta m_j - i\Gamma_j/2$, where Γ_j is the total width of the resonance. Contribution from other resonances are small. Isgur-Wise functions are given by

$$\begin{aligned}\xi(\nu) &= \exp\left[\tfrac{\bar\Lambda^2}{4\beta^2}(\nu^2-1)\right] \\ \xi^{(1)}(\nu) &= -\sqrt{\tfrac{2}{3}}\left[\tfrac{\bar\Lambda^2}{4\beta^2}(\nu^2-1)\right]\exp\left[\tfrac{\bar\Lambda^2}{4\beta^2}(\nu^2-1)\right] \\ \rho_1(\nu) &= \tfrac{1}{\sqrt2}\tfrac{\bar\Lambda}{\beta}\left(\tfrac{2\beta\beta'}{\beta^2+\beta'^2}\right)^{5/2}\exp\left[\tfrac{\bar\Lambda^2}{2(\beta^2+\beta'^2)}(\nu^2-1)\right] \\ \rho_2(\nu) &= \tfrac{1}{2\sqrt2}\left(\tfrac{\bar\Lambda}{\beta}\right)^2\left(\tfrac{2\beta\beta'}{\beta^2+\beta'^2}\right)^{7/2}\exp\left[\tfrac{\bar\Lambda^2}{2(\beta^2+\beta'^2)}(\nu^2-1)\right]\end{aligned} \tag{467}$$

where β and β' are the harmonic oscillator parameters of the ground and excited states, respectively. $\bar\Lambda$ is defined by

$$M_{(0^-,1^-)} = m_Q + \bar\Lambda \tag{468}$$

Ω_μ can be, in general, expressed as

$$\Omega_\mu = -ihm_Bm_D\epsilon_{\mu\nu\rho\sigma}v^\nu v'^\rho p_\pi^\sigma + A_1p_{\pi\mu} + A_2m_Bv_\mu + A_3m_Dv'_{mu} \tag{469}$$

where h, A_1, A_2 and A_3 are the form factors and p_π is the 4-momentum of the pion. The non-resonant contribution to the form factors are

$$\begin{aligned}
h_{NR} &= \frac{g}{2F_0}\frac{\xi(\nu)}{m_B m_D}\left(\frac{1}{p_\pi\cdot v+\delta m_B - i\varepsilon} - \frac{1}{p_\pi\cdot v'-\delta m_D + i\varepsilon}\right)\\
A_{1NR} &= -\frac{g}{2F_0}\xi(\nu)(1+\nu)\left(\frac{1}{p_\pi\cdot v+\delta m_B - i\varepsilon} - \frac{1}{p_\pi\cdot v'-\delta m_D + i\varepsilon}\right)\\
A_{2NR} &= \frac{g}{2F_0}\frac{\xi(\nu)}{m_B}\left(\frac{p_\pi\cdot v + p_\pi\cdot v'}{p_\pi\cdot v+\delta m_B - i\varepsilon}\right)\\
A_{3NR} &= -\frac{g}{2F_0}\frac{\xi(\nu)}{m_D}\left(\frac{p_\pi\cdot v + p_\pi\cdot v'}{p_\pi\cdot v'-\delta m_D + i\varepsilon}\right)
\end{aligned} \tag{470}$$

In SP5/SP6, the contribution from $B \to D^*\ell\nu \to D\pi\ell\nu$ was removed. Hence

$$\begin{aligned}
h_{NR} &= \frac{g}{2F_0}\frac{\xi(\nu)}{m_B m_D}\left(\frac{1}{p_\pi\cdot v+\delta m_B - i\varepsilon}\right)\\
A_{1NR} &= -\frac{g}{2F_0}\xi(\nu)(1+\nu)\left(\frac{1}{p_\pi\cdot v+\delta m_B - i\varepsilon}\right)\\
A_{2NR} &= \frac{g}{2F_0}\frac{\xi(\nu)}{m_B}\left(\frac{p_\pi\cdot v + p_\pi\cdot v'}{p_\pi\cdot v+\delta m_B - i\varepsilon}\right)\\
A_{3NR} &= 0
\end{aligned} \tag{471}$$

The resonant contribution to the form factors are

$$\begin{aligned}
h_R &= \frac{\alpha_2\rho_2(\nu)}{6F_0 m_B m_D}(\nu-1)\left(\frac{1}{p_\pi\cdot v+\delta\tilde{m}_2} - \frac{1}{p_\pi\cdot v'-\delta\tilde{m}_2}\right) + \frac{\alpha_3\xi^{(1)}(\nu)}{2F_0 m_B m_D}\left(\frac{1}{p_\pi\cdot v+\delta\tilde{m}_3} - \frac{1}{p_\pi\cdot v'-\delta\tilde{m}_3}\right)\\
A_{1R} &= -\frac{\alpha_2\rho_2(\nu)}{6F_0}(\nu^2-1)\left(\frac{1}{p_\pi\cdot v+\delta\tilde{m}_2} - \frac{1}{p_\pi\cdot v'-\delta\tilde{m}_2}\right) - \frac{\alpha_3\xi^{(1)}(\nu)}{2F_0}(1+\nu)\left(\frac{1}{p_\pi\cdot v+\delta\tilde{m}_3} - \frac{1}{p_\pi\cdot v'-\delta\tilde{m}_3}\right)\\
A_{2R} &= \frac{\alpha_1\rho_1(\nu)}{2F_0 m_B}\left(\frac{p_\pi\cdot v}{p_\pi\cdot v+\delta\tilde{m}_1} + \frac{p_\pi\cdot v'}{p_\pi\cdot v'-\delta\tilde{m}_2}\right)\\
&\quad + \frac{\alpha_2\rho_2(\nu)}{F_0 m_B}\left\{\frac{1}{p_\pi\cdot v+\delta\tilde{m}_2}\left[\frac{1}{6}(\nu p_\pi\cdot v' - p_\pi\cdot v) + \frac{1}{3}(p_\pi\cdot v' - \nu p_\pi\cdot v)\right] + \frac{1}{2}\frac{1}{p_\pi\cdot v'-\delta\tilde{m}_2}(p_\pi\cdot v - \nu p_\pi\cdot v')\right\}\\
&\quad + \frac{\alpha_3\xi^{(1)}(\nu)}{2F_0 m_B}\left(\frac{p_\pi\cdot(v+v')}{p_\pi\cdot v+\delta\tilde{m}_3}\right)\\
A_{3R} &= -\frac{\alpha_1\rho_1(\nu)}{2F_0 m_D}\left(\frac{p_\pi\cdot v}{p_\pi\cdot v+\delta\tilde{m}_1} + \frac{p_\pi\cdot v'}{p_\pi\cdot v'-\delta\tilde{m}_1}\right)\\
&\quad - \frac{\alpha_2\rho_2(\nu)}{F_0 m_D}\left\{\frac{1}{p_\pi\cdot v'-\delta\tilde{m}_2}\left[\frac{1}{6}(\nu p_\pi\cdot v - p_\pi\cdot v') + \frac{1}{3}(p_\pi\cdot v - \nu p_\pi\cdot v')\right] + \frac{1}{2}\frac{1}{p_\pi\cdot v+\delta\tilde{m}_2}(p_\pi\cdot v' - \nu p_\pi\cdot v)\right\}\\
&\quad - \frac{\alpha_3\xi^{(1)}(\nu)}{2F_0 m_D}\left(\frac{p_\pi\cdot(v+v')}{p_\pi\cdot v'-\delta\tilde{m}_3}\right)
\end{aligned} \tag{472}$$

In SP5/SP6 contributions from D^{**} was removed

$$
\begin{aligned}
h_R &= \tfrac{\alpha_2\rho_2(\nu)}{6F_0 m_B m_D}(\nu-1)\left(\tfrac{1}{p_\pi\cdot v+\delta\tilde{m}_2}\right)+\tfrac{\alpha_3\xi^{(1)}(\nu)}{2F_0 m_B m_D}\left(\tfrac{1}{p_\pi\cdot v+\delta\tilde{m}_3}\right)\\
A_{1R} &= -\tfrac{\alpha_2\rho_2(\nu)}{6F_0}(\nu^2-1)\left(\tfrac{1}{p_\pi\cdot v+\delta\tilde{m}_2}\right)-\tfrac{\alpha_3\xi^{(1)}(\nu)}{2F_0}(1+\nu)\left(\tfrac{1}{p_\pi\cdot v+\delta\tilde{m}_3}\right)\\
A_{2R} &= \tfrac{\alpha_1\rho_1(\nu)}{2F_0 m_B}\left(\tfrac{p_\pi\cdot v}{p_\pi\cdot v+\delta\tilde{m}_1}\right)\\
&\quad+\tfrac{\alpha_2\rho_2(\nu)}{F_0 m_B}\left\{\tfrac{1}{p_\pi\cdot v+\delta\tilde{m}_2}\left[\tfrac{1}{6}(\nu p_\pi\cdot v'-p_\pi\cdot v)+\tfrac{1}{3}(p_\pi\cdot v'-\nu p_\pi\cdot v)\right]\right\}\\
&\quad+\tfrac{\alpha_3\xi^{(1)}(\nu)}{2F_0 m_B}\left(\tfrac{p_\pi\cdot(v+v')}{p_\pi\cdot v+\delta\tilde{m}_3}\right)\\
A_{3R} &= -\tfrac{\alpha_1\rho_1(\nu)}{2F_0 m_D}\left(\tfrac{p_\pi\cdot v}{p_\pi\cdot v+\delta\tilde{m}_1}\right)\\
&\quad-\tfrac{\alpha_2\rho_2(\nu)}{F_0 m_D}\left\{\tfrac{1}{2}\tfrac{1}{p_\pi\cdot v+\delta\tilde{m}_2}(p_\pi\cdot v'-\nu p_\pi\cdot v)\right\}
\end{aligned}
\tag{473}
$$

Numerical values used in SP5/SP6 are

$$
\begin{aligned}
&g=0.5\\
&\alpha_1=-1.430\\
&\alpha_2=-0.140\\
&\alpha_3=0.690\\
&F_0=0.093\\
&\delta m_B=0.0460-\tfrac{0.00001}{2}i\\
&\delta m_D=0.1421-\tfrac{0.00006}{2}i\\
&\delta\tilde{m}_1=0.392-\tfrac{1.040}{2}i\\
&\delta\tilde{m}_2=0.709-\tfrac{0.405}{2}i\\
&\delta\tilde{m}_3=0.563-\tfrac{0.191}{2}i\\
&\beta=0.285\\
&\beta'=0.280\quad\text{for}\quad\rho_1(\nu)\\
&\beta'=0.260\quad\text{for}\quad\rho_2(\nu)\\
&\bar{\Lambda}=0.750
\end{aligned}
\tag{474}
$$

H.5.2 $B\to D^*\pi\ell\nu$

The amplitude for this process has the general form

$$T=\kappa j_\mu \Omega^{\mu\nu}\varepsilon_{D^*\nu} \tag{475}$$

where $\varepsilon_{D^*\nu}$ is the polarization vector of the D^*.

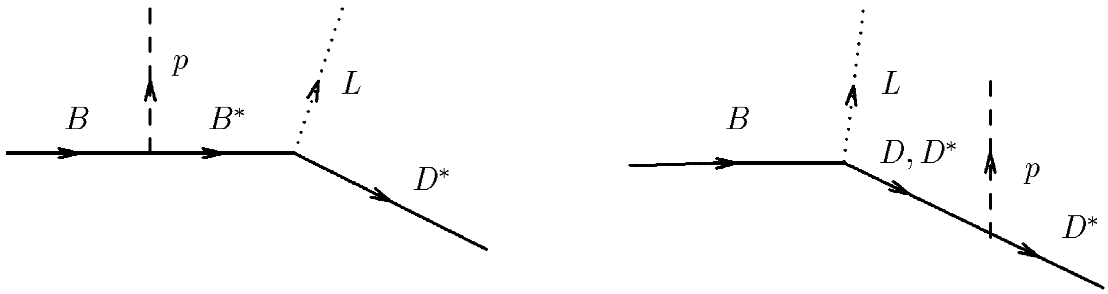

(a)

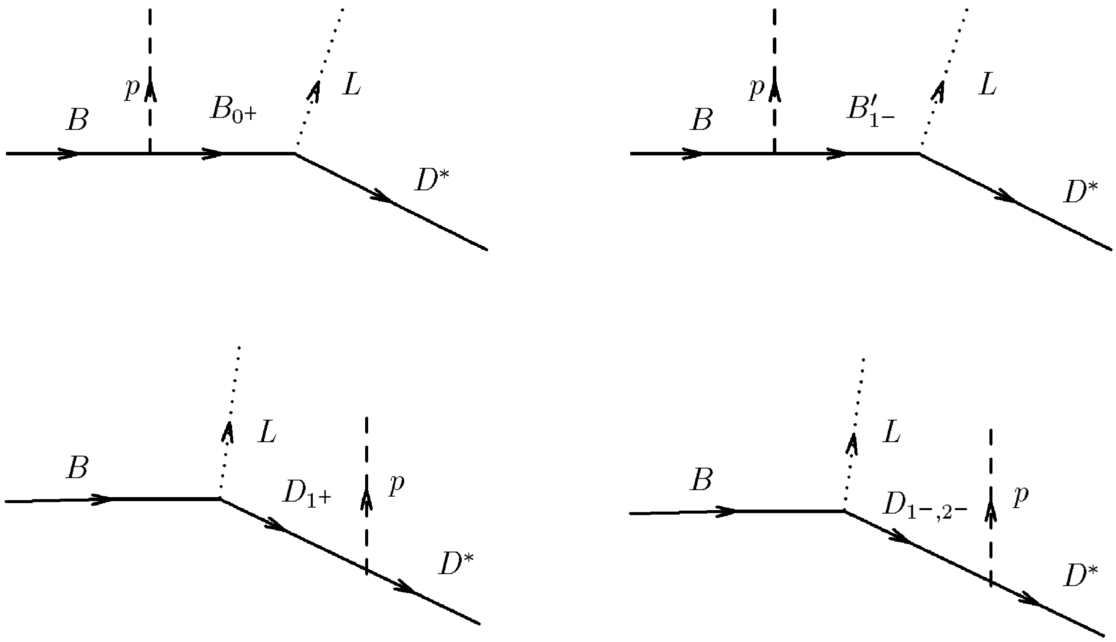

(b)

(a) shows two non-resonant decays , (b) shows four resonant decays. The non-resonant portion of $\Omega_{\mu\nu}$ is

$$
\begin{aligned}
\Omega_{\mu\nu}^{NR} \;=\; & \tfrac{g}{2F_0}\xi(\nu)\Big\{(v+v')_\mu \tfrac{p_\nu}{p\cdot v'+\delta m_D+i\varepsilon} \\
& -p^\rho \tfrac{\Theta_{\rho\sigma}(v)}{-(p\cdot v+\delta m_B)+i\varepsilon}\left[g_{\nu\sigma}(v+v')_\mu - g_{\mu\sigma}v_\nu - g_{\mu\nu}v'_\sigma + i\epsilon_{\mu\alpha\sigma\nu}(v+v')^\alpha\right] \\
& +\tfrac{\Theta_{\rho\delta}(v')}{p\cdot v'+i\varepsilon}\left[-i\epsilon_{\mu\rho\alpha\beta}v'^\alpha v^\beta + g_{\mu\rho}(1+\nu) - v_\rho v'_\mu\right] i\epsilon_{\omega\nu\gamma\delta}p^\gamma v'^\omega\Big\}
\end{aligned} \tag{476}
$$

The resonant portion of $\Omega_{\mu\nu}$ is

$$
\begin{aligned}
\Omega_{\mu\nu}^{R} \;=\; & \tfrac{\alpha_1}{F_0}\rho_1(\nu)\left[-g_{\mu\nu}(\nu-1)+v'_\mu v_\nu - i\epsilon_{\mu\nu\alpha\beta}v^\alpha v'^\beta\right]\left[-\tfrac{p\cdot v}{2(-p\cdot v-\delta\tilde{m}_1)}+\tfrac{p\cdot v'}{2(p\cdot v'-\delta\tilde{m}_1)}\right] \\
& -\tfrac{\alpha_2}{3F_0}\rho_2(\nu)\Big\{p_\rho \tfrac{\Theta^{\rho\sigma}(v)}{2(-p\cdot v-\delta\tilde{m}_2)}\left[-g_{\nu\sigma}(v+v')_\mu(\nu-1)+3v_\nu v'_\mu v'_\sigma - 2g_{\mu\nu}v'_\sigma(\nu-1)\right. \\
& \left.+g_{\mu\sigma}v_\nu(\nu-1)+i\epsilon_{\mu\sigma\alpha\nu}(v-v')^\alpha(1+\nu)+2i\epsilon_{\sigma\nu\alpha\beta}v'^\alpha v^\beta v'_\mu + i\epsilon_{\mu\nu\alpha\beta}v'_\sigma v'^\alpha v^\beta\right] \\
& +3p^\gamma \tfrac{\Theta^{\sigma\rho}_{\gamma\nu}(v')}{2(p\cdot v'-\delta\tilde{m}_2)+i\varepsilon}\left[v_\delta g_{\rho\mu}(\nu-1)-v_\delta v_\rho v'_\mu + i\epsilon_{\mu\delta\alpha\beta}v_\rho v^\alpha v'^\beta\right] \\
& +\tfrac{i}{2}\tfrac{\Theta^{\sigma\rho}(v)}{2(p\cdot v'-\delta\tilde{m}_2)}\epsilon_{\rho\delta\gamma\nu}p_\pi^\delta v'^\gamma\left[i\epsilon_{\mu\sigma\alpha\beta}v^\alpha v'^\beta(\nu-1)+g_{\mu\sigma}(\nu^2-1)-v_\alpha\left(v'_\mu(2+\nu)-3v_\mu\right)\right]\Big\} \\
& +\tfrac{\alpha_3}{F_0}\xi^{(1)}(\nu)\Big\{(v+v')_\mu \tfrac{p_\nu}{2(p\cdot v'-\delta\tilde{m}_3)} \\
& +p^\rho \tfrac{\Theta_{\rho\sigma}(v)}{-2(-p\cdot v-\delta\tilde{m}_3)}\left[g_{\nu\sigma}(v+v')_\mu - g_{\mu\sigma}v_\nu - g_{\mu\nu}v'_\sigma + i\epsilon_{\mu\alpha\sigma\nu}(v+v')^\alpha\right] \\
& +\tfrac{\Theta_{\rho\delta}(v')}{2(p\cdot v'-\delta\tilde{m}_3)}\left[-i\epsilon_{\mu\rho\alpha\beta}v'^\alpha v^\beta + g_{\mu\rho}(1+\nu)-v_\rho v'_\mu\right] i\epsilon_{\omega\nu\gamma\delta}p^\gamma v'^\omega\Big\}
\end{aligned} \tag{477}
$$

The tensor $\Omega_{\mu\nu}$ can be expressed as

$$
\begin{aligned}
\Omega_{\mu\nu} \;=\; & \tfrac{i}{2}\epsilon_{\mu\nu\rho\sigma}\left[h_1 m_B m_D v^\rho v'^\sigma + h_2 m_B v^\rho p_\pi^\sigma + h_3 m_D v'^\rho p_\pi^\sigma\right] \\
& +f_1 m_B v_\mu p_{\pi\nu} + f_2 m_D v'_\mu p_{\pi\nu} + f_3 p_{\pi\mu}p_{\pi\nu} + f_4 m_B^2 v_\mu v_\nu + f_5 m_B m_D v'_\mu v_\nu + f_6 m_B p_{\pi\mu} v_\nu \\
& +k g_{\mu\nu} \\
& +\tfrac{i}{2}\epsilon_{\mu\delta\rho\sigma}v^\delta v'^\rho p_\pi^\sigma(g_1 p_{\pi\nu}+g_2 m_B v_\nu)+\tfrac{i}{2}\epsilon_{\nu\delta\rho\sigma}v^\delta v'^\rho p_\pi^\sigma(g_3 m_B v_\mu + g_4 m_D v'_\mu + g_5 p_{\pi\mu})
\end{aligned} \tag{478}
$$

The non-resonant contribution to the form factors are

$$
\begin{aligned}
h_{1NR} &= -\frac{g\xi(\nu)}{F_0 m_B m_D}\frac{p_\pi\cdot v}{p_\pi\cdot v+\delta m_B - i\varepsilon}\\
h_{2NR} &= -\frac{g\xi(\nu)}{F_0 m_B}\frac{1}{p_\pi\cdot v+\delta m_B - i\varepsilon}\\
h_{3NR} &= -\frac{g\xi(\nu)}{F_0 m_D}\left(\frac{1}{p_\pi\cdot v+\delta m_B - i\varepsilon} - \frac{1+\nu}{p_\pi\cdot v' + i\varepsilon}\right)\\
f_{1NR} &= -\frac{g\xi(\nu)}{2F_0 m_B}\left(\frac{1}{p_\pi\cdot v+\delta m_B - i\varepsilon} - \frac{1}{p_\pi\cdot v' + \delta m_D + i\varepsilon}\right)\\
f_{2NR} &= \frac{m_B}{m_D} f_{1NR}\\
f_{3NR} &= 0\\
f_{4NR} &= 0\\
f_{5NR} &= -\frac{g\xi(\nu)}{2F_0 m_B m_D}\left(1 + \frac{p_\pi\cdot v}{p_\pi\cdot v+\delta m_B - i\varepsilon}\right)\\
f_{6NR} &= -\frac{g\xi(\nu)}{2F_0 m_B}\left(\frac{1}{p_\pi\cdot v+\delta m_B - i\varepsilon} - \frac{1}{p_\pi\cdot v' + i\varepsilon}\right)\\
k_{NR} &= \frac{g\xi(\nu)}{2F_0}\left(\frac{p_\pi\cdot v' - \nu p_\pi\cdot v}{p_\pi\cdot v+\delta m_B - i\varepsilon} + \frac{p_\pi\cdot v - \nu p_\pi\cdot v'}{p_\pi\cdot v' + i\varepsilon}\right)\\
g_{1NR} &= 0\\
g_{2NR} &= 0\\
g_{3NR} &= 0\\
g_{4NR} &= \frac{g\xi(\nu)}{F_0 m_D}\frac{1}{p_\pi\cdot v' + i\varepsilon}\\
g_{5NR} &= 0
\end{aligned}
\tag{479}
$$

The resonant contribution to the form factors are

$$
\begin{aligned}
h_{1R} &= \frac{\alpha_1\rho_1(\nu)}{F_0 m_B m_D}\left(\frac{p_\pi\cdot v}{-p_\pi\cdot v-\delta\tilde m_1}-\frac{p_\pi\cdot v'}{p_\pi\cdot v'-\delta\tilde m_1}\right)+\frac{\alpha_2\rho_2(\nu)}{3F_0 m_B m_D}\left(\frac{p_\pi\cdot v(1+2\nu)-p_\pi\cdot v'}{p_\pi\cdot v+\delta\tilde m_2}+\frac{3}{2}\frac{\nu p_\pi\cdot v'-p_\pi\cdot v}{p_\pi\cdot v'-\delta\tilde m_2}\right)\\
&\quad -\frac{\alpha_3\xi^{(1)}(\nu)}{F_0 m_B m_D}\frac{p_\pi\cdot v}{p_\pi\cdot v+\delta\tilde m_3}\\
h_{2R} &= \frac{\alpha_2(1+\nu)\rho_2(\nu)}{3F_0 m_B}\frac{1}{-p_\pi\cdot v-\delta\tilde m_2}-\frac{\alpha_3\xi^{(1)}(\nu)}{F_0 m_B}\frac{1}{p_\pi\cdot v+\delta\tilde m_3}\\
h_{3R} &= \frac{\alpha_2\rho_2(\nu)}{3F_0 m_D}\left(\frac{1+\nu}{p_\pi\cdot v+\delta\tilde m_2}-\frac{\nu^2-1}{2(p_\pi\cdot v'-\delta\tilde m_2)}\right)-\frac{\alpha_3\xi^{(1)}(\nu)}{F_0 m_D}\left(\frac{1}{p_\pi\cdot v+\delta\tilde m_3}-\frac{1+\nu}{p_\pi\cdot v'-\delta\tilde m_3}\right)\\
f_{1R} &= -\frac{\alpha_2\rho_2(\nu)(\nu-1)}{6F_0 m_B}\left(\frac{1}{p_\pi\cdot v+\delta\tilde m_2}-\frac{1}{p_\pi\cdot v'-\delta\tilde m_2}\right)-\frac{\alpha_3\xi^{(1)}(\nu)}{2F_0 m_B}\left(\frac{1}{p_\pi\cdot v+\delta\tilde m_3}-\frac{1}{p_\pi\cdot v'-\delta\tilde m_3}\right)\\
f_{2R} &= \frac{m_B}{m_D}f_{1R}\\
f_{3R} &= 0\\
f_{4R} &= 0\\
f_{5R} &= -\frac{\alpha_1\rho_1(\nu)}{2F_0 m_B m_D}\left(\frac{p_\pi\cdot v}{p_\pi\cdot v+\delta\tilde m_1}+\frac{p_\pi\cdot v'}{p_\pi\cdot v'-\delta\tilde m_1}\right)+\frac{\alpha_2\rho_2(\nu)}{2F_0 m_B m_D}\left(\frac{p_\pi\cdot v'-\frac{1}{3}p_\pi\cdot v(1+2\nu)}{p_\pi\cdot v+\delta\tilde m_2}+\frac{p_\pi\cdot v-\frac{1}{3}p_\pi\cdot v'(1+2\nu)}{p_\pi\cdot v'-\delta\tilde m_2}\right)\\
&\quad +\frac{\alpha_3\xi^{(1)}(\nu)}{F_0 m_B m_D}\left(\frac{p_\pi\cdot v}{p_\pi\cdot v+\delta\tilde m_3}+\frac{p_\pi\cdot v'}{p_\pi\cdot v'-\delta\tilde m_3}\right)\\
f_{6R} &= \frac{\alpha_2\rho_2(\nu)(\nu-1)}{6F_0 m_B}\left(\frac{1}{p_\pi\cdot v+\delta\tilde m_2}-\frac{1}{p_\pi\cdot v'-\delta\tilde m_2}\right)+\frac{\alpha_3\xi^{(1)}(\nu)}{2F_0 m_B}\left(\frac{1}{p_\pi\cdot v+\delta\tilde m_3}-\frac{1}{p_\pi\cdot v'-\delta\tilde m_3}\right)\\
k_R &= -\frac{\alpha_1\rho_1(\nu)(\nu-1)}{2F_0}\left(\frac{p_\pi\cdot v}{p_\pi\cdot v+\delta\tilde m_1}+\frac{p_\pi\cdot v'}{p_\pi\cdot v'-\delta\tilde m_1}\right)-\frac{\alpha_2\rho_2(\nu)(\nu-1)}{3F_0}\left(\frac{p_\pi\cdot v'-\nu p_\pi\cdot v}{p_\pi\cdot v+\delta\tilde m_2}+\frac{p_\pi\cdot v-\nu p_\pi\cdot v'}{p_\pi\cdot v'-\delta\tilde m_2}\right)\\
&\quad +\frac{\alpha_3\xi^{(1)}(\nu)}{2F_0}\left(\frac{p_\pi\cdot v'-\nu p_\pi\cdot v}{p_\pi\cdot v+\delta\tilde m_3}+\frac{p_\pi\cdot v-\nu p_\pi\cdot v'}{p_\pi\cdot v'-\delta\tilde m_3}\right)\\
g_{1R} &= 0\\
g_{2R} &= -\frac{\alpha_2\rho_2(\nu)}{2F_0 m_B}\frac{1}{p_\pi\cdot v'-\delta\tilde m_2}\\
g_{3R} &= -g_{2R}\\
g_{4R} &= \frac{\alpha_2\rho_2(\nu)}{3F_0 m_D}\left(\frac{2}{p_\pi\cdot v+\delta\tilde m_2}-\frac{1+\frac{1}{2}\nu}{p_\pi\cdot v'-\delta\tilde m_2}\right)+\frac{\alpha_3\xi^{(1)}(\nu)}{F_0}\frac{1}{p_\pi\cdot v'-\delta\tilde m_3}\\
g_{5R} &= 0
\end{aligned}
\tag{480}
$$

In SP5/SP6 contributions from D^{**} was removed

$$
\begin{aligned}
h_{1R} &= \tfrac{\alpha_1\rho_1(\nu)}{F_0 m_B m_D}\left(\tfrac{p_\pi\cdot v}{-p_\pi\cdot v-\delta\tilde m_1}\right)+\tfrac{\alpha_2\rho_2(\nu)}{3F_0 m_B m_D}\left(\tfrac{p_\pi\cdot v(1+2\nu)-p_\pi\cdot v'}{p_\pi\cdot v+\delta\tilde m_2}\right)\\
&\quad -\tfrac{\alpha_3\xi^{(1)}(\nu)}{F_0 m_B m_D}\tfrac{p_\pi\cdot v}{p_\pi\cdot v+\delta\tilde m_3}\\
h_{2R} &= \tfrac{\alpha_2(1+\nu)\rho_2(\nu)}{3F_0 m_B}\tfrac{1}{-p_\pi\cdot v-\delta\tilde m_2}-\tfrac{\alpha_3\xi^{(1)}(\nu)}{F_0 m_B}\tfrac{1}{p_\pi\cdot v+\delta\tilde m_3}\\
h_{3R} &= \tfrac{\alpha_2\rho_2(\nu)}{3F_0 m_D}\left(\tfrac{1+\nu}{p_\pi\cdot v+\delta\tilde m_2}\right)-\tfrac{\alpha_3\xi^{(1)}(\nu)}{F_0 m_D}\left(\tfrac{1}{p_\pi\cdot v+\delta\tilde m_3}\right)\\
f_{1R} &= -\tfrac{\alpha_2\rho_2(\nu)(\nu-1)}{6F_0 m_B}\left(\tfrac{1}{p_\pi\cdot v+\delta\tilde m_2}\right)-\tfrac{\alpha_3\xi^{(1)}(\nu)}{2F_0 m_B}\left(\tfrac{1}{p_\pi\cdot v+\delta\tilde m_3}\right)\\
f_{2R} &= \tfrac{m_B}{m_D}f_{1R}\\
f_{3R} &= 0\\
f_{4R} &= 0\\
f_{5R} &= -\tfrac{\alpha_1\rho_1(\nu)}{2F_0 m_B m_D}\left(\tfrac{p_\pi\cdot v}{p_\pi\cdot v+\delta\tilde m_1}\right)+\tfrac{\alpha_2\rho_2(\nu)}{2F_0 m_B m_D}\left(\tfrac{p_\pi\cdot v'-\frac{1}{3}p_\pi\cdot v(1+2\nu)}{p_\pi\cdot v+\delta\tilde m_2}\right)\\
&\quad +\tfrac{\alpha_3\xi^{(1)}(\nu)}{F_0 m_B m_D}\left(\tfrac{p_\pi\cdot v}{p_\pi\cdot v+\delta\tilde m_3}\right)\\
f_{6R} &= \tfrac{\alpha_2\rho_2(\nu)(\nu-1)}{6F_0 m_B}\left(\tfrac{1}{p_\pi\cdot v+\delta\tilde m_2}\right)+\tfrac{\alpha_3\xi^{(1)}(\nu)}{2F_0 m_B}\left(\tfrac{1}{p_\pi\cdot v+\delta\tilde m_3}\right)\\
k_R &= -\tfrac{\alpha_1\rho_1(\nu)(\nu-1)}{2F_0}\left(\tfrac{p_\pi\cdot v}{p_\pi\cdot v+\delta\tilde m_1}\right)-\tfrac{\alpha_2\rho_2(\nu)(\nu-1)}{3F_0}\left(\tfrac{p_\pi\cdot v'-\nu p_\pi\cdot v}{p_\pi\cdot v+\delta\tilde m_2}\right)\\
&\quad +\tfrac{\alpha_3\xi^{(1)}(\nu)}{2F_0}\left(\tfrac{p_\pi\cdot v'-\nu p_\pi\cdot v}{p_\pi\cdot v+\delta\tilde m_3}\right)\\
g_{1R} &= 0\\
g_{2R} &= 0\\
g_{3R} &= -g_{2R}\\
g_{4R} &= \tfrac{\alpha_2\rho_2(\nu)}{3F_0 m_D}\left(\tfrac{2}{p_\pi\cdot v+\delta\tilde m_2}\right)\\
g_{5R} &= 0
\end{aligned}
\tag{481}
$$

Numerical values used in SP5/SP6 are

$$
\begin{aligned}
&g = 0.5\\
&\alpha_1 = -1.430\\
&\alpha_2 = -0.140\\
&\alpha_3 = 0.690\\
&F_0 = 0.093\\
&\delta m_B = 0.0460 - \tfrac{0.00001}{2} i\\
&\delta m_D = 0.1421 - \tfrac{0.00006}{2} i\\
&\delta \tilde{m}_1 = 0.392 - \tfrac{1.040}{2} i\\
&\delta \tilde{m}_2 = 0.709 - \tfrac{0.405}{2} i\\
&\delta \tilde{m}_3 = 0.563 - \tfrac{0.191}{2} i\\
&\beta = 0.285\\
&\beta' = 0.280 \quad \text{for} \quad \rho_1(\nu)\\
&\beta' = 0.260 \quad \text{for} \quad \rho_2(\nu)\\
&\bar{\Lambda} = 0.750
\end{aligned}
\tag{482}
$$

References

[1] N. Cabbibo, Phys. Rev. Lett. **10**, 531 (1963).

[2] M. Kobayashi and T. Maskawa, Prog. Theor. Phys. **49**, 652 (1973).

[3] BELLE Collaboration, K. Abe *et al.*, Phys. Lett. B**526**, 247 (2002), hep-ex/0111060.

[4] DELPHI Collaboration, P. Abreu *et al.*, Phys. Lett. B**510**, 55 (2001), hep-ex/0104026.

[5] BABAR Collaboration, B. Aubert *et al.*, Phys. Rev. D**71**, 051502 (2005), hep-ex/0408027.

[6] OPAL Collaboration, G. Abbiendi *et al.*, Phys. Lett. B**482**, 15 (2000), hep-ex/0003013.

[7] ALEPH Collaboration, D. Buskulic *et al.*, Phys. Lett. B**395**, 373 (1997).

[8] DELPHI Collaboration, J. Abdallah *et al.*, European. Phys. J. C**33**, 213 (2004), hep-ex/0401023.

[9] CLEO Collaboration, N. E. Adam *et al.*, Phys. Rev. D**67**, 032001 (2003), hep-ex/0210040.

[10] Particle Data Group, W. M. Yao *et al.*, J. Phys. G**33**, 1 (2006).

[11] BABAR Collaboration., BAD1565 (2006).

[12] BELLE Collaboration, Liventsev, D. *et al.*, Phys. Rev. D**72**, 051109 (2005), hep-ex/0507060.

[13] BABAR Collaboration, hep-ex/0607067.

[14] ALEPH Collaboration, D. Buskulic *et al.*, Phys. Lett. B**395**, 373 (1997).

[15] BELLE Collaboration, K. Abe *et al.*, Phys. Lett. B**526**, 258 (2002), hep-ex/0111082.

[16] CLEO Collaboration, J. Bartelt *et al.*, Phys. Rev. Lett.**82**, 3746 (2003), hep-ex/9811042.

[17] BABAR Collaboration, B. Aubert *et al.*, Nucl. Instrum. Meth. **A479**, 1 (2002), hep-ex/0105044.

[18] CLEO Collaboration, T. E. Coan *et al.*, Phys. Rev. Lett. **95**, 181801 (2005), hep-ex/0506053.

[19] CLEO Collaboration, N. E. Adam *et al.*, Phys. Rev. Lett. , (2006), hep-ex/0604044.

[20] BABAR Collaboration, B. Aubert *et al.*, Phys. Rev. Lett. **93**, 011803 (2004), hep-ex/0404017.

[21] BABAR Collaboration, B. Aubert *et al.*, Phys. Rev. Lett. **92**, 071802 (2004), hep-ex/0307062.

[22] CLEO Collaboration, Q. He *et al.*, Phys. Rev. Lett. **95**, 121801 (2005), Erratum-*ibid.* 96, 199903 (2006), hep-ex/0504003.

[23] Scora, D and N. Isgur., Phys. Rev. D**52**, 2783 (1995), hep-ph/9503486.

[24] Isgur, N, D. Scora, B. Grinstein and M. B. Wise., Phys. Rev. D**39**, 2783 (1989).

[25] Neubert, M., Phys. Rept. **245**, 259 (1994), hep-ph/9306320.

[26] Richman, J. D. and P. R. Burchat., Rev. Mod. Phys. **67**, 893 (1995), hep-ph/9508250.

[27] Okamoto, M. *et al.*, Nucl. Phys. Proc. Suppl. **140**, 461 (2005), hep-lat/0409116.

[28] Caprini, I, L. Lellouch and M.Neubert., Nucl. Phys. B**530**, 153 (1998), hep-ph/9712417.

[29] Leibovich, A. K., Z. Ligeti, I. W. Stewart, M. B. Wise., Phys. Rev. D**57**, 308 (1998), hep-ph/9705467.

[30] Goity, J. L. and W. Roberts., Phys. Rev. D**51**, 3459 (1995), hep-ph/9406236.

[31] BABAR Collaboration, B. Aubert *et al.*, Phys. Rev. D, (2006), hep-ex/0602023.

[32] BABAR Collaboration, B. Aubert *et al.*, Phys. Rev. D**69**, 071101 (2004), hep-ex/0401028.

[33] BABAR Collaboration, P. F. Harrison, ed. *et al.*, *"The BABAR Physics Book"* (1997), SLAC-R-504.